



National Library
of Canada

Acquisitions and
Bibliographic Services Branch

395 Wellington Street
Ottawa, Ontario
K1A 0N4

Bibliothèque nationale
du Canada

Direction des acquisitions et
des services bibliographiques

395, rue, Wellington
Ottawa (Ontario)
K1A 0N4

Your file *Votre référence*

Our file *Notre référence*

NOTICE

The quality of this microform is heavily dependent upon the quality of the original thesis submitted for microfilming. Every effort has been made to ensure the highest quality of reproduction possible.

If pages are missing, contact the university which granted the degree.

Some pages may have indistinct print especially if the original pages were typed with a poor typewriter ribbon or if the university sent us an inferior photocopy.

Reproduction in full or in part of this microform is governed by the Canadian Copyright Act, R.S.C. 1970, c. C-30, and subsequent amendments.

AVIS

La qualité de cette microforme dépend grandement de la qualité de la thèse soumise au microfilmage. Nous avons tout fait pour assurer une qualité supérieure de reproduction.

S'il manque des pages, veuillez communiquer avec l'université qui a conféré le grade.

La qualité d'impression de certaines pages peut laisser à désirer, surtout si les pages originales ont été dactylographiées à l'aide d'un ruban usé ou si l'université nous a fait parvenir une photocopie de qualité inférieure.

La reproduction, même partielle, de cette microforme est soumise à la Loi canadienne sur le droit d'auteur, SRC 1970, c. C-30, et ses amendements subséquents.

Canada

The Kinetics and Mechanism of the Reaction of
1,1-difluoro-2,2-diarylethylene with Amines and
pK_a Measurements of Amines in Acetonitrile.

by

Kohilathevy Thanapaalasingham.

A Thesis

Submitted to the Faculty of Graduate Studies
in Partial Fulfillment of the Requirements for the degree of
DOCTOR OF PHILOSOPHY.

© copyright by Kohilathevy Thanapaalasingham. 1992.



National Library
of Canada

Acquisitions and
Bibliographic Services Branch

395 Wellington Street
Ottawa, Ontario
K1A 0N4

Bibliothèque nationale
du Canada

Direction des acquisitions et
des services bibliographiques

395, rue Wellington
Ottawa (Ontario)
K1A 0N4

Your file *Votre référence*

Our file *Notre référence*

The author has granted an irrevocable non-exclusive licence allowing the National Library of Canada to reproduce, loan, distribute or sell copies of his/her thesis by any means and in any form or format, making this thesis available to interested persons.

L'auteur a accordé une licence irrévocable et non exclusive permettant à la Bibliothèque nationale du Canada de reproduire, prêter, distribuer ou vendre des copies de sa thèse de quelque manière et sous quelque forme que ce soit pour mettre des exemplaires de cette thèse à la disposition des personnes intéressées.

The author retains ownership of the copyright in his/her thesis. Neither the thesis nor substantial extracts from it may be printed or otherwise reproduced without his/her permission.

L'auteur conserve la propriété du droit d'auteur qui protège sa thèse. Ni la thèse ni des extraits substantiels de celle-ci ne doivent être imprimés ou autrement reproduits sans son autorisation.

ISBN 0-315-80193-X

Canada

TABLE OF CONTENTS

Table of Contents	iv
Table of Figures	vii
Abstract	xv
Abbreviations and Symbols Used.	xvi
Acknowledgements	xvii
1. INTRODUCTION	1
1.1 General	2
1.2 Factors favoring nucleophilic attack on vinylic carbon.	4
1.3 Possible products from the nucleophilic attack on vinylic carbon.	7
1.4 Mechanism of nucleophilic vinylic substitution.	11
1.5 Literature survey on nucleophilic vinylic substitution.	23
1.6 Scope of our present study.	32
2. KINETICS AND MECHANISM OF THE REACTION OF PHENYL SUBSTITUTED 1,1-DIFLUORO-2,2-DIPHENYLETHYLENES WITH PIPERIDINE IN ACETONITRILE.	39
2.1 General	40
2.2 A preliminary qualitative study of the reaction of para substituted 1,1-difluoro-2,2-diphenylethylene with piperidine.	41

2.3 Kinetics of the reaction of para substituted 1,1-difluoro-2,2-diphenylethylene with piperidine.	57
2.4 The Hammett Relationship.	87
3. pK_a VALUES OF CONJUGATE ACIDS OF AMINES IN ACETO- NITRILE.	95
3.1 Introduction.	96
3.2 Results and discussion	98
4. KINETICS OF THE REACTION OF 1,1-DIFLUORO-2,2-DI(4-CYANO- PHENYL)ETHYLENE WITH AMINES.	110
4.1 General.	111
4.2 Results and discussion.	111
4.3 The Brønsted relationship.	148
5. KINETICS OF THE REACTION OF 1,1-DIFLUORO-2,2-DI(4-CYANO- PHENYL)ETHYLENE WITH PIPERIDINE IN PRESENCE OF ADDED TERTIARY AMINES.	153
5.1 General.	154
5.2 Results and discussion.	155
6. EXPERIMENTAL.	177
6.1 General	178
6.2 Solvents	178
6.3 Reagents	179

6.4 Kinetic measurements	187
6.5 EMF measurements	204
7. REFERENCES	207

Table of Figures

- 1 Figure 1(a): The UV-Vis. spectrum of 1,1-difluoro-2,2-diphenylethylene in acetonitrile and the UV-Vis spectra of the reaction mixture of 1,1-difluoro-2,2-diphenylethylene and piperidine in acetonitrile. 44
- 2 Figure 1(b): The UV-Vis. spectrum of 1,1-difluoro-2,2-diphenylethylene in acetonitrile and the UV-Vis spectra of the reaction mixture of 1,1-difluoro-2,2-diphenylethylene and piperidine in acetonitrile (ie, continuation of Figure 1(a)). 46
- 3 Figure 2: The UV-Vis. spectra of 1,1-difluoro-2,2-di(4-bromophenyl)ethylene and the reaction mixture of 1,1-difluoro-2,2-di(p-bromophenyl)ethylene and piperidine in acetonitrile. 50
- 4 Figure 3: The UV-Vis. spectra of 1,1-difluoro-2,2-di(4-trifluoromethylphenyl)ethylene and the reaction mixture of 1,1-difluoro-2,2-di(4-trifluoromethylphenyl)ethylene and piperidine in acetonitrile. 52
- 5 Figure 4: The UV-Vis. spectra of 1,1-difluoro-2,2-di(4-cyanophenyl)ethylene and the reaction mixture

- of 1,1-difluoro-2,2-di(p-cyanophenyl)ethylene and piperidine in acetonitrile. 54
- 6 Figure 5: k_1 obs vs [piperidine] plot for the reaction of 1,1-difluoro-2,2-diphenylethylene with piperidine in acetonitrile at different temperatures. 63
- 7 Figure 6: k_1 obs vs [piperidine] plot for the reaction of 1,1-difluoro-2,2-di(4-bromophenyl)ethylene with piperidine in acetonitrile at different temperatures. 64
- 8 Figure 7: k_1 obs vs [piperidine] plot for the reaction of 1,1-difluoro-2,2-di(4-trifluoromethylphenyl)ethylene with piperidine in acetonitrile at different temperatures. 65
- 9 Figure 8: k_1 obs vs [piperidine] plot for the reaction of 1,1-difluoro-2,2-di(4-cyanophenyl)ethylene with piperidine in acetonitrile at different temperatures. 66
- 10 Figure 9: k_2 obs vs [piperidine] plot for the reaction of 1,1-difluoro-2,2-diphenylethylene with piperidine in acetonitrile at different temperatures. 68
- 11 Figure 10: k_2 obs vs [piperidine] plot for the reaction of 1,1-difluoro-2,2-di(4-bromophenyl)ethylene

- with piperidine in acetonitrile at different temperatures. 69
- 12 Figure 11: k_2 , obs vs [piperidine] plot for the reaction of 1,1-difluoro-2,2-di(4-trifluoromethylphenyl)ethylene with piperidine in acetonitrile at different temperatures. 70
- 13 Figure 12: k_2 , obs vs [piperidine] plot for the reaction of 1,1-difluoro-2,2-di(p-cyanophenyl)ethylene with piperidine in acetonitrile at different temperatures. 71
- 14 Figure 13: The Hammett plots for the amine catalysed and uncatalysed rate constants for the reaction of para substituted 1,1-difluoro-2,2-diphenylethylenes with piperidine in acetonitrile at 25°C. 91
- 15 Figure 14: The calibration curve for glass electrode in acetonitrile. 103
- 16 Figure 15: EMF vs $\log \{ [B]/ [BH^+] \}$ plots for different amines in acetonitrile at constant salt concentration. 107
- 17 Figure 16: The UV-Vis. spectra of 1,1-difluoro-2,2-

- di(4-cyanophenyl)ethylene and the reaction mixture of 1,1-difluoro-2,2-di(4-cyanophenyl)ethylene and 1,1,3,3-tetramethylguanidine in acetonitrile. 114
- 18 Figure 17: The UV-Vis. spectra of 1,1-difluoro-2,2-di(p-cyanophenyl)ethylene and the reaction mixture of 1,1-difluoro-2,2-di(4-cyanophenyl)ethylene and 1,2,3,4-tetrahydroisoquinoline in acetonitrile. 116
- 19 Figure 18: k_1 obs vs [pyrrolidine] plot for the reaction of 1,1-difluoro-2,2-di(4-cyanophenyl)-ethylene with pyrrolidine in acetonitrile at different temperatures. 129
- 20 Figure 19: k_1 obs vs [morpholine] plot for the reaction of 1,1-difluoro-2,2-di(4-cyanophenyl)-ethylene with morpholine in acetonitrile at different temperatures. 130
- 21 Figure 20: k_1 obs vs [1,2,3,4-tetrahydroisoquinoline] plot for the reaction of 1,1-difluoro-2,2-di(4-cyanophenyl)ethylene with 1,2,3,4-tetrahydroisoquinoline in acetonitrile at different temperatures. 131
- 22 Figure 21: k_1 obs vs [thiomorpholine] plot for the reaction of 1,1-difluoro-2,2-di(4-cyanophenyl)ethyl-

ene with thiomorpholine in acetonitrile at 25°C, 132

23 Figure 22: k_1 obs vs [n-propylamine] plot for the reaction of 1,1-difluoro-2,2-di(4-cyanophenyl)ethylene with n-propylamine in acetonitrile at different temperatures. 133

24 Figure 23: k_1 obs vs [TMG] plot for the reaction of 1,1-difluoro-2,2-di(4-cyanophenyl)ethylene with 1,1,3,3-tetramethylguanidine in acetonitrile at different temperatures. 134

25 Figure 24: k_2 obs vs [pyrrolidine] plot for the reaction of 1,1-difluoro-2,2-di(4-cyanophenyl)ethylene with pyrrolidine in acetonitrile at different temperatures. 135

26 Figure 25: k_2 obs vs [morpholine] plot for the reaction of 1,1-difluoro-2,2-di(4-cyanophenyl)ethylene with morpholine in acetonitrile at different temperatures. 136

27 Figure 26: k_2 obs vs [1,2,3,4-tetrahydroisoquinoline] plot for the reaction of 1,1-difluoro-2,2-di(4-cyanophenyl)ethylene with 1,2,3,4-tetrahydroisoquinoline in acetonitrile at different

temperatures.	137
28 Figure 27: k_2 obs vs [thiomorpholine] plot for the reaction of 1,1-difluoro-2,2-di(4-cyanophenyl)ethylene with thiomorpholine in acetonitrile at 25°C.	138
29 Figure 28: k_2 obs vs [n-propylamine] plot for the reaction of 1,1-difluoro-2,2-di(4-cyanophenyl)ethylene with n-propylamine in acetonitrile at different temperatures.	139
30 Figure 29: $\log k_2$ vs pK_a plot for the reaction of 1,1-difluoro-2,2-di(4-cyanophenyl)ethylene with various amines.	143
31 Figure 30: $\log k_2$ vs pK_a plot for the reaction of 1,1-difluoro-2,2-di(4-cyanophenyl)ethylene with various amines.	152
32 Figure 31: k_2 obs. vs [amine] plot for the reaction of 1,1-difluoro-2,2-di(4-cyanophenyl)ethylene with piperidine in presence of N-methylpyrrolidine.	158
33 Figure 32: k_2 obs. vs [amine] plot for the reaction of 1,1-difluoro-2,2-di(4-cyanophenyl)ethylene with piperidine in the presence of N-methylpiperidine.	160

- 34 Figure 33: $k_{2,obs.}$ vs [amine] plot for the reaction of 1,1-difluoro-2,2-di(4-cyanophenyl)ethylene with piperidine in the presence of N-methylmorpholine. 162
- 35 Figure 34: $k_{2,obs.}$ vs [amine] plot for the reaction of 1,1-difluoro-2,2-di(4-cyanophenyl)ethylene with piperidine in the presence of DBU. 164
- 36 Figure 35: $k_{2,obs.}$ vs [amine] plot for the reaction of 1,1-difluoro-2,2-di(4-cyanophenyl)ethylene with piperidine in the presence of 1,3-diphenylguanidine. 166
- 37 Figure 36: $\log k_{cat}$ vs pK_a plot for the reaction of 1,1-difluoro-2,2-di(4-cyanophenyl)ethylene with piperidine in the presence of different tertiary amines. 168
- 38 Figure 37: The cell used for the kinetic measurements of the reaction of 1,1-difluoro-2,2-diphenyl-ethylene with piperidine in acetonitrile. 189
- 39 Figure 38: The kinetic curve for the reaction of 1,1-difluoro-2,2-di(4-trifluoromethylphenyl)ethylene with piperidine at 20°C in acetonitrile. 194
- 40 Figure 39: The Guggenheim plot for the reaction of 1,1-difluoro-2,2-di(4-trifluoromethylphenyl)-

ethylene with piperidine at 20°C in acetonitrile.	196
41 Figure 40: The kinetic curve for the reaction of 1,1-difluoro-2,2-diphenylethylene with piperidine at 50°C in acetonitrile.	200
42 Figure 41: The Guggenheim plot for the reaction of 1,1-difluoro-2,2-diphenylethylene with piperidine at 50°C in acetonitrile.	203
43 Figure 42: The H-shaped cell that was used for the pK_a measurements.	206

ABSTRACT

1,1-difluoro-2,2-diphenylethylene and its para-phenyl substituted analogs have been synthesised and their reactions with piperidine in acetonitrile have been studied. The substrates are reactive only with primary and secondary amines. Tertiary amines do not react with the substrates directly, but they catalyse reactions with primary and secondary amines. Reactions with primary and secondary amines give 1-amino-1-fluoro-2,2-diarylethylenes as the initial products. The kinetics for the formation of 1-amino-1-fluoro-2,2-diarylethylene have been studied. The reaction proceeds via both amine catalysed and uncatalysed paths. The rate constants and the activation parameters for both amine catalysed and uncatalysed routes have been obtained and the rate constants show good correlation with the substituent constants, σ .

The rate constants and the activation parameters for the reaction of 1,1-difluoro-2,2-di(4-cyanophenyl)ethylene with various amines have been obtained and the catalysed rate constants show a good correlation with the pK_a values of the conjugate acids of the amines in acetonitrile.

The catalytic rate constants of tertiary amines for the reaction of 1,1-difluoro-2,2-di(4-cyanophenyl)ethylene with piperidine in acetonitrile have been obtained and correlated with the pK_a values of the conjugate acids of the amines. Based on the results, a mechanism for the formation of 1-amino-1-fluoro-2,2-diarylethylene has been proposed.

In order to obtain the Brønsted relationship, the pK_a values of the conjugate acids of the amines have been measured in acetonitrile using a potentiometric method.

Abbreviations and Symbols used

A	absorbance
B	base (amine)
BH ⁺	conjugate acid (ammonium ion)
D	dielectric constant
DBU	1,8-diazabicyclo[5.4.0]undec-7-ene
DMF	dimethylformamide
E ⁺	electrophile
f	activity coefficient
ΔH	enthalpy of activation
HMPA	hexamethylphosphoramide
HMPT	hexamethylphosphoroustriamide
HPI	picric acid
k	rate constant
K	equilibrium constant
Nu	nucleophile
S	ionic strength
ΔS	entropy of activation
Pi ⁻	picrate ion
SET	single electron transfer
TMG	1,1,3,3-tetramethylguanidine
σ	substituent constant
ρ	reaction constant
λ	wavelength

ACKNOWLEDGEMENT

I would like to express my sincere gratitude to my supervisor, Professor K. T. Leffek, for his guidance and encouragement during the course of this work, and his valuable advice and patience.

I am grateful to Dalhousie University for financial support during my period of study.

1. INTRODUCTION

1.1 General.

In 1925, Lapworth recognised that polar reagents can be classified into two groups depending on their properties, and he termed them as "cationoid" and "anionoid" (1). Later, in 1933, Ingold termed these two classes as "electrophilic" (electron seeking) and "nucleophilic" (nucleus seeking) respectively (2). According to Ingold, nucleophiles are reagents which donate their electrons to, or share them with, another atomic nucleus (3). This definition fails to distinguish reducing agents from nucleophiles. In order to eliminate this confusion, Bunnett defined a nucleophile as a reagent which supplies a pair of electrons to form a new bond between itself and another atom (4).

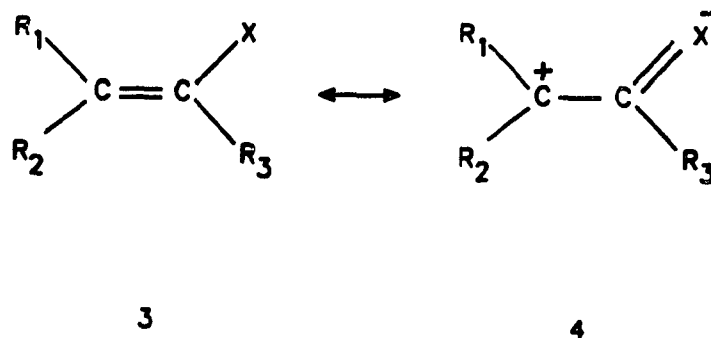
From the definition for a nucleophile, it is reasonable to believe that nucleophilic attack on an unsaturated carbon atom would be difficult, due to the presence of π -electrons. This may be the reason why nucleophilic substitution at aromatic or vinylic carbon did not receive much attention until the 1950's while the intensive work on the nucleophilic substitution at saturated carbon atom began in the 1930's.

Nucleophilic attack on carbon-carbon double bonds has not been studied or systemized as much as that of electrophilic addition. Nucleophilic attack on a carbon-oxygen double bond is rather common and it is used widely for

avored by the structural factors which favor nucleophilic aromatic substitution and these reactions will become as important as those of aromatic nucleophilic substitution in synthetic organic chemistry.

1.2 Factors favoring nucleophilic attack on vinylic carbon.

Although nucleophilic attack on vinylic carbon does not take place under normal conditions, some structural factors activate vinylic carbons towards nucleophilic attack. The presence of groups which diminish electron density in the carbon-carbon double bond either by an electron-withdrawing inductive(-I) or by a mesomeric(-M) effect is the most common factor among those which facilitate nucleophilic attack on the vinylic carbon atom. Michael addition to an α,β -unsaturated ketone is an example of nucleophilic attack on a carbon-carbon double bond that is activated by the carbonyl group. Systems activated by nitro(5-6), cyano(7-9), alkoxy-carbonyl(10-12) and arylsulphonyl(13) groups are also known. Substitution of such a group on a carbon-carbon double bond develops a positive charge on the β -carbon atom by its mesomeric(-M) effect, and hence directs the nucleophile towards this carbon atom. In other words, the contribution of structure 4 of Scheme 2 aids nucleophilic attack.



with electron-withdrawing substituents, the polarization of the double bond is lowered and causes a decrease in reactivity. However, multiple substitution, (eg: as in tetracyanoethylene) increases the overall reactivity. Nucleophilic attack on fluoro olefins (14) is a good example where the olefin is activated by the inductive effect of the substituent.

In addition to the presence of electron-withdrawing substituents, there are some other factors which could facilitate nucleophilic attack at vinylic carbon. There is some evidence that in a system activated by ground state strain, nucleophilic attack occurs even in the absence of electron-withdrawing substituents (15). It is also reported that phenolate oxygen adds rapidly to a neighboring monoalkyl ethylene when the groups are brought together in a system

exhibiting high effective molarity (16,17). Some enzyme catalysed nucleophilic attacks are also known to occur in the absence of other activating factors (18).

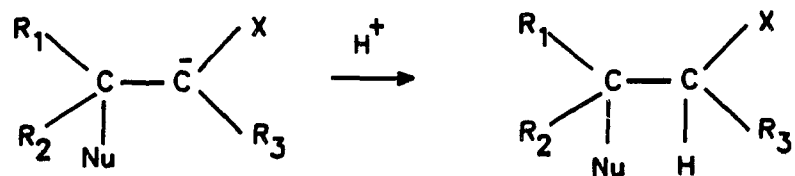
In more recent studies, it was also found that nucleophilic attack by thiolate and selenide anions occurs even on unactivated vinyl halides such as β -bromostyrene under mild conditions in aprotic solvents such as HMPA and DMF (19, 20). When HMPA was the solvent reaction occurs at room temperature with complete retention of configuration and the yield reported was above 90%.

In the nucleophilicity scale established for nucleophilic substitution at saturated carbon atom, thiolate and selenide anions have been given high nucleophilic constants (21). According to a qualitative nucleophilicity scale established by Rappoport for nucleophilic substitution at vinylic carbon atoms, thiolate ion was one of the strongest nucleophiles (22). Moreover, the reactivity of these nucleophiles is enhanced in HMPA by specific solvation of the cation. Hence HMPA facilitates nucleophilic attack on unactivated vinyl halides.

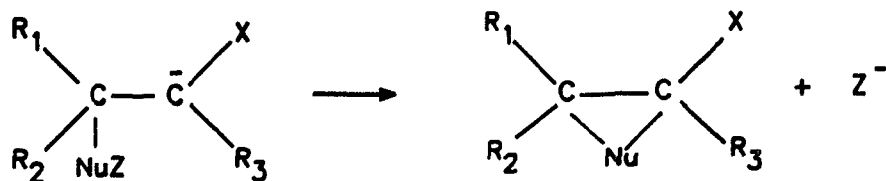
This carbanion or zwitterion can undergo several reactions as shown in Scheme 4. Among these reactions, addition, substitution, fragmentation and *cis-trans* isomerization reactions are the most frequently observed. Competition between these reactions often leads to a mixture of two or more products and hence complicates the kinetic and mechanistic investigation and limits the synthetic applications. However, careful selection of nucleophile, substrate and solvent may help to simplify the situation.

Scheme 4

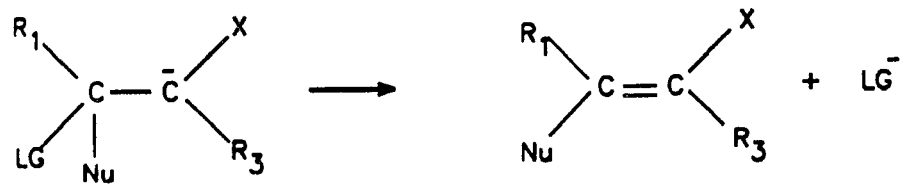
(i) addition :



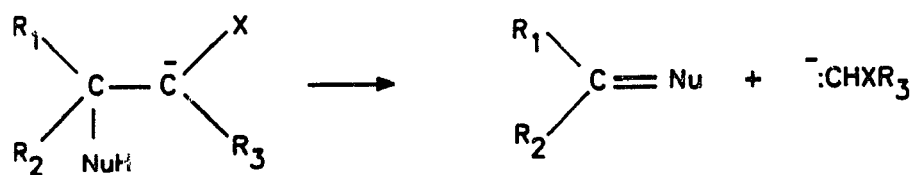
(ii) internal cyclization :



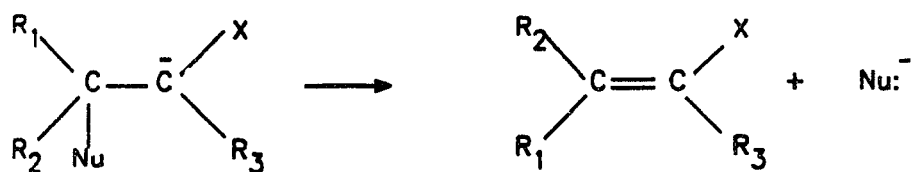
(iii) substitution:



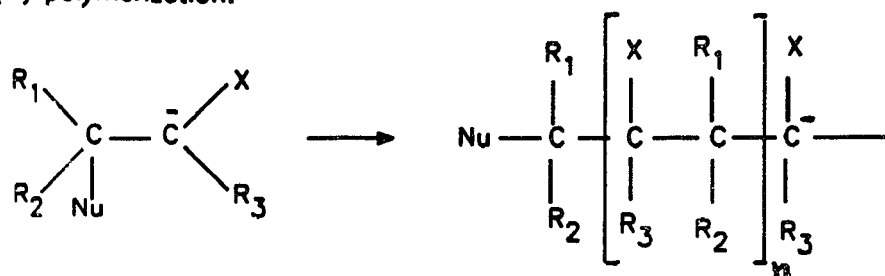
(iv) fragmentation:



(v) cis-trans isomerization:



(vi) polymerization:



In the presence of a proton source, such as a protic solvent, nucleophilic addition across the double bond is the common reaction. Michael addition and the cyanoethylation reaction are well known examples of such addition reactions (23,24). Numerous examples of nucleophilic vinylic substitution can be found in the literature (25-28). Since we are mainly interested in nucleophilic vinylic substitution, the mechanism of the substitution reaction will be discussed in detail. Attack of hydroxide ion or water on the activated carbon - carbon double bond often leads to a fragmentation reaction (10). Bernasconi and co-workers have reported a considerable number of such fragmentation reactions (29-31). For example, base catalysed hydrolysis of benzylidene malononitrile gives benzaldehyde and malononitrile anion as products (32), as shown in equation [1].



Some data are also available on nucleophile assisted *cis-trans* isomerization of an activated olefin (33). In a few cases, nucleophilic attack on carbon - carbon double bonds leads to cyclic dimers, trimers and short chain polymers (34,35).

1.4 Mechanism of nucleophilic vinylic substitution.

Any factors which stabilize the intermediate carbanion (or zwitterion) allow more opportunity for expulsion of the leaving group. Since there are similarities between aryl halides and vinyl halides, nucleophilic substitution at vinylic centres could be merely a further chapter of aromatic nucleophilic substitution. However, reactions of ethylenic substrates are mechanistically more diverse. Vinyl halides undergo β -elimination to acetylenes with greater ease than aromatic compounds form arynes. The competition between substitution and elimination is, indeed, one of the most intriguing features of the reactions of vinylic compounds with nucleophiles. *Cis-trans* isomerism of substituted ethylenes makes available substrates of known configuration for the study of mechanisms of β -elimination. Moreover, a vinylic substrate necessarily carries an α -substituent with respect to the leaving group. This α -substituent may exert a steric and an electronic effect on the reaction rate and may itself be attacked by the nucleophile, thus opening new reaction pathways. Ethylenic substrates of suitable structure may undergo an S_N1 type reaction even at room temperature (36).

In fact, nucleophilic substitution on a vinylic system can take place via mechanistic routes that operate both in nucleophilic substitution at saturated carbon atoms and at

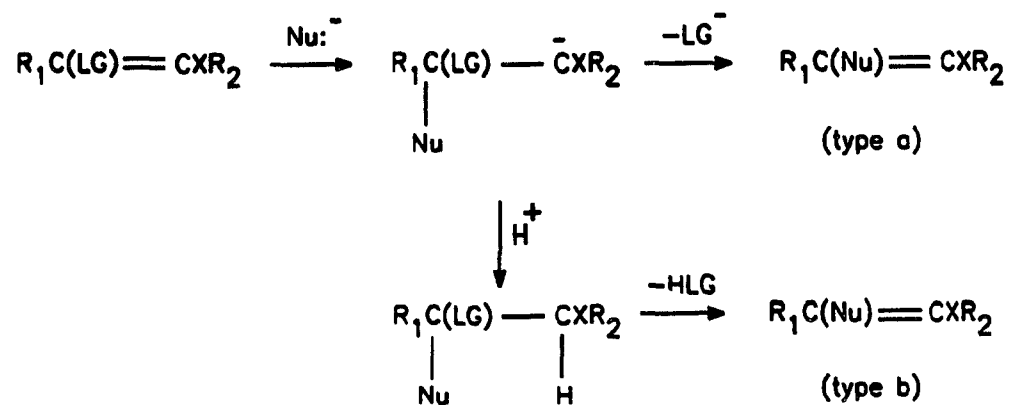
aromatic carbon atoms. Therefore, nucleophilic substitution at vinylic carbon is richest in mechanistic possibilities in comparison to saturated and aromatic systems.

The mechanisms of nucleophilic substitution in the vinylic systems have been reviewed from time to time by different authors during the last forty years. As time went on, the number of mechanistic routes on the list increased. In fact, 38 theoretical mechanistic variations have been suggested in the latest review published by Rappoport (37). Although all these 38 routes are theoretically possible, only a few of them are experimentally supported. These observed routes are summarized in Scheme 5.

The mechanism of a particular nucleophilic vinylic substitution depends on the substrate, nucleophile, solvent and the leaving group. The most important routes in Scheme 5 are (i), (ii) and (iii) while (iv) and (v) are observed only in special cases.

Scheme 5

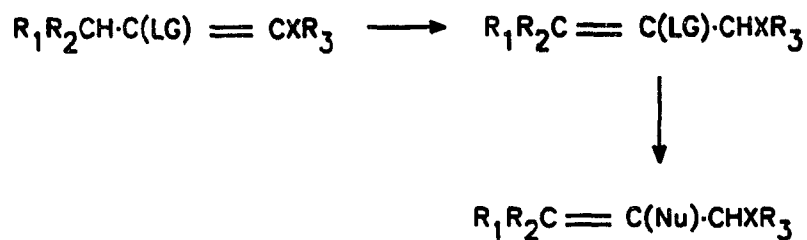
(i) addition-elimination:



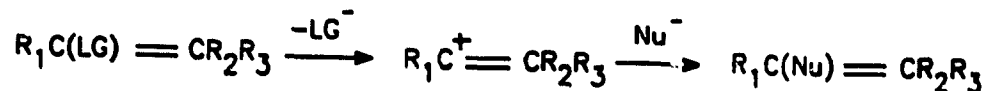
(ii) elimination-addition:



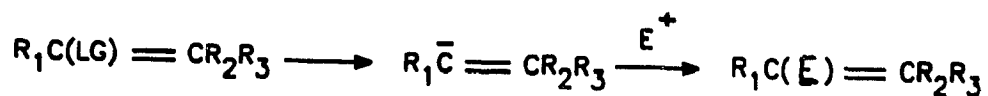
(iii) substitution with primary rearrangement of substrate:



(iv) S_N1 type vinylic substitution:



(v) substitution involving a vinylic carbanion:



(i) The addition - elimination mechanism.

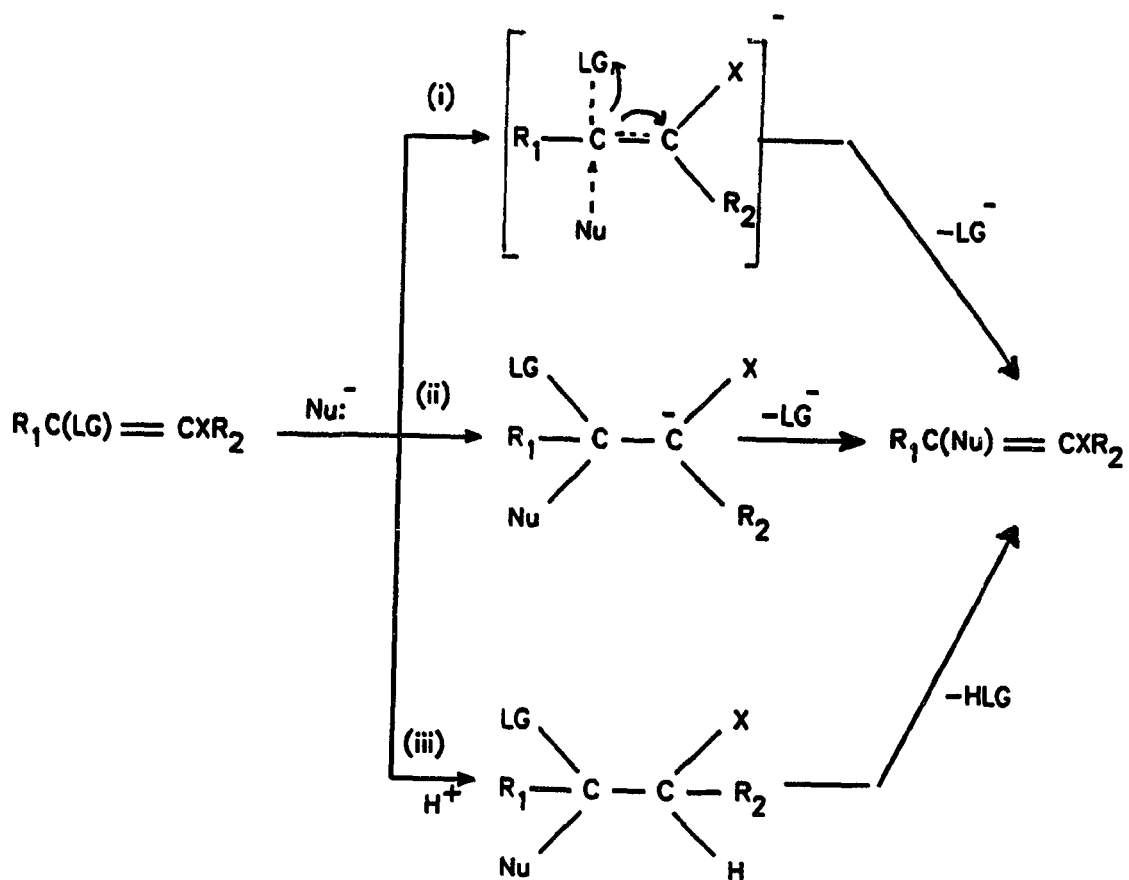
Most of the substitution reactions take place via the addition - elimination route. Therefore, this is the most studied one in Scheme 5. In fact this is the only route which involves direct attack of the nucleophile on a vinylic carbon atom.

In the elimination-addition route the primary step is the attack on the vinylic H-atom not on the vinylic carbon. These two mechanisms can be distinguished by isotopic studies. Deuterium exchange will take place if the primary attack take place on the vinylic hydrogen. In the addition - elimination mechanism, the product configuration will be determined by the path of attack and by the configuration and the life time of the carbanion(or

zwitterion) intermediate. Since it involves the direct attack of a nucleophile on the vinylic carbon atom, it is also the one which, in actual fact, is most correctly described as a nucleophilic vinylic substitution.

If we consider the addition-elimination mechanism, the attack of the nucleophile could lead to three types of reactions, as shown in Scheme 6.

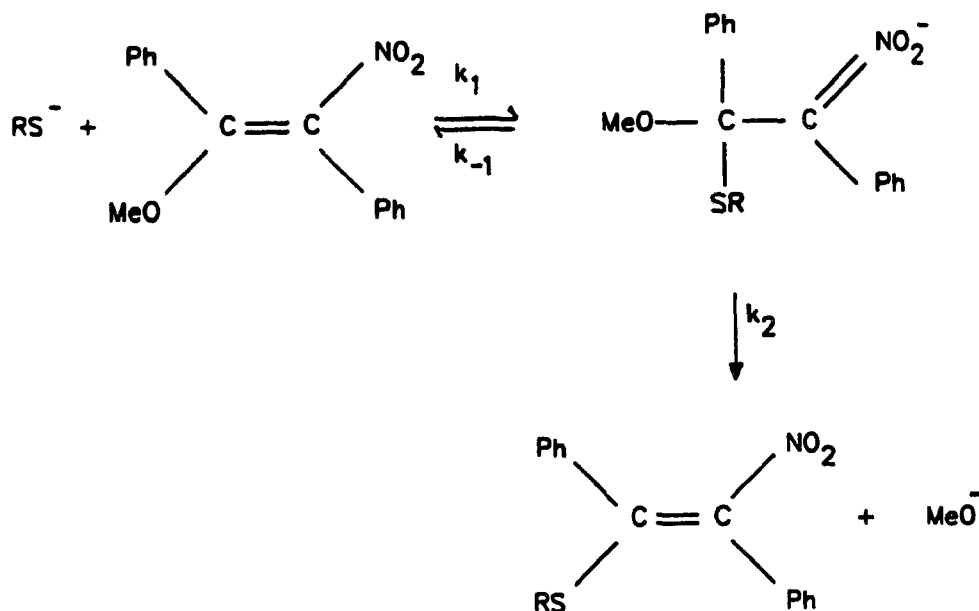
Scheme 6



In the first one(i), which involves no intermediate, bond breaking and bond forming take place simultaneously. In the second one(ii), bond breaking takes place after the bond formation and the intermediate is a carbanion(or a zwitterion) and in the third one (iii), the α,β -addition product is formed as the intermediate. That is, the first reaction is a single step reaction and the second and third ones are multistep reactions. The stereochemistry and the element effect can give information about the type of intermediate. Most of the experimental evidence points to a short lived carbanionic intermediate, but in some cases , an α,β -adduct seems essential. These variations have been discussed by Rappoport in terms of the variable transition state concept (38).

Although the presence of a carbanionic intermediate has been suggested for most nucleophilic vinylic substitution reactions, and carbanionic adducts were detected when there was no leaving group in the adduct, such intermediates were not detected under the reaction conditions where vinylic substitution actually occurred. But such a carbanionic intermediate was recently observed in the reaction of alkyl thiolate ions with (E)- β -methoxy- α -nitrostilbene in 50% DMSO - 50% water solvent at 20°C (39, 40).

The reaction takes place according to following equation.



The following conditions are necessary for the detection of the intermediate.

- (i) The equilibrium for the formation of the intermediate must be favorable. ie, $k_1[\text{Nu}]/k_{-1} \gg 1$.
- (ii) The decay of the intermediate must be slower than its formation. ie, $k_1[\text{Nu}] \gg k_2$.
- (iii) The absolute value of k_2 must be low enough to allow detection by suitable techniques.

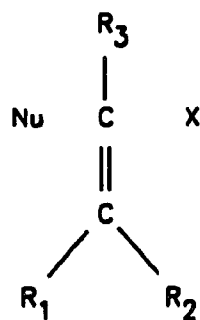
When one or more of these conditions are not satisfied in a reaction, the detection of the intermediate becomes difficult. For example, after the detection of the intermediate in the above reaction, the reaction of pyrrolidine, piperidine, morpholine and n-butylamine with

(E)- β -methoxy- α -nitrostilbene was studied in a solvent mixture containing 50% DMSO - 50% water at 20° with the intention of observing the intermediate. However, no intermediate was observed (41). In another example, a search for the intermediate carbanion in the reaction of OH⁻ with Ph(LG)C = CPh(NO₂) (LG = Cl, I, SEt and OMe) in 50% DMSO - H₂O solvent was unsuccessful (42).

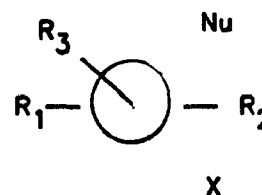
Two transition state structures were proposed by Gold for the single step process (type (i)) (43). One involved an in-plane attack of the nucleophile leading to the transition state (structure 5) which is analogous to that in aliphatic S_N2 reactions but with sp hybridization for the co-linear R₃-C _{α} -C _{β} bonds where one of the p-orbitals is involved in the weak binding to the entering and the leaving groups while the other participates in the formation of π -bond between C _{α} and C _{β} . This would lead to the product with complete inversion of configuration. Such exclusive inversion of configuration is not reported in the literature. Most of the experimental results show that the substitution takes place either with retention of configuration or with stereoconvergence. This in turn suggests that the attack in fact takes place perpendicular to the plane of the molecule. Moreover, theoretical calculations show that in-plane attack requires more energy than perpendicular attack (44).

The second type of transition state is formed when the nucleophilic attack takes place perpendicular to the plane

of the molecule. In this case, C_α is tetrahedral, the carbon has sp^3 hybridization and the $C_\alpha - C_\beta$ bond has single bond character (structure 6).



5



6

The stereochemical outcome of the addition - elimination mechanism has been analyzed by Miller (45). He analyzed how the overall stereoselectivity depends on one or two of the following factors (rate constants),

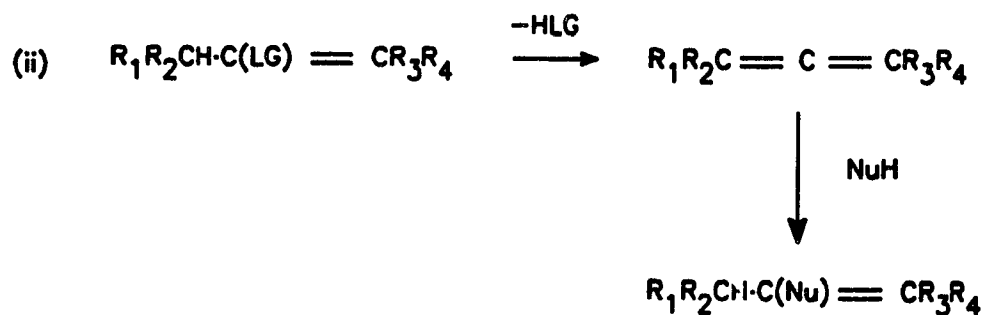
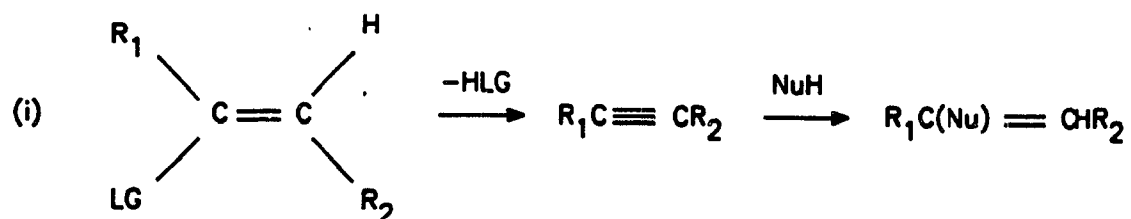
- (i) formation of the intermediate anion,
- (ii) isomerization of the anion by rotation,
- (iii) isomerization of the anion by inversion, and
- (iv) dissociation of the anion to reactant or product.

According to his analysis, substitution with retention of configuration or with stereoconvergence is the preferred path in the addition-elimination mechanism. This is consistent with the experimental observations.

(ii) The elimination-addition mechanism.

When there is a vinylic or allylic proton in the substrate, in the presence of a basic nucleophile, the substitution could take place via the elimination - addition mechanism (Scheme 7).

Scheme 7



In this mechanism, the proton and the leaving group are eliminated initially and then the addition of the NuH to the intermediate leads to the substituted product. Depending on the position of the proton, the first step of the reaction involves either α, β - β, β - or β, γ - elimination.

The α, β - elimination - addition route which involves an acetylene intermediate is the most common one. This is similar to the benzyne mechanism in nucleophilic aromatic substitution. Alternatively, if there is an activated hydrogen on the γ - carbon, then β, γ - elimination could take place resulting in an allene intermediate. Then attack of the nucleophile on the central carbon atom would lead to the overall substitution. The β, β - elimination route which involves a carbene intermediate is observed only in special cases (46). In the elimination - addition mechanism, there will be no relation between the configuration of the starting material and that of product as both *cis* and *trans* isomers give the same acetylenic intermediate.

(iii) Substitution with primary rearrangement.

In a suitable system, migration of the double bond takes place in the presence of a basic nucleophile. This migration places the leaving group either in an allylic position, or in a vinylic position at which the attack of the nucleophile becomes easier than it was in the original substrate. Substitution followed by another double bond

migration gives the final product.

(iv) S_N1 type reaction.

The S_N1 type reaction can take place when there are powerful electron donating substituents present in the olefin to stabilize the intermediate carbocation. This mechanism has been reviewed by Stang and Rappoport (47).

(v) Substitution involving a vinylic carbanion.

A vinylic carbanion is formed as the intermediate when the nucleophile attacks the leaving group instead of vinylic carbon atom.

In addition to the above discussed mechanisms, a single electron transfer (SET) process in the attack step could also be considered as one of the possible mechanistic routes. This process is considered to be one of the mechanistic routes in nucleophilic aromatic substitution and designated as $S_{RN}1$ mechanism. The involvement of such SET processes in classical organic reactions has been investigated extensively during last 25 years, and evidence has been presented for the involvement of an SET step in many organic reactions which were previously considered to proceed via polar pathways (48-51). Therefore, it becomes necessary to consider this mechanism for nucleophilic substitution on vinylic carbon atom.

In fact, a mechanism with an SET process has been considered as one of the competing routes for the reaction of 2,2-bis(4-nitrophenyl)-1-bromo-1-chloroethylene and 9-(bromochloromethylene)fluorene with thiolate anion (52).

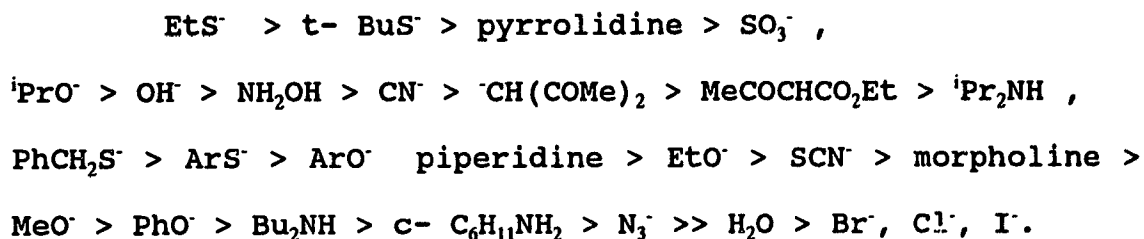
1.5 Literature survey of nucleophilic vinylic substitution.

Since the late fifties the kinetics and mechanism of nucleophilic vinylic substitution have been an interesting subject for physical-organic chemists. A considerable amount of work has been done on the nucleophilic attack on olefins by varying the nucleophile, leaving group, activating group and solvents. These investigations led to the study of nucleophilic addition (32), elimination (34), rearrangement, degradation of the double bond (29-31) and also substitution. Rappoport and co-workers have continued to contribute to this subject since 1962. Bernasconi and co-workers have also studied numerous different systems all of which involve nucleophilic attack on olefins, since 1978. Their recent work involves the study of transition state imbalances and the application of the Principle of Nonperfect Synchronization for nucleophilic addition reactions (53-55). Comprehensive reviews on nucleophilic vinylic substitution are available (25-28).

In most of the systems reported, nucleophilic

vinyllic substitution takes place through an addition - elimination mechanism and most of them involve a carbanionic intermediate. In addition to kinetic measurements, other methods such as stereochemistry of the product (52), element effect (56,57) product distribution (58) and linear free energy relationships have also been used to investigate the mechanism. Although many systems show the common addition - elimination mechanism, the rate-determining step varies from one system to another. In some systems nucleophilic attack is the rate determining step, while in others leaving group expulsion becomes rate determining (59).

For most of the systems studied by Rappoport and co-workers, nucleophilic attack is the rate determining step. The following qualitative nucleophilicity scale has been suggested for reactions in which nucleophilic attack is the rate determining step (22).

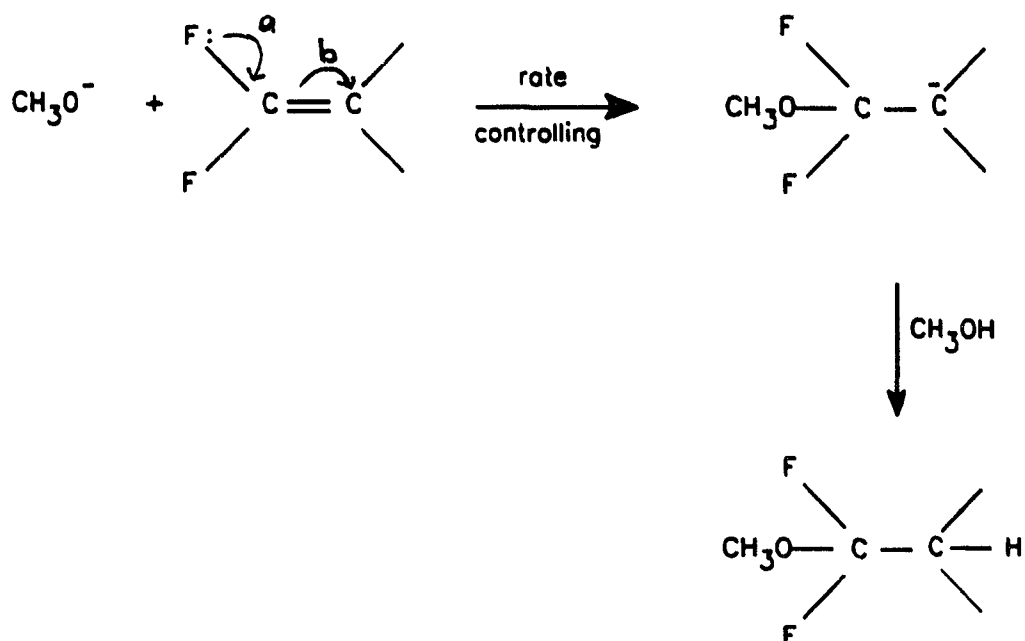


Nucleophilic vinyllic substitution has also received some attention from theoretical chemists. In a recent theoretical study, the energies associated with the attack

phase and the expulsion phase have been calculated. This calculation supports and explains some of the experimentally observed results (60).

As might be predicted from the electronegativity of fluorine, the replacement of H by F in ethylene diminishes the electron density on the double bond and hence facilitates the attack of nucleophiles. Nucleophilic reactions of perfluoro- and chlorofluoroolefins containing two to four carbon atoms in the molecule have been reported in numerous publications. The reaction of fluoroolefins with various nucleophiles have been collected in a review by Chambers and Mobbs (61). A considerable number of publications which describe nucleophilic addition to fluoroolefins began with a patent by Hanford and Rigby (62) which describes the addition of various alcohols to tetrafluoroethylene and of ethanol to chlorotrifluoroethylene and 1-chloro-2,2-difluoroethylene using the corresponding alkoxides or KCN as catalyst. Following this patent, base-catalysed addition of methanol to these compounds and to 1,1-dichloro-2,2-difluoroethylene (63) was shown to occur.

In the above experiments, specific addition was observed with these α,α -difluoroethylenes to give products in which the nucleophile becomes attached to the difluoromethylene part of the molecule. The authors postulated the following mechanism for the reaction.



They also observed that trichlorofluoroethylene reacts readily with methanol at 0°C whereas tetrachloroethylene does not react at all at this temperature. They suggest that the role of fluorine relative to chlorine in promoting addition of nucleophilic reagents and effecting the orientation is due to fluorine's greater tendency to enter into resonance with the double bond. This effect predisposes the double bond to polar activation as indicated by the arrow 'b' in the diagram above. Fluorine differs from other activating groups such as $-\text{CN}$, $-\text{NO}_2$, etc., in directing the nucleophile. This observation is also supported by theoretical studies (60).

These reactions give the corresponding saturated ethers as major or sole products. Small amounts of

unsaturated ethers, formed by replacement of the vinylic fluorine by the nucleophile, were obtained occasionally. The tendency to form unsaturated ethers in the reaction with perfluoroisobutene seems to increase with the basicity of the alkoxy anions. That is, the tendency increases in the order of $\text{EtO}^- < {}^n\text{PrO}^- < {}^i\text{PrO}^- < {}^t\text{BuO}^-$. The reactions of alcohols with branched higher perfluoroolefins gave unsaturated ethers exclusively, regardless of the nature of the nucleophile (64). 1-(2-Tetrahydrofuryl)-pentafluoropropene also seems to react with alkoxide to give unsaturated ethers as the major product (65).

Following Miller's (63) suggestion, J.D.Park and his coworkers explained the displacement of vinylic halogens by alkoxides in both cyclic and acyclic systems in terms of carbanionic intermediates (66). In the later fifties, Miller's group studied the reactions of various nucleophiles with acyclic fluoroolefins and concluded that, depending on the structure of the olefin, such reactions could result in addition to form saturated products, direct substitution of vinylic halogen or displacement of allylic halogen accompanied by rearrangement (67-70). In 1966, Park and coworkers suggested a set of rules (which is known as Park's carbanionic theory) for the nucleophilic vinylic displacement on the basis of their results on the reaction between ethoxide and a variety of halogenated cyclobutenes (71). The rules are;

(1) Nucleophilic displacement reactions of olefins, which are highly substituted with electron withdrawing substituents, may best be considered as proceeding through a carbanion intermediate.

(11) Usually, a nucleophile will attack the carbon atom leading to the carbanion best stabilized by an α -substituent.

(111) If either position of nucleophilic attack leads to carbanions with equivalent stabilization by α -substituents, the effect of β -substituents and steric interaction will prevail.

(1V) The relative importance of the β -effect diminishes with increasing stabilization by either α - or β -effects.

(V) Carbanions which are adequately stabilized are discrete intermediates with no knowledge of their origin. That is, loss of a substituent may occur from either β -carbon atom, irrespective of whether it was vinylic or allylic in the reacting olefin.

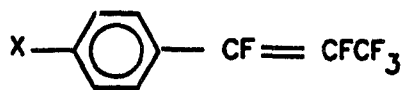
(V1) The less basic the β -substituent is, the better it is as a leaving group. Hence, the order of leaving group from the carbanion is: $I > Br > Cl > F > OR > H$.

(V11) Fluorine will not be lost from a geminal difluoro group if there is another β -halogen which can leave.

(V111) If a choice must be made between two equivalent leaving moieties, loss will occur so as to give the more stable olefin.

Although unsaturated ethers arising from the displacement of fluoride from cyclic fluoroolefins were common, such products from acyclic fluoroolefins were obtained only when the olefin was branched (71). In 1970, it was found by Koch and his coworkers that the reactions of $\text{PhCR}=\text{CF}_2$, where $\text{R} = -\text{F}$, $-\text{CF}_3$, and $-\text{CF}_2\text{Cl}$, with ethoxide in ethanol all give vinyl ethers as one of the products (72). Later, they studied the rate and Arrhenius parameters as well as the product distribution for the above reactions (73). In this reaction, the initially formed carbanion adduct partitions into the vinylic substitution product and the protonated adduct to give the saturated ether.

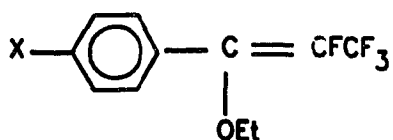
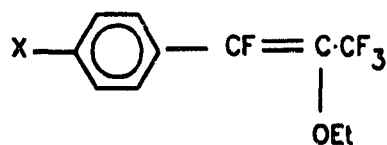
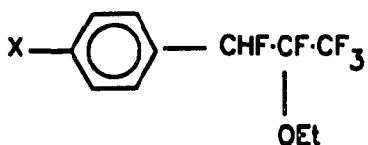
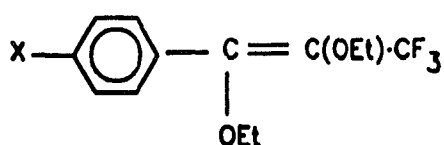
In 1982, Dmowski (58) found that the reaction of 1-phenylpentafluoropropene and its *para* substituted derivatives 7 with ethanolic sodium ethoxide gave predominantly substitution products with only a little formation of adducts.



7

$\text{X} = \text{CH}_3\text{O}-, \text{CH}_3-, \text{H}, \text{Cl}$ and CF_3

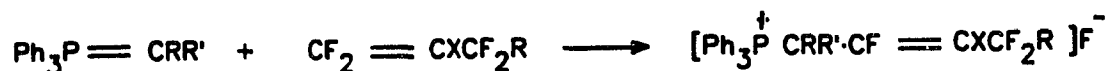
These compounds seem to be susceptible to nucleophilic attack at both vinylic carbons C-1 and C-2. This should be due to the presence of a fluorine atom on both carbons. As a result, he obtained 1-ethoxy-1-phenyltetrafluoropropenes **8** and 2-ethoxy-1-phenyltetrafluoropropenes **9** with a small amount of the addition product 2-ethoxy-1,1,1,2,3-pentafluoro-3-phenylpropanes **10** and the disubstituted product 1,2-diethoxy-1-phenyltrifluoropropenes **11**.

**8****9****10****11**

From the product distribution and on the assumption that the attack of the nucleophile on the olefin is the rate

determining step, he showed that the logarithm of the ratio of the rate constants for the attack at C-1 and C-2 is linearly related to the σ_p constant. That is, the overall regioselectivity of nucleophilic attack of the ethoxide ion on these alkenes exhibits a Hammett type correlation with σ_p .

All the above discussed experiments concern the reaction between fluoroolefins and alkoxide ions. In 1981, the reaction of fluoroolefins with stabilized carbon nucleophiles was studied by Shaw and coworkers (74). Reactions of phosphorous ylides with fluoroolefins gave an initial phosphonium salt via an addition-elimination process. Again, the point of attack by the ylides was exclusively at the terminal difluoromethylene carbon. Hydrolysis of the initially formed phosphonium salt gives the mixture of diene, olefin and allene.



The reaction of lithium dimethylcuprate with 1-fluoro-2-phenylethylene and 1-fluoro-2-phenylsulphonyl ethylene leads to the product of methyl-substitution. A concerted mechanism for the former substrate and an addition-elimination mechanism for the latter substrate has been

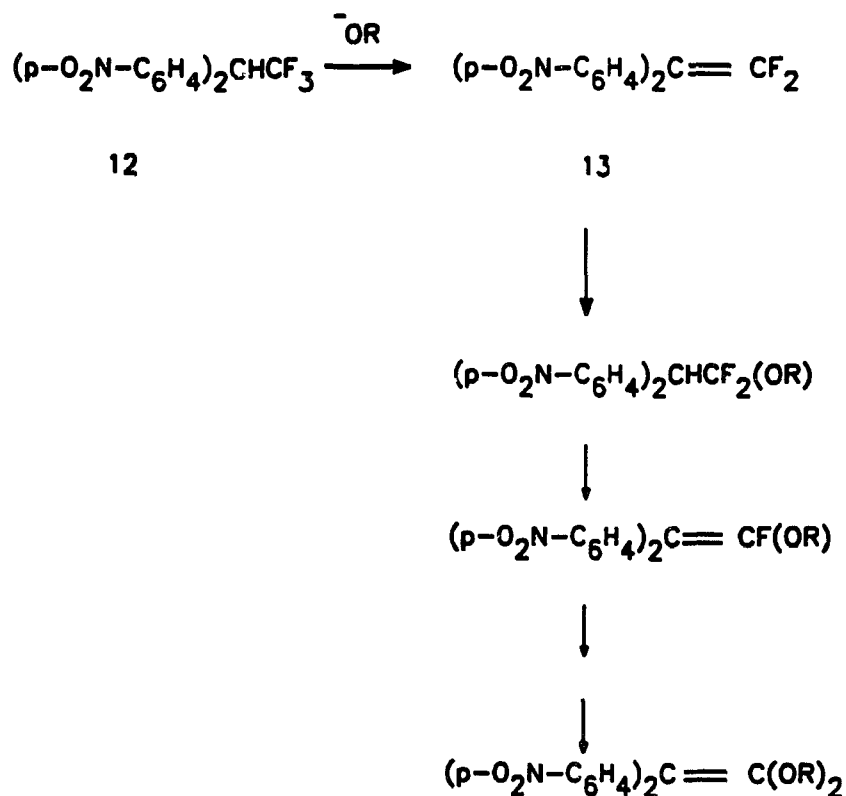
proposed (75).

Tetrafluoroethylene reacts with cyanide, phenoxide, methylmercaptide and azide ions and gives the corresponding carbanions. These carbanions were captured by CO_2 (76).

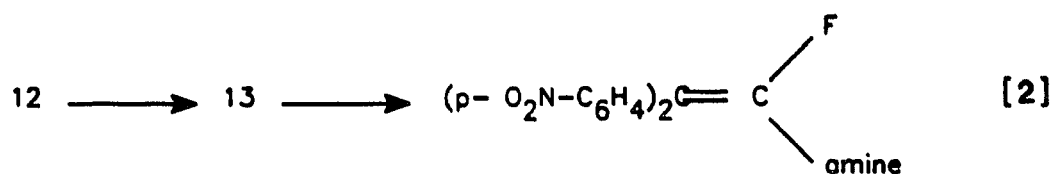
1.6 Scope of our present study.

In a kinetic study of the reaction between 2,2-di(4-nitrophenyl)-1,1,1-trifluoroethane (12) and alkoxide bases in alcohols as solvents conducted in our laboratory. 2,2-di(4-nitro-phenyl)-1-alkoxy-1-fluoroethylenes and 2,2-di(4-nitrophenyl)-1,1-dialkoxyethylenes were obtained as final products, instead of the expected 2,2-di(4-nitrophenyl)-1,1-difluoro-ethylene (13) (77). It was shown that these products were formed from the initial elimination product 2,2-di(4-nitrophenyl)-1,1-difluoroethylene by the attack of alkoxide anions (Scheme 8). The reaction between the olefin and the alkoxide anion seems to go via the addition-elimination mechanism of the type b (Scheme 5).

Scheme 8



In an attempt to study the β -elimination reaction of 2,2-di(4-nitrophenyl)-1,1,1-trifluoroethane (12) promoted by piperidine and pyrrolidine bases, 2,2-di(4-nitrophenyl)-1-fluoro-1-piperidinoethylene and 2,2-di(4-nitrophenyl)-1-fluoro-1-pyrrolidinoethylene were obtained as the final products as shown in equation [2] (78). These products also proved to be formed from the initial elimination product 2,2-di(4-nitrophenyl)-1,1-difluoroethylene. The reaction was first order with respect to the amine.



The reaction of 1,1-dicyanoolefin with various amines had been studied by Rappoport (7, 56, 59) and his co-workers. They found the reaction to go via the most common addition-elimination route in which the nucleophilic attack was the rate-determining step in most of the systems they investigated. They also observed that the reaction involved both amine-catalysed and uncatalysed routes. The relative importance of catalysed and uncatalysed routes depends on the leaving group and the nucleophile.

Amine catalysis in nucleophilic aromatic substitution is a well-known phenomenon. The most accepted mechanism in these systems involves base-catalysed proton transfer from the dipolar intermediate formed by the initial attack of the amine (79, 80). A similar mechanism for a vinylic system has been proposed by Rappoport. Amine catalysis was also observed in the addition reaction of amines to trans-(2-furyl)nitroethylene (81 - 83).

Recently, the kinetics and the mechanism of the reaction of 2,2-di(4-nitrophenyl)-1,1-difluoroethylene with these amines was studied in our laboratory (84). It was found

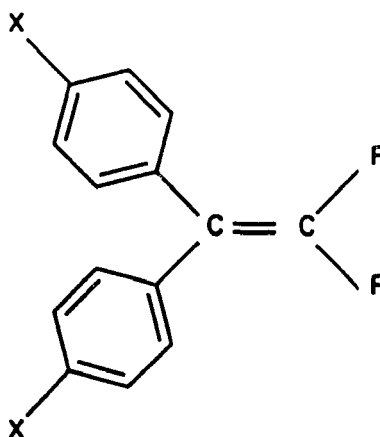
that the reaction proceeds via both amine catalysed and uncatalysed routes. The second order and the third order rate coefficients were obtained for these reactions.

In order to obtain more mechanistic information, the effect of the substituents in the aromatic ring on the reaction mechanism, and also the effect of basicity of the amine have been studied in our present work.

Data on such Hammett type relationships for various combinations of nucleophile and activated olefin have been collected by Rappoport and Ladkani (85). Although ten of the fortyfive reaction series listed in this paper were substitution reactions, the aryl group was not attached directly to the vinylic carbon. The reaction involves substitution by different nucleophiles on *cis* and *trans* $\text{ArSO}_2\text{CH} = \text{CHCl}$.

The Hammett type correlation was established between σ and the rate constants. The reaction constants reported for these reaction ranges from 1.21 to 1.85. Among these ten reaction series five contain only three different substituents on the aryl group making the ρ values unreliable.

In our present study, the *para* substituted analogs, 14 - 17, of 1,1-difluoro-2,2-diphenylethylene have been synthesized and their reactions with amines in acetonitrile have been studied.



14. X = H

16. X = CF₃

15. X = Br

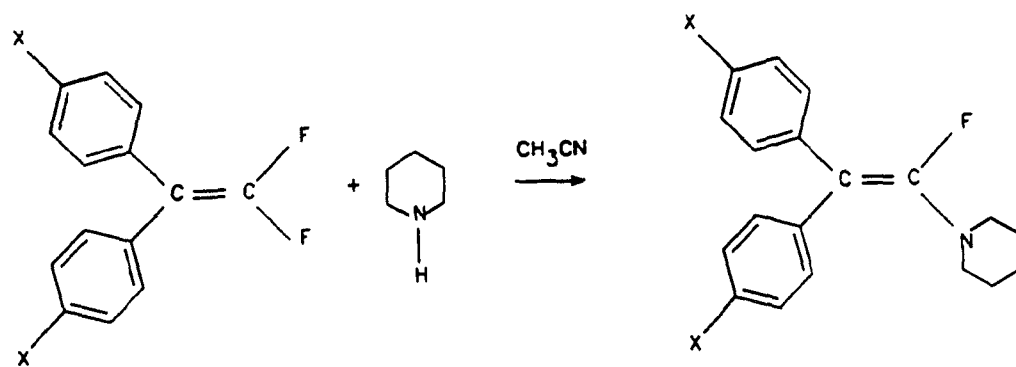
17. X = CN

Scheme 9 shows the three different systems that have been investigated in this work. In the first system, substrates with different substituents in the *para* positions of 1,1-difluoro-2,2-diphenylethylene have been used. The reaction of these substrates with piperidine in acetonitrile was investigated.

In the second system, the reaction of 1,1-difluoro-2,2-di-(4-cyanophenyl)ethylene with different amines was studied, and in the third one, the reaction of 1,1-difluoro-2,2-di(4-cyanophenyl)ethylene with piperidine catalysed by tertiary amines with different base strengths was studied.

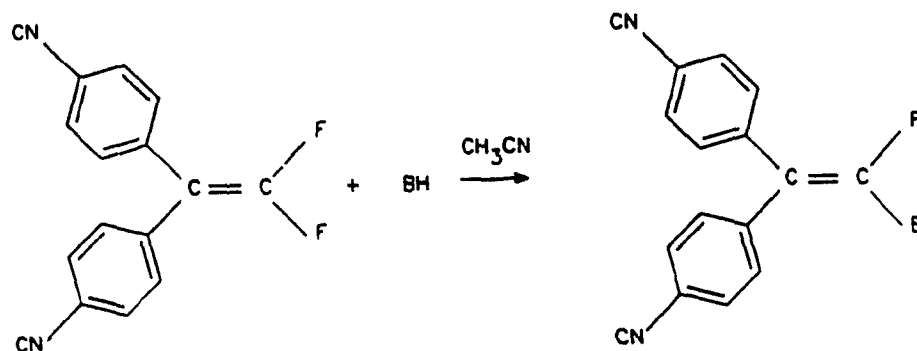
Scheme 9

System 1



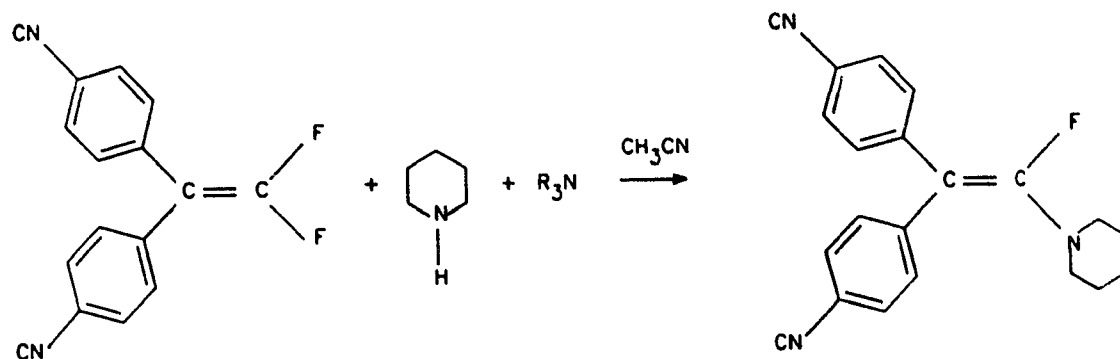
For X = H, Br, CN, CF_3 and NO_2 .

System 2



For BH = pyrrolidine, piperidine, morpholine, thiomorpholine, 1,2,3,4-tetrahydroisoquinoline, 1,1,3,3-tetramethylguanidine (TMG), and n-propylamine.

System 3

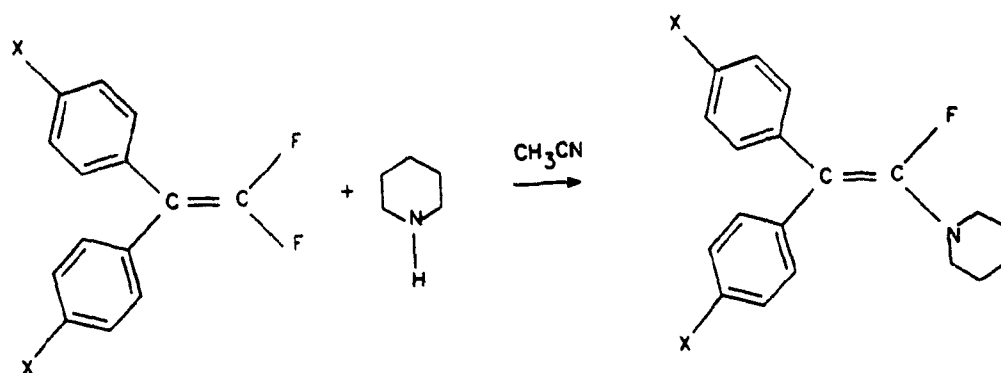


For R_3N = N-methylpyrrolidine, N-methylpiperidine, N-methylmorpholine, 1,3-diphenylguanidine and DBU.

**2. Kinetics and Mechanism of the Reaction of Phenyl
Substituted 1,1-Difluoro-2,2-diphenylethylene with
Piperidine in acetonitrile as solvent.**

phenyl ring, the *para* substituted analogs, 14 - 17, of 1,1-difluoro-2,2-diphenylethylene have been synthesized and their reaction with amines in acetonitrile (System 1) studied.

System 1.



For X = H, Br, CN, CF₃ and NO₂.

2.2. A preliminary qualitative study of the reaction of *para*-substituted 1,1-difluoro-2,2-diphenylethylene with piperidine.

In a preliminary study, the reaction of 1,1-difluoro-2,2-diphenylethylene, 14, with amines in acetonitrile was followed spectrophotometrically. The UV - visible spectrum of the substrate as well as the reaction mixture were recorded between 190 and 500nm. The substrate

showed λ_{\max} at 237nm. Neither the reaction spectrum nor the TLC analysis showed detectable product with morpholine, methoxyethylamine, propylamine, isobutylamine, benzylamine and cyclohexylamine at room temperature (25°C) and 50°C, at a substrate concentration of 9.5×10^{-3} mol.L⁻¹. The concentration of amines was kept about 9.5×10^{-1} mol.L⁻¹.

In the case of piperidine the reaction spectrum (Figure 1(a)) showed a peak at about $\lambda \sim 286$ nm a few hours after mixing. The absorbance at this wavelength increases with time. After 24 hours at 50°C, a shoulder was observed with this peak and the absorbance at 286nm began to decrease. As this absorbance continued to decrease, the shoulder moved towards longer wavelength. After 70 hours a sharp peak was observed at $\lambda = 328$ nm (Figure 1(b)), and the absorbance at this wavelength increased with time while λ_{\max} remained approximately the same. This indicates that the reaction leads to two products, one which absorbs at about 286nm (P_1), and a second one (P_2), which absorbs at 328nm in a consecutive manner (equation [3]). As the reaction proceeds, the ratio $[P_1]/[P_2]$ varies and this variation causes the observed changes in the reaction spectra. It also indicates that the formation of the second product is much slower than that of the first one which allows us to study the formation of the first product without interference by the subsequent reaction.



$$\lambda_{\text{max}} = 237 \text{ nm.}$$

$$\lambda_{\text{max}} \sim 286 \text{ nm.}$$

$$\lambda_{\text{max}} = 328 \text{ nm.}$$

The extinction coefficient of the final product (P_2) was comparable to that of the substrate. The bathochromic shift in λ_{max} indicates the presence of an extended conjugation in the product.

Figure 1(a): (1) The UV-Vis. spectrum of 1,1-difluoro-2,2-diphenylethylene in acetonitrile [$8.97 \times 10^{-3} \text{M}$] and (2) - (6) the UV-Vis spectra of the reaction mixture of 1,1-difluoro-2,2-diphenylethylene and piperidine [$9 \times 10^{-1} \text{M}$] in acetonitrile at different time after mixing. (2) 1.5 hrs, (3) 2.5 hrs, (4) 3.5 hrs, (5) 4.5 hrs and (6) 25 hrs.

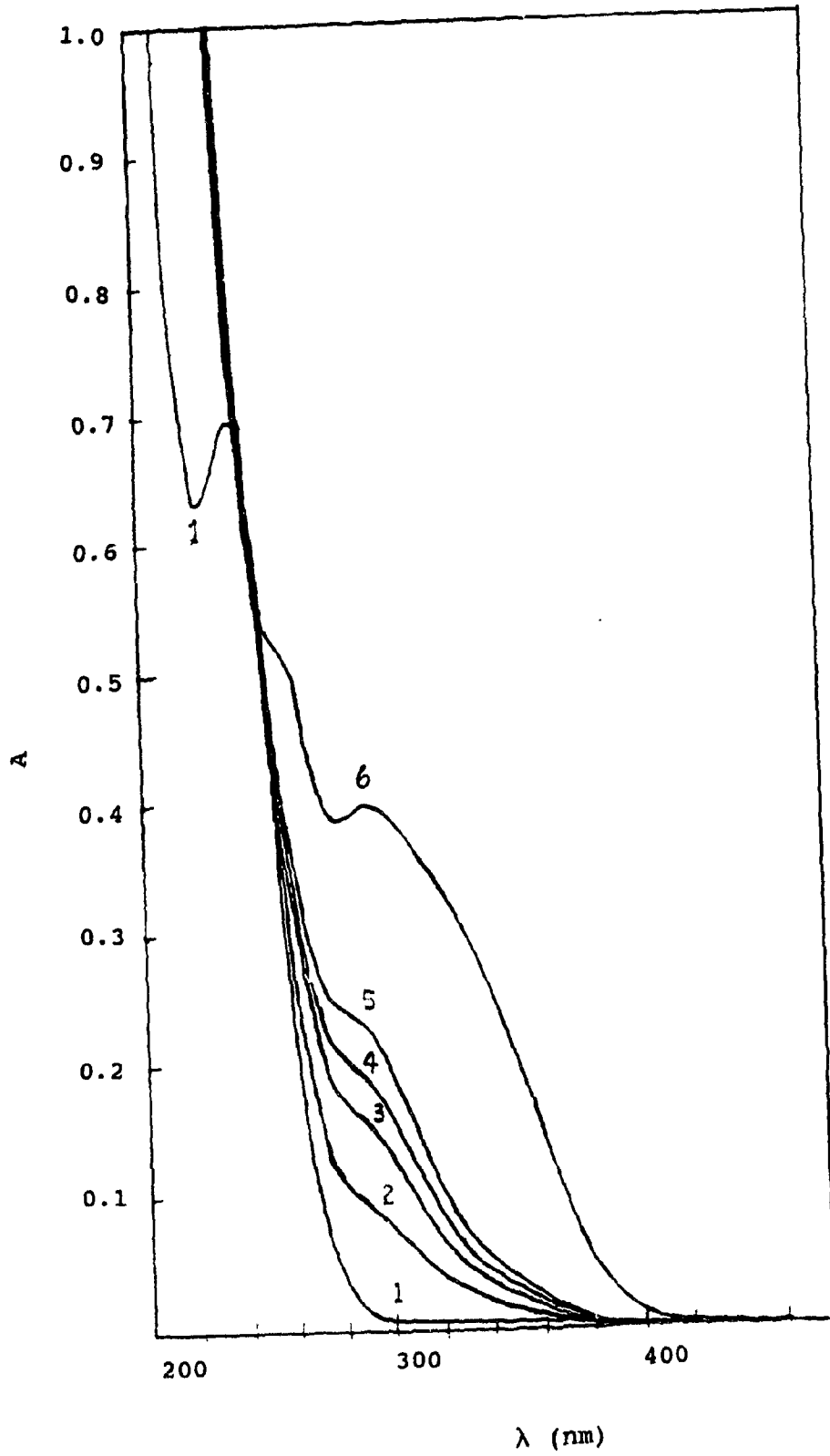


Figure 1(a)

Figure 1(b): (1) The UV-Vis. spectrum of 1,1-difluoro-2,2-diphenylethylene in acetonitrile [$8.97 \times 10^{-3}M$] and (6) - (12) the UV-Vis spectra of the reaction mixture of 1,1-difluoro-2,2-diphenylethylene and piperidine [$9 \times 10^{-1} M$] in acetonitrile at different time after mixing (ie, continuation of figure 1(a)). (6) 25 hrs, (7) 27 hrs, (8) 48 hrs, (9) 70 hrs, (10) 92 hrs, (11) 145hrs and (12)165 hrs.

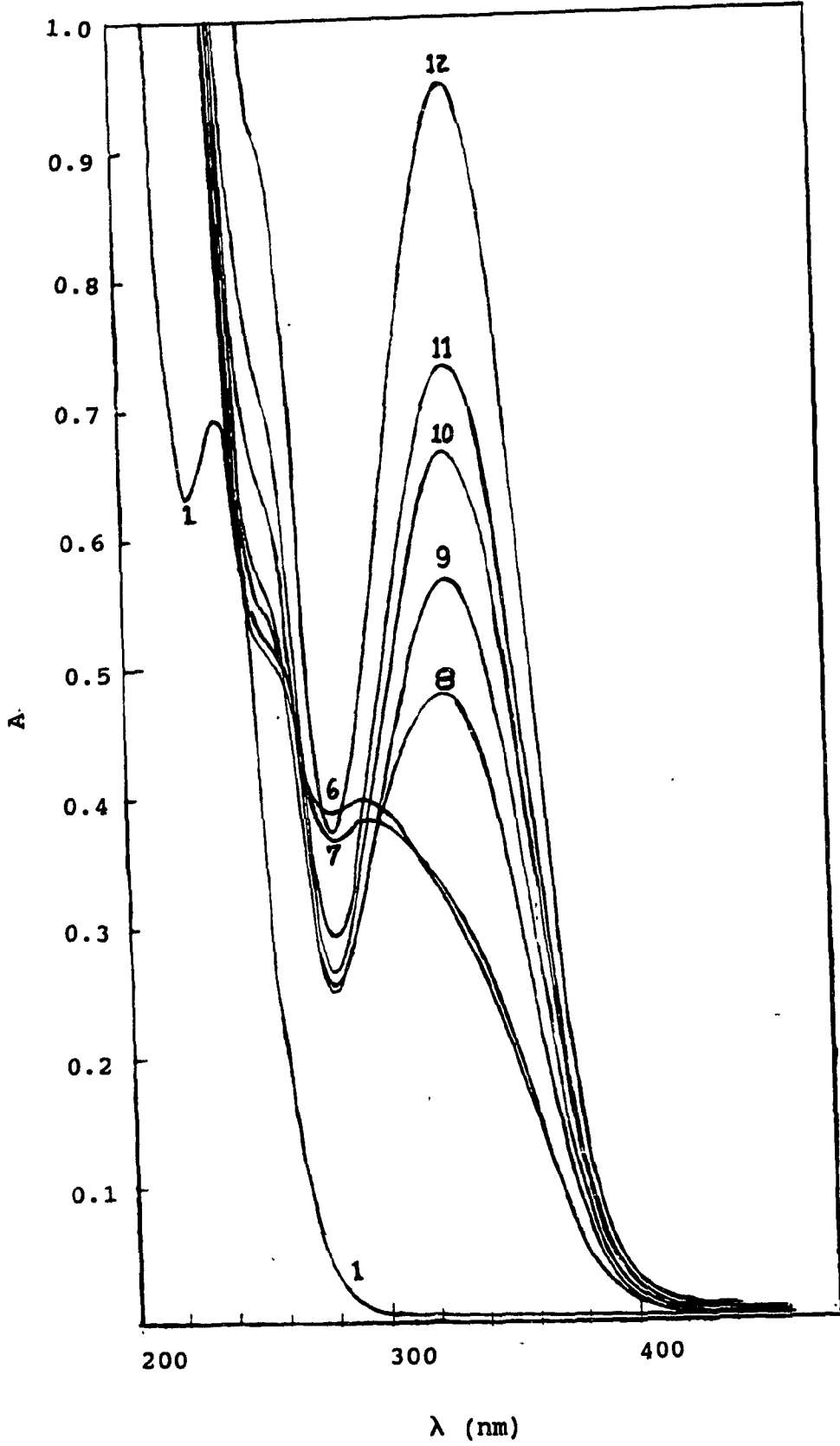


Figure 1(b)

Considering the possible products from the reaction, together with the spectral properties, the structure of the final product (P_2), could be assigned as either 1-fluoro-1-piperidino-2,2-diphenylethylene or 1,1-dipiperidino-2,2-diphenylethylene.

After separation from the reaction mixture, the mass spectral analysis of the product which absorbs at 328nm (P_2) shows a molecular peak at m/z ratio 346 together with the M + 1 isotopic peak of intensity 27.79% of that molecular ion peak. The recorded molecular peak fits the molecular weight of 1,1-dipiperidino-2,2-diphenylethylene 19. The relative intensity of M+1 isotopic peak also agrees with the number of carbon atoms in 19. Therefore, the product P_2 is assigned as 1,1-diphenyl-2,2-dipiperidinoethylene 19.

The $^1\text{H-NMR}$ of P_2 shows signals at δ 7.50 (t), 7.41 (t), 7.21 (d), 3.65 (t), 1.42 (m) and 1.26 (m). This is in agreement with the proposed structure of P_2 . Due to the interference of the solvents that were used for the chromatographic separation of the compound, the relative intensity of these peaks were not obtained.

The similar bathochromic shift in both steps of the reaction (equation [3]) suggests that the structural change in each step is similar. This suggests that the product which absorbs at 286nm is 1-fluoro-1-piperidino-2,2-diphenylethylene 18. That is, the reaction follows Scheme 11. Such disubstitution has also been reported for the reaction of

Figure 2: (1) The UV-Vis. spectra of 1,1-difluoro-2,2-di(4-bromophenyl)ethylene [$4.55 \times 10^{-5} \text{M}$] and the reaction mixture of 1,1-difluoro-2,2-di(4-bromophenyl)ethylene and piperidine [$5 \times 10^{-3} \text{M}$] in acetonitrile at different time after mixing. (2) 2.5 hrs, (3) 24 hrs, (4) 28.5 hrs and (5) 72 hrs.

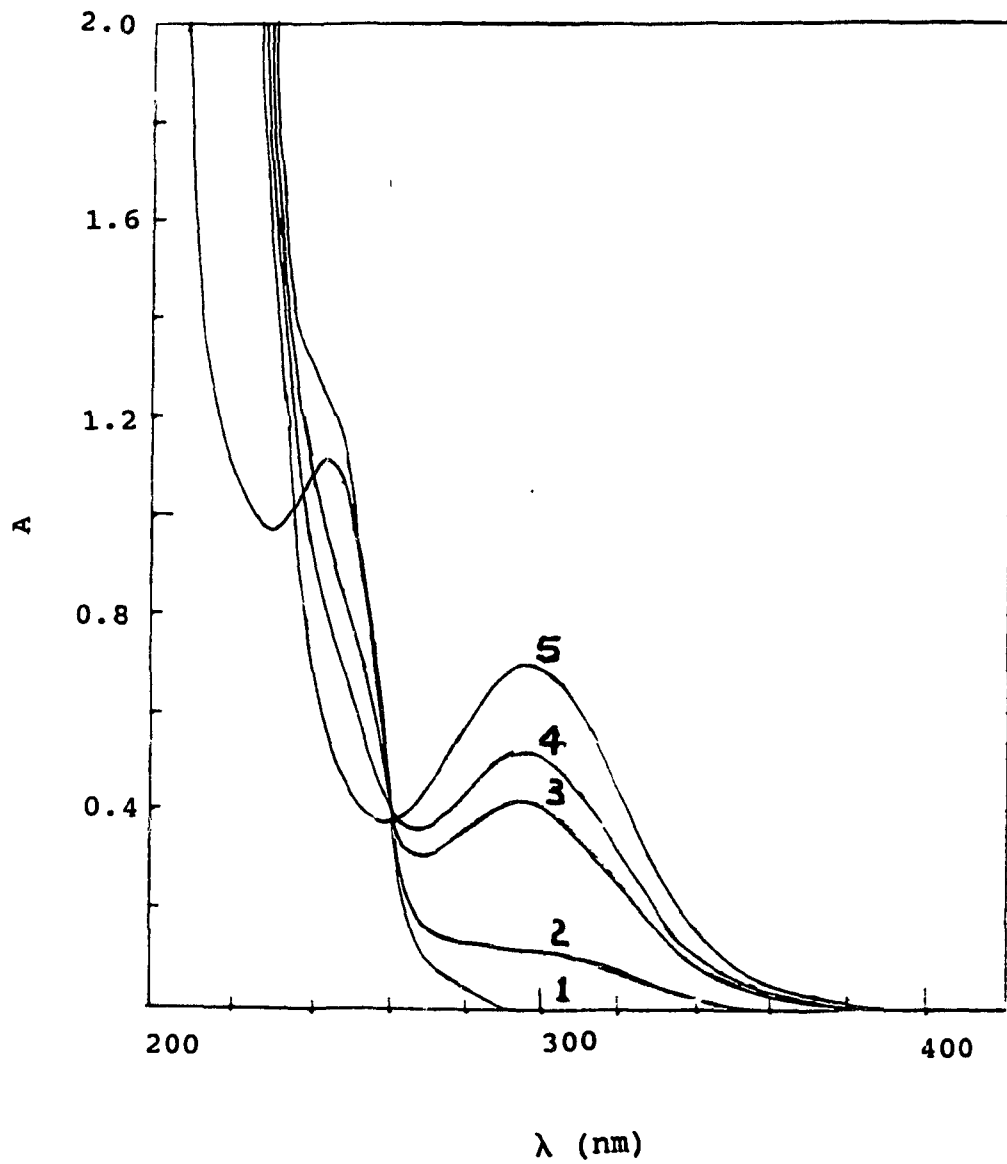


Figure 2

Figure 3: (1) The UV-Vis. spectra of 1,1-difluoro-2,2-di(4-trifluoromethylphenyl)ethylene [$5.6 \times 10^{-5} \text{M}$] and the reaction mixture of 1,1-difluoro-2,2-di(4-trifluoromethylphenyl)ethylene and piperidine [$6 \times 10^{-3} \text{M}$] in acetonitrile at different time after mixing. (2) 5 min., (3) 25 min, (4) 45 min, (5) 1 hr (6) 1.5 hrs, (7) 2.5 hrs (8) 3.5 hrs and (9) 20 hrs .

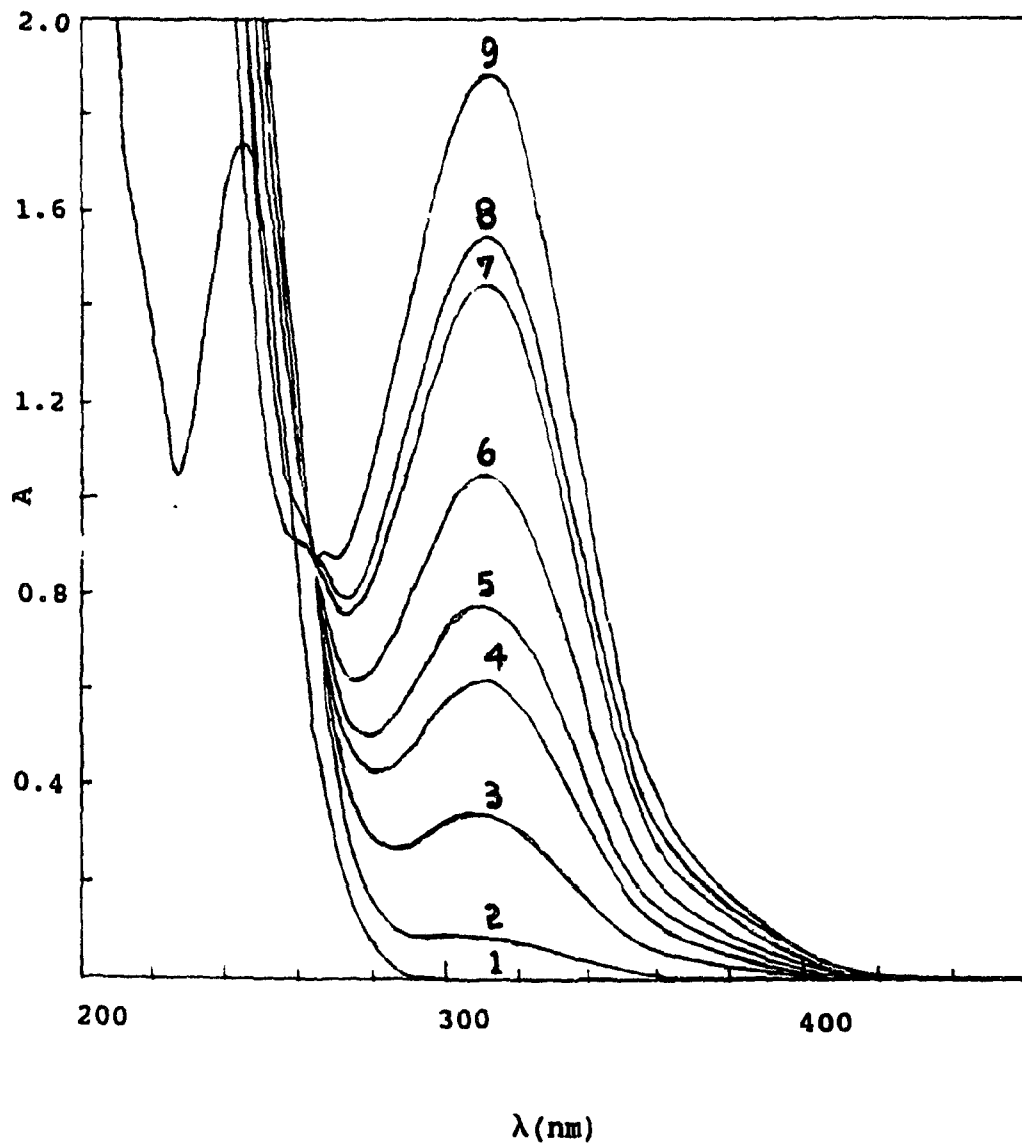


Figure 3

Figure 4: (1) The UV-Vis. spectra of 1,1-difluoro-2,2-di(4-cyanophenyl)ethylene [$8.97 \times 10^{-5} \text{M}$] and the reaction mixture of 1,1-difluoro-2,2-di(4-cyanophenyl)ethylene and piperidine [$9 \times 10^{-3} \text{M}$] in acetonitrile at different time after mixing. (2) 15 min, (3) 30 min, (4) 50 min, (5) 1 hr, (6) 2 hrs, (7) 3 hrs and (8) 22hrs.

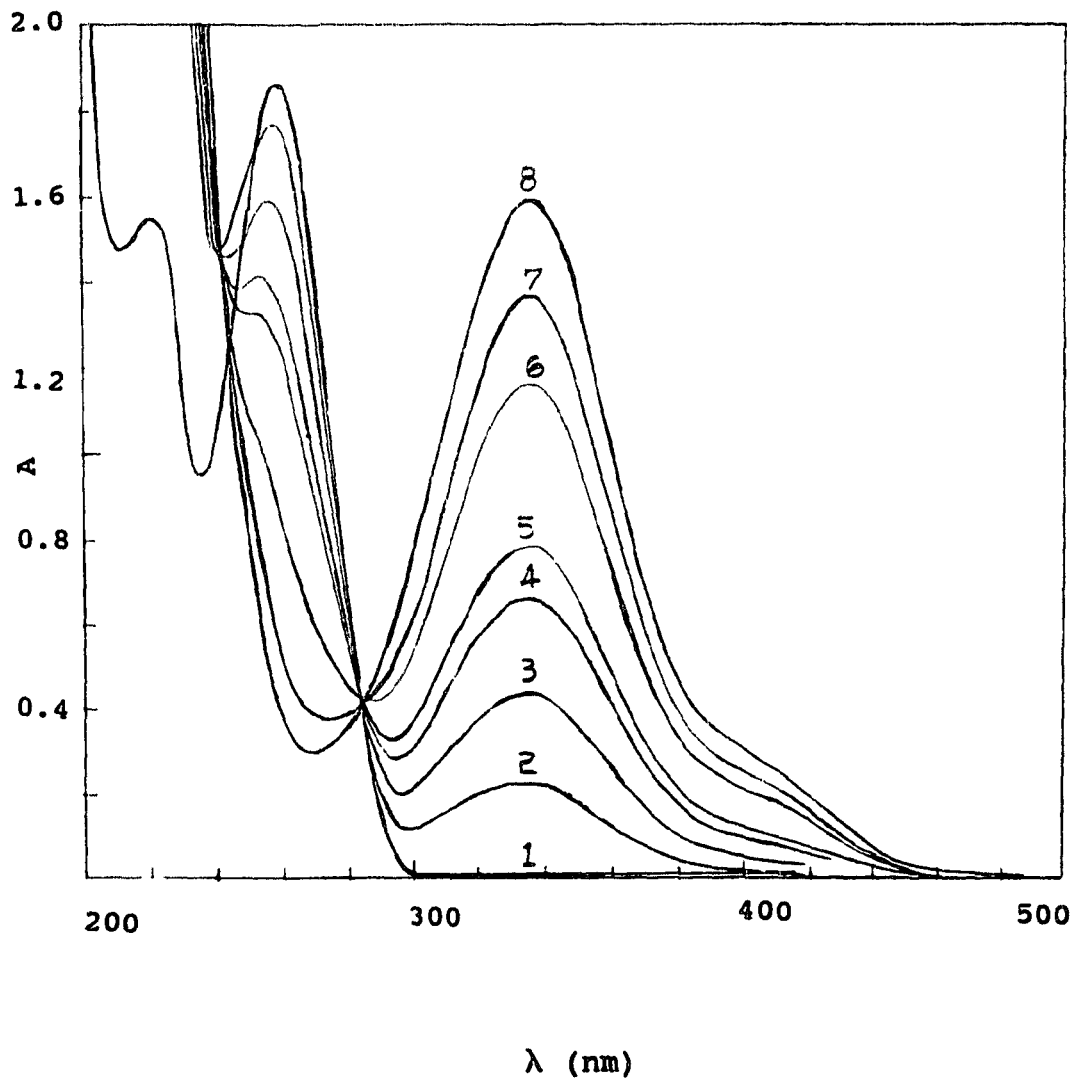


Figure 4

Table 1

The λ_{\max} of $(p\text{-XC}_6\text{H}_4)_2\text{C} = \text{CF}_2$ and that of mono piperidinoethylene.

X	λ_{\max} of substrate(nm)	λ_{\max} of product(nm)
H	237	286
Br	244	295
CF ₃	244	310
CN	259	336
*NO ₂	296	400

* obtained from reference (84).

2.3 Kinetics of the reaction of *para*-substituted 1,1-difluoro-2,2-diphenylethylene with piperidine.

The kinetics of the reaction of 1,1-difluoro-2,2-diphenylethylene and its *para*-substituted analogs with piperidine were studied spectrophotometrically by monitoring the formation of the monoamino products at the λ_{max} of the corresponding product. The reactions were carried out in presence of a large excess of base so that pseudo first-order rate constants were obtained. The pseudo first-order rate constants were calculated using the Guggenheim method (90).

The observed pseudo first-order rate constants at five different temperatures and a range of concentrations of piperidine for each substrate are tabulated in Tables 2 to 5, together with their standard deviations. These rate constants are plotted as a function of base concentrations in Figures 5 to 8.

Table 2

Pseudo first-order rate constants for the reaction of 1,1-difluoro-2,2-diphenylethylene* with piperidine in acetonitrile to give 1-fluoro-1-piperidino-2,2-diphenylethylene .

Temp. (°C)	$10^5 \times k_{1,obs.} (s^{-1})$				
	50	55	60	65	70
[pip] x 10 (mol.l ⁻¹)					
3.03	0.84 ± 0.03	1.28 ± 0.02	1.75 ± 0.05	2.37 ± 0.05	2.88 ± 0.07
4.04	1.19 ± 0.01	2.11 ± 0.03	2.50 ± 0.17	3.43 ± 0.06	4.06 ± 0.04
5.05	1.96 ± 0.07	2.68 ± 0.05	3.43 ± 0.24	4.42 ± 0.14	5.13 ± 0.08
6.06	2.72 ± 0.07	3.67 ± 0.07	4.53 ± 0.24	5.54 ± 0.08	6.43 ± 0.23
7.07	3.51 ± 0.07	4.26 ± 0.06	5.50 ± 0.15	6.41 ± 0.13	8.11 ± 0.41

* initial concentration = $(4 \times 10^{-3} \text{ mol.l}^{-1})$

Table 3

Pseudo first-order rate constants for the reaction of 1,1-difluoro-2,2-di(4-bromophenyl)-ethylene* with piperidine in acetonitrile to give 1-fluoro-1-piperidino-2,2-di(4-bromophenyl)ethylene.

Temp. (°C)	$k_{\text{obs}} \times 10^5 \text{ (s}^{-1}\text{)}$				
	25	30	35	40	45
[pip] $\times 10^2 \text{ (mol.l}^{-1}\text{)}$					
2.50					0.50 ± 0.01
3.75					1.00 ± 0.01
5.00					1.63 ± 0.01
5.20	1.09 ± 0.01				
6.00		1.60 ± 0.01	1.79 ± 0.01	2.00 ± 0.02	
6.25					2.46 ± 0.01
7.50					3.37 ± 0.02
7.81	2.34 ± 0.01				

continued

table 3 continued

Temp. (°C)	$k_{1\text{obs}} \times 10^5 \text{ (s}^{-1}\text{)}$				
	25	30	35	40	45
[pip] $\times 10^2$					
9.00		3.54 ± 0.03	3.84 ± 0.02	4.26 ± 0.01	
10.4	** 3.73 ± 0.01				
12.0		6.02 ± 0.02	6.76 ± 0.02	7.34 ± 0.02	
13.0	6.24 ± 0.02				
15.0		9.17 ± 0.03	10.3 ± 0.01	11.1 ± 0.04	
15.6	9.14 ± 0.03				
18.0		13.2 ± 0.1	14.5 ± 0.04	15.9 ± 0.1	

* initial concentration = $1.07 \times 10^{-4} \text{ mol.l}^{-1}$.

** not used for the calculation of k_2° and k_3

Table 4

Pseudo-first-order rate constants for the reaction of 1,1-difluoro-2,2-di- (4-trifluoromethylphenyl)ethylene* with piperidine in acetonitrile to give 1-fluoro-1-piperidino-2,2-di(p-trifluoromethylphenyl)ethylene.

Temp. (°C)	$k_{\text{obs.}} \times 10^5 \text{ (s}^{-1}\text{)}$				
	20	25	30	35	40
[pip] $\times 10^3 \text{ (mol.l}^{-1}\text{)}$					
9.43	1.46 \pm 0.01	1.62 \pm 0.02	1.79 \pm 0.01	1.98 \pm 0.01	2.25 \pm 0.01
14.1	3.06 \pm 0.01	3.31 \pm 0.02	3.77 \pm 0.01	4.17 \pm 0.01	4.52 \pm 0.03
18.9	5.27 \pm 0.01	5.58 \pm 0.04	6.29 \pm 0.02	6.91 \pm 0.01	7.71 \pm 0.02
23.6	8.08 \pm 0.01	8.68 \pm 0.07	9.41 \pm 0.04	10.5 \pm 0.04	11.6 \pm 0.04
28.3	11.5 \pm 0.03	12.4 \pm 0.10	13.8 \pm 0.04	15.2 \pm 0.05	16.4 \pm 0.07

* initial concentration = $7.09 \times 10^{-5} \text{ mol. l}^{-1}$

Table 5

Pseudo-first order rate constants for the reaction of 1,1-difluoro-2,2-di (4-cyano-phenyl)ethylene* with piperidine in acetonitrile to give 1-fluoro-1-piperidino-2,2-di-(4-cyanophenyl)ethylene.

Temp. (°C)	$k_{1,obs.} \times 10^5 \text{ (s}^{-1}\text{)}$				
	15	20	25	32.5	40
[pip] $\times 10^3 \text{ (mol.l}^{-1}\text{)}$					
4.10	**4.03 \pm 0.02	**4.91 \pm 0.02	5.24 \pm 0.04	5.90 \pm 0.04	6.92 \pm 0.08
6.15	7.93 \pm 0.04	9.07 \pm 0.03	9.71 \pm 0.04	11.6 \pm 0.10	13.7 \pm 0.10
8.20	13.0 \pm 0.10	15.1 \pm 0.10	16.6 \pm 0.10	20.3 \pm 0.10	22.1 \pm 0.10
10.3	20.6 \pm 0.10	23.0 \pm 0.10	24.4 \pm 0.10	29.0 \pm 0.20	32.5 \pm 0.10
12.3	27.8 \pm 0.20	31.8 \pm 0.20	35.2 \pm 0.20	40.2 \pm 0.50	44.3 \pm 0.30

* initial concentration = $5.25 \times 10^{-5} \text{ mol.l}^{-1}$.

** not used for the calculation of k_2° and k_3

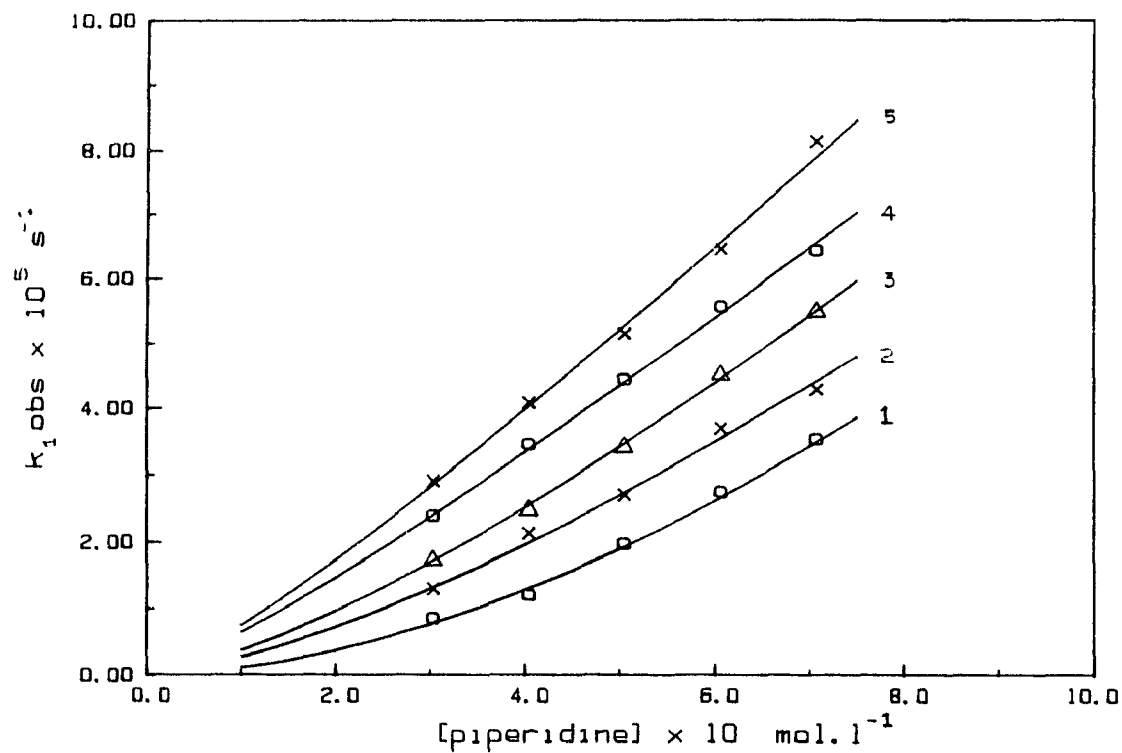


Figure 5: k_1 obs vs [piperidine] plot for the reaction of 1,1-difluoro-2,2-diphenylethylene with piperidine in acetonitrile at different temperatures. (1) 50, (2) 55, (3) 60, (4) 65 and (5) 70°C.

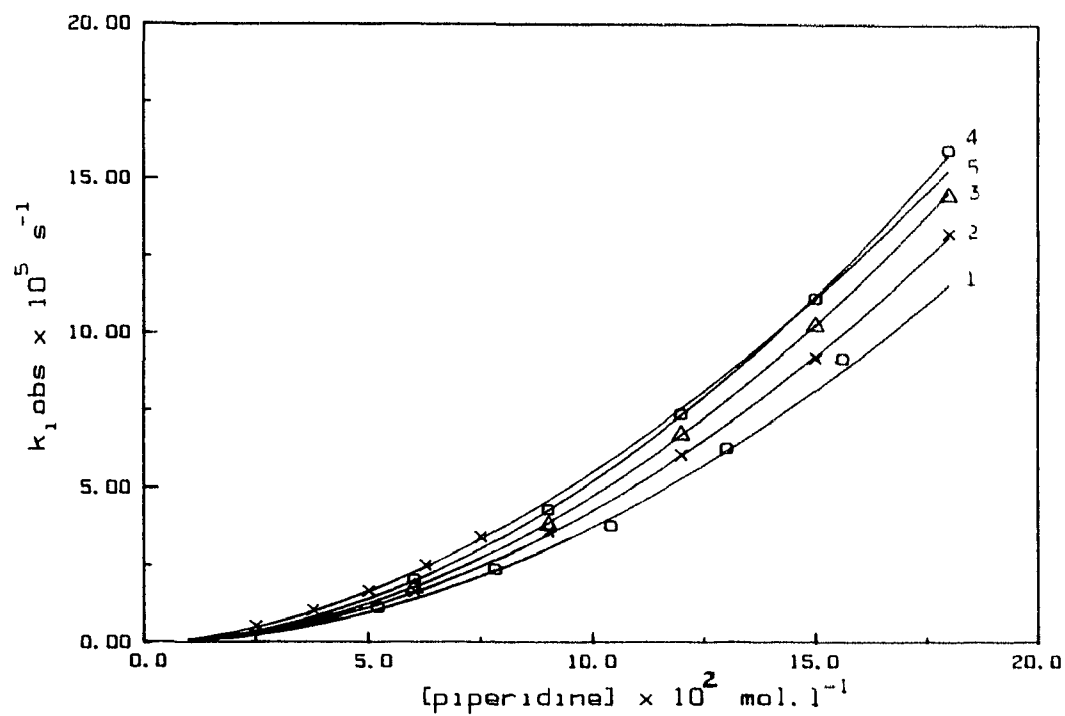


Figure 6: k_1 obs vs [piperidine] plot for the reaction of 1,1-difluoro-2,2-di(4-bromophenyl)ethylene with piperidine in acetonitrile at different temperatures. (1) 25, (2) 30, (3) 35, (4) 40 and (5) 45°C.

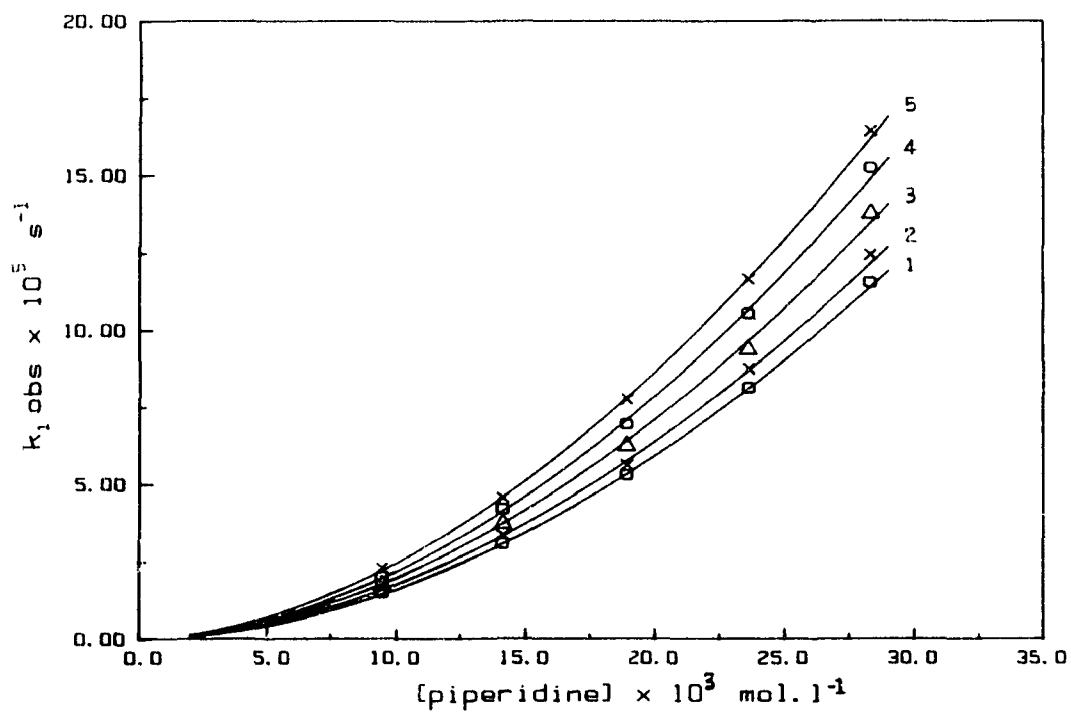


Figure 7: $k_1 \text{ obs}$ vs [piperidine] plot for the reaction of 1,1-difluoro-2,2-di(4-trifluoromethylphenyl)ethylene with piperidine in acetonitrile at different temperatures. (1) 20, (2) 25, (3) 30, (4) 35 and (5) 40°C.

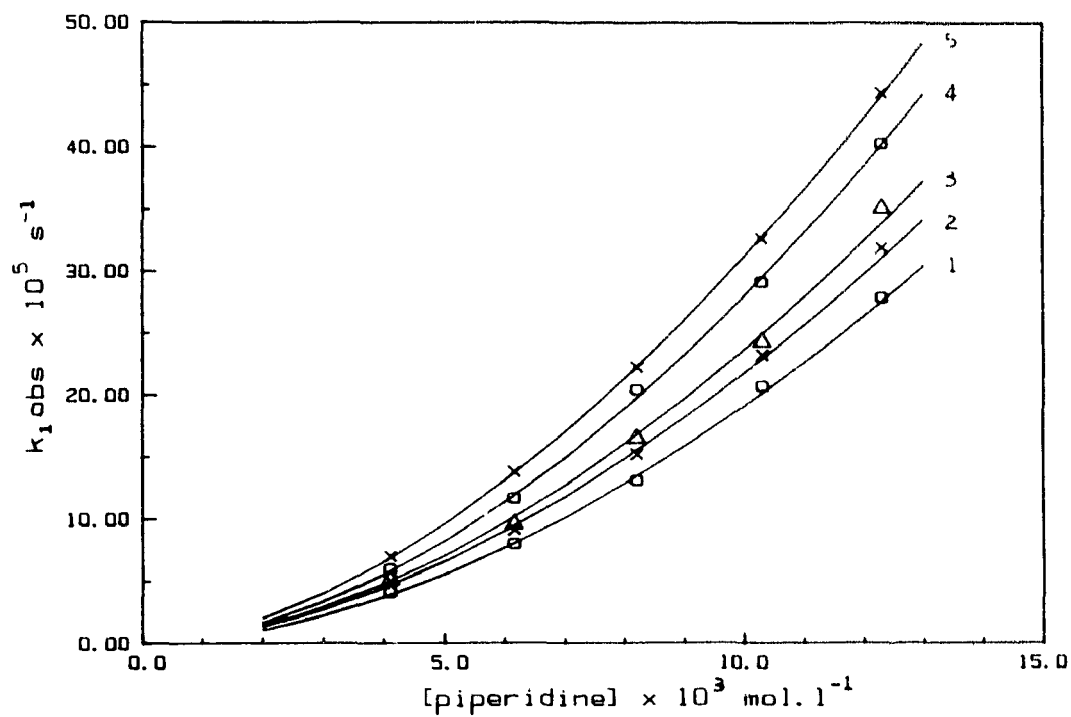


Figure 8: k_1 obs vs [piperidine] plot for the reaction of 1,1-difluoro-2,2-di(4-cyanophenyl)ethylene with piperidine in acetonitrile at different temperatures. (1) 15, (2) 20, (3) 25, (4) 32.5 and (5) 40°C.

The $k_{1,obs}$. vs. [piperidine] plot is not linear as would be expected if the reaction is first order with respect to amine. Instead, it is a curve (Figures 5-8) giving a linear relationship between $k_{1,obs}/[\text{piperidine}]$ and [piperidine]. The results were fitted (Figures 9-12) to equation [4].

$$k_{2,obs} = k_2^\circ + k_3[\text{piperidine}] \quad [4]$$

where, $k_{2,obs} = k_{1,obs}/[\text{piperidine}]$.

This indicates that the reaction takes place by two different mechanisms which operate simultaneously, one of which is second order with respect to amine (the amine catalysed route) and the other one is first order with respect to amine (the uncatalysed route). This result is similar to that obtained by Rappoport in the case of cyanoethylene (7,52 & 55). The least squares intercept and the slope of the plot (Figures 9 to 12) give the rate coefficients k_2° and k_3 respectively, where k_2° is the rate coefficient for the uncatalysed route and k_3 is the rate coefficient for the catalysed route. Calculated values of these rate coefficients at different temperatures and their standard deviations are listed in Tables 6 to 9. The activation parameters for these reactions are given in Table 10 together with their standard deviations.

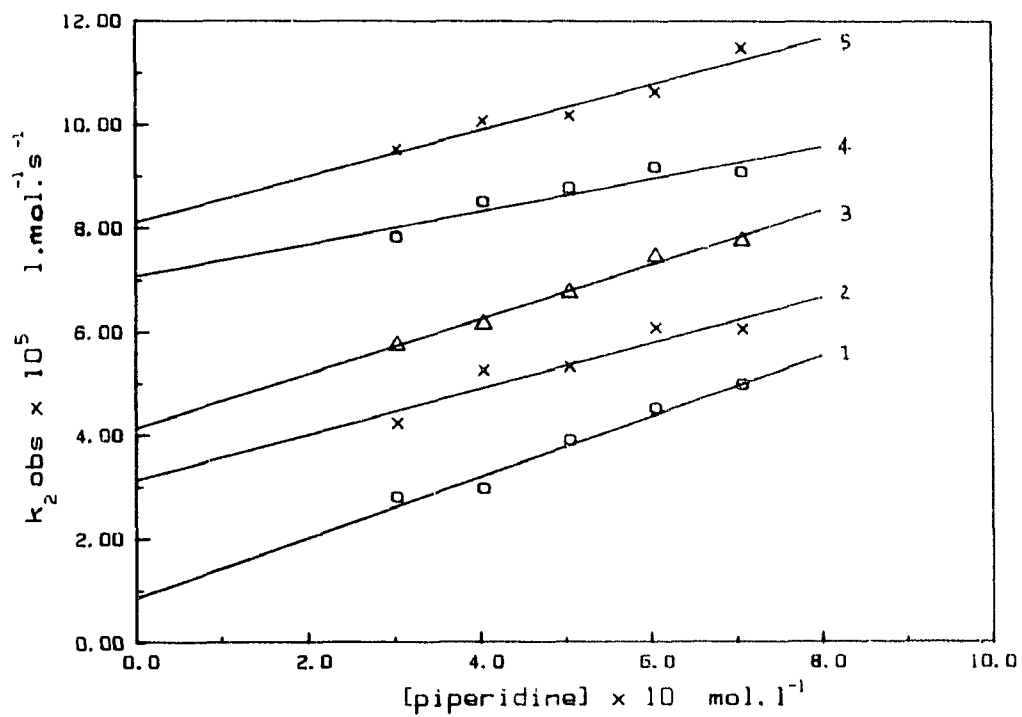


Figure 9: k_2 obs vs [piperidine] plot for the reaction of 1,1-difluoro-2,2-diphenylethylene with piperidine in acetonitrile at different temperatures. (1) 50, (2) 55, (3) 60, (4) 65 and (5) 70°C.

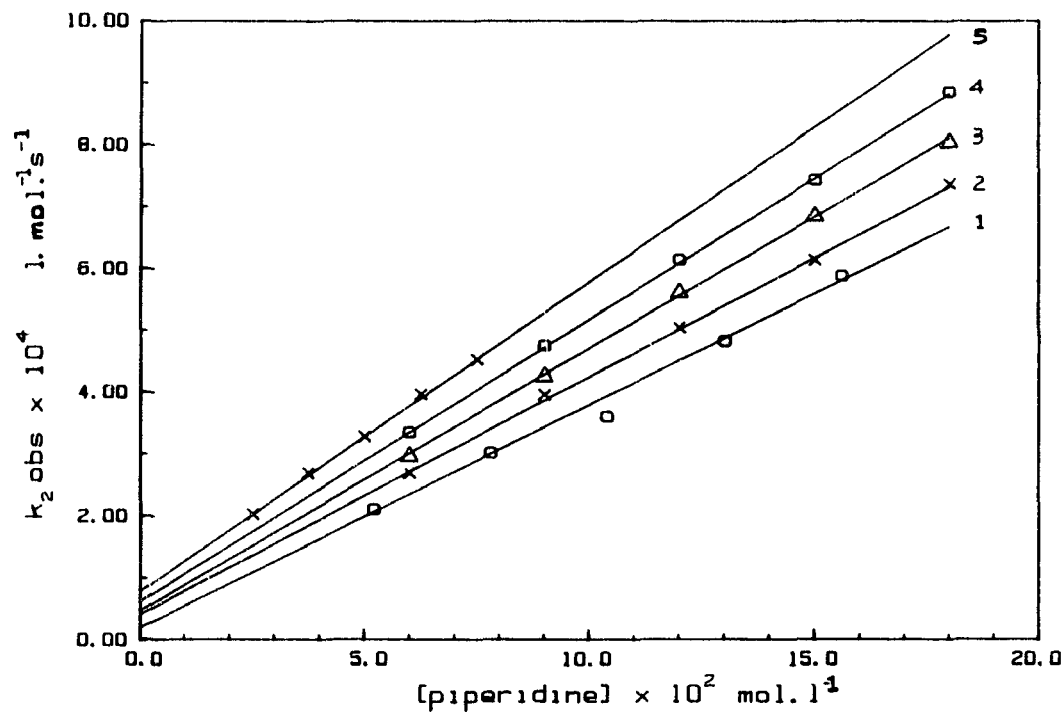


Figure 10: k_2 obs vs [piperidine] plot for the reaction of 1,1-difluoro-2,2-di(4-bromophenyl)ethylene with piperidine in acetonitrile at different temperatures. (1) 25, (2) 30, (3) 35, (4) 40 and (5) 45°C.

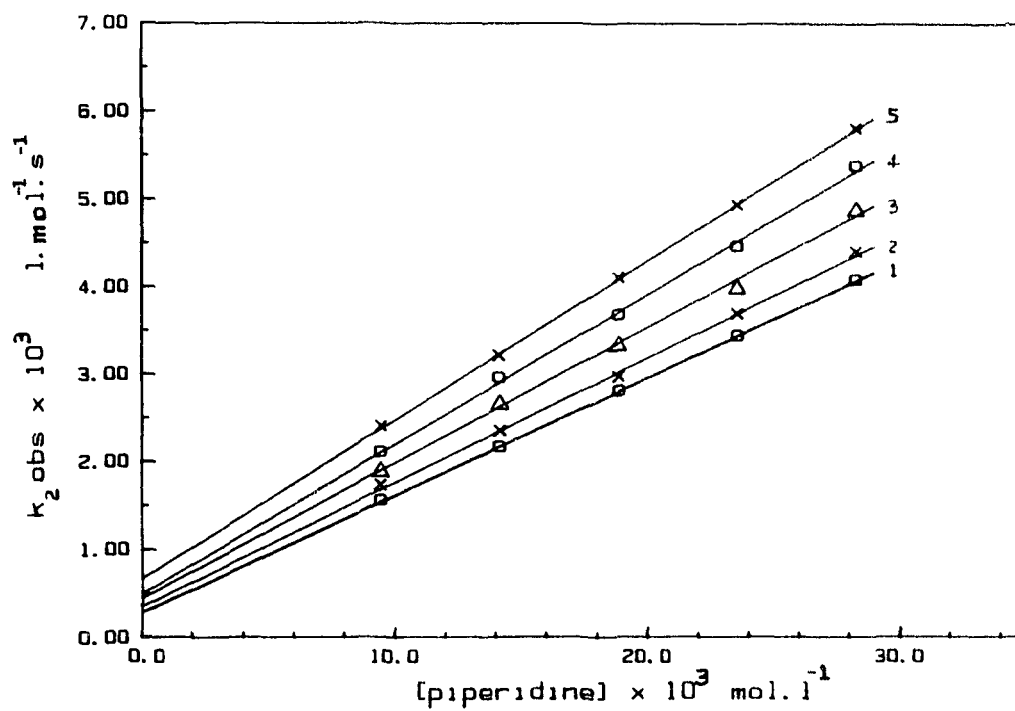


Figure 11: k_2 obs vs [piperidine] plot for the reaction of 1,1-difluoro-2,2-di(4-trifluoromethylphenyl)ethylene with piperidine in acetonitrile at different temperatures. (1) 20, (2) 25, (3) 30, (4) 35 and (5) 40°C.

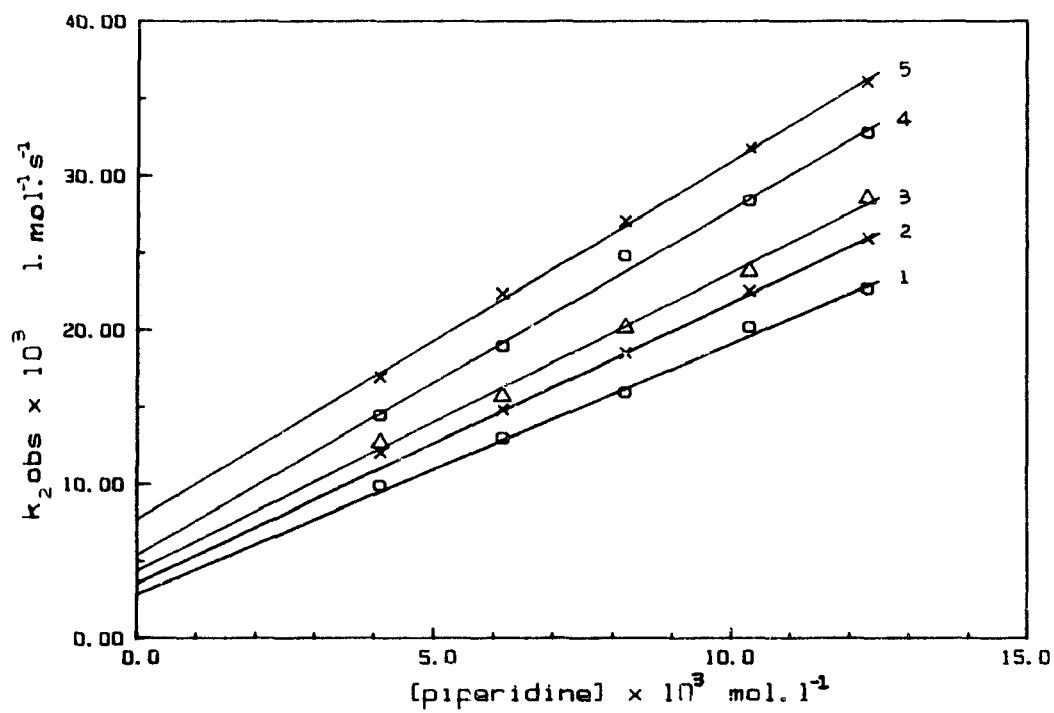


Figure 12: k_2, obs vs [piperidine] plot for the reaction of 1,1-difluoro-2,2-di(4-cyanophenyl)ethylene with piperidine in acetonitrile at different temperatures. (1) 15, (2) 20, (3) 25, (4) 32.5 and (5) 40°C.

Table 6

Calculated second-order and third-order rate constants (k_2^0 and k_3 , respectively) for the reaction of 1,1-difluoro-2,2-diphenylethylene with piperidine to give 1-fluoro-1-piperidino-2,2-diphenylethylene.

Temp (°C)	$k_2^0 \times 10^5$ (l.mol ⁻¹ .s ⁻¹)	$k_3 \times 10^5$ (l ² .mol ⁻² .s ⁻¹)	k_3/k_2^0
50	0.86 ± 0.31	5.86 ± 0.59	6.8
55	3.13 ± 0.50	4.49 ± 0.96	1.4
60	4.14 ± 0.18	5.26 ± 0.34	1.3
65	7.07 ± 0.38	3.13 ± 0.72	0.4
70	8.12 ± 0.36	4.44 ± 0.69	0.5

Table 7

Calculated second-order and third-order rate constants (k_2° and k_3 , respectively) for the reaction of 1,1-difluoro-2,2-di(4-bromophenyl)ethylene with piperidine to give 1-fluoro-1-piperidino-2,2-di(4-bromophenyl)ethylene.

Temp. (° C)	$k_2^\circ \times 10^5$ ($l.mol^{-1}.s^{-1}$)	$k_3 \times 10^3$ ($l^2.mol^{-2}.s^{-1}$)	k_3 / k_2°
25	2.07 ± 0.90	3.58 ± 0.08	173
30	4.11 ± 0.79	3.83 ± 0.06	93
35	4.67 ± 0.81	4.24 ± 0.06	91
40	6.20 ± 0.55	4.55 ± 0.04	73
45	7.86 ± 0.41	4.99 ± 0.07	63

Table 8

Calculated second-order and third-order rate constants (k_2° and k_3 , respectively) for the reaction of 1,1-difluoro-2,2-di(4-trifluoromethylphenyl)ethylene with piperidine in acetonitrile to give 1-fluoro-1-piperidino-2,2-di(4-trifluoromethylphenyl)ethylene.

Temp. (°C)	$k_2^\circ \times 10^4$ ($l.mol^{-1}.s^{-1}$)	$k_3 \times 10$ ($l^2.mol^{-2}.s^{-1}$)	k_3 / k_2°
20	2.79 ± 0.11	1.34 ± 0.01	480
25	3.47 ± 0.60	1.42 ± 0.03	409
30	4.39 ± 0.93	1.55 ± 0.05	353
35	4.89 ± 0.80	1.71 ± 0.04	350
40	6.59 ± 0.30	1.81 ± 0.01	275

Table 9

Calculated second-order and third-order rate constants (k_2° and k_3 , respectively) for the reaction of 1,1-difluoro-2,2-di(4-cyanophenyl)ethylene with piperidine to give 1-fluoro-1-piperidino-2,2-di(4-cyanophenyl)ethylene.

Temp. (°C)	$k_2^\circ \times 10^3$ ($l \cdot mol^{-1} \cdot s^{-1}$)	k_3 ($l^2 \cdot mol^{-2} \cdot s^{-1}$)	k_3 / k_2°
15	2.85 ± 1.05	1.63 ± 0.11	572
20	3.56 ± 0.37	1.82 ± 0.04	511
25	4.34 ± 0.66	1.94 ± 0.08	447
32.5	5.39 ± 0.84	2.24 ± 0.10	416
40	7.68 ± 0.46	2.32 ± 0.05	302

Table 10

The activation parameters for the amine catalysed and uncatalysed reactions of $(p\text{-XC}_6\text{H}_4)_2\text{C} = \text{CF}_2$ with piperidine in acetonitrile.

X	Act. parameters for uncatalysed reaction		Act. parameters for catalysed reaction	
	ΔH^\ddagger (kJ.mol ⁻¹)	ΔS^\ddagger (J.mol ⁻¹ .K ⁻¹)	ΔH^\ddagger (kJ.mol ⁻¹)	ΔS^\ddagger (J.mol ⁻¹ .K ⁻¹)
H	96 ± 20	-43 ± 61	-20 ± 13	-387 ± 38
Br	46 ± 8	-178 ± 25	11 ± 0.4	-256 ± 2
CN	26 ± 1	-202 ± 5	8 ± 1	-211 ± 4
CF ₃	29 ± 3	-214 ± 8	10 ± 1	-229 ± 2
^o NO ₂	16 ± 3	-217 ± 10	-9 ± 1	-239 ± 4

* obtained from the reference (84)

From Tables 6 to 9, it can be seen that for all substrates, the ratio between the catalysed and the uncatalysed rate constants, k_3 / k_2° , decreases with temperature. This means that the uncatalysed route becomes more important at high temperatures. This is due to the higher enthalpy of activation for the uncatalysed reaction.

The unsubstituted substrate 14 shows a very low k_3 / k_2° ratio in the temperature range studied. This in turn suggests that the contribution of the catalytic route is very low under these experimental conditions. This, together with the high amine concentration and high temperature used during these kinetic measurements, might have contributed to the large percentage error in the rate constants and the activation parameters for this substrate.

Table 10 shows that the enthalpy of activation for the uncatalysed reaction decreases with increasing electron-withdrawing power of the substituent. The enthalpy of activation for the amine catalysed reaction is almost independent of the nature of the substituent group. It is also rather small, even negative for some substrates. A negative enthalpy of activation for the amine catalysed reaction was also reported by Rappoport (59) and for the reaction of 2,2-di(4-nitrophenyl)-1,1-difluoroethylene (84). The Arrhenius activation energy for the amine catalysed route for the addition reaction of piperidine to trans-(2-furyl)-nitroethylene was also found to be negative (81). These

differences suggest that the temperature dependence of the catalytic rate constant is distinctly different from that of uncatalysed second order rate constant. The negative enthalpy of activation suggests that k_2 is more complex than the rate constant of a single step of the reaction.

The entropies of activation for both the amine catalysed and uncatalysed reactions are large and negative. Large negative entropies of activation have been reported for many reactions which involve formation of dipolar zwitterion (7,56, 55, 81). This must be due to an increase in solvation of the transition state relative to the initial state.

Nucleophilic vinylic substitutions occur by many mechanistic pathways as illustrated in Scheme 5. The absence of vinylic or allylic hydrogens in the substrates studied, eliminates many competing routes such as elimination-addition. If we consider the possible addition - elimination routes for the system studied (Scheme 12), the initial nucleophilic attack of the amine would take place on the carbon atom which carries the fluorine atoms to form the zwitterion, Z^+ . This zwitterion can either revert to the starting material (S), or it can transfer the proton from the positively charged nitrogen atom to another amine molecule to form the carbanion, Z^- , or it can transfer the proton intramolecularly to the carbanionic center to form a neutral α,β - adduct, Z.

Now the substitution product could be formed either from the zwitterion by departure of fluoride ion followed by proton transfer (path (a)), or from the carbanion by expulsion of F^- (path (b)), or from the α,β - adduct by base catalysed β -elimination (path (c)).

Expulsion of fluoride ion from the carbanion should be much easier than from the zwitterion, due to the electrostatic attraction between the negatively charged leaving group and the positively charged nitrogen atom. Since the C - F bond is a strong bond and fluoride ion is a poor leaving group, expulsion of fluoride ion could be the rate determining step in the scheme.

If the assumption that the expulsion of fluoride as the rate determining step is correct, then paths (b) and (c) would show a second-order kinetics with respect to the amine but path (a) would show a first-order kinetics with respect to the amine.

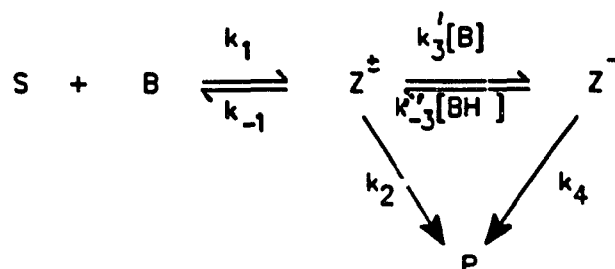
As mentioned earlier, our kinetic results show that the reaction takes place via both amine catalysed and uncatalysed routes. Therefore, it is clear that path (b) or (c) or even both should be considered together with path (a). The only difference between the two amine catalysed paths is that in path (b), the proton is removed from a positively charged nitrogen atom but in path (c), the proton is removed from a saturated carbon atom. Removal of proton in path (b) must be easier than in path (c) at least in the case of the

In this case, the amine catalysis does not take place in an equilibrium step, but in the breaking of the C-F bond step. Since the reaction step must have a positive enthalpy of activation, the catalysed and the uncatalysed route would both show positive enthalpies of activation. However, this is contrary to the experimental results. Furthermore, in the study of the reaction of 2,2-di(4-nitrophenyl)-1,1-difluoroethylene with amines, it was found that the reaction was not catalysed by alkylammonium ion (84). This indicates that the reaction does not take place according to Scheme 13.

The negative enthalpy of activation for the catalysed reaction and a high positive enthalpy of activation for the uncatalysed reaction suggest that the reaction is not catalysed in the third step. It also suggests that an equilibrium step is followed by the rate determining step. The amine acting as the catalyst in the equilibrium step could produce a negative enthalpy of activation for the overall reaction, as will be discussed later in terms of rate equations.

If it is assumed that paths (a) and (b) are operative in the reaction with the rate constants shown in Scheme 14, the rate of appearance of the product can be expressed by equation (5).

Scheme 14



According to Scheme 14,

$$\frac{d[\text{P}]}{dt} = k_2 [\text{Z}^\pm] + k_4 [\text{Z}^-] \quad [5]$$

Application of the steady state approximation to the intermediates Z^\pm and Z^- gives equations [6] and [7].

$$\frac{d[\text{Z}^\pm]}{dt} = k_1 [\text{S}][\text{B}] + k_3^1 [\text{BH}^+][\text{Z}^-] - (k_{-1} + k_2 + k_3^1 [\text{B}])[\text{Z}^\pm] = 0 \quad [6]$$

$$\frac{d[\text{Z}^-]}{dt} = k_3^1 [\text{B}][\text{Z}^\pm] - (k_4 + k_3^1 [\text{BH}^+])[\text{Z}^-] = 0 \quad [7]$$

From equation [7],

$$[\text{Z}^-] = \frac{k_3^1 [\text{B}][\text{Z}^\pm]}{k_4 + k_3^1 [\text{BH}^+]} \quad [8]$$

Substituting this in equation [6],

$$k_1[S][B] + \frac{k_3'[BH^+] k_3'[B][Z^\pm]}{k_4 + k_3'[BH^+]} - (k_1 + k_2 + k_3'[B])[Z^\pm] = 0$$

Therefore,

$$[Z^\pm] = \frac{k_1[S][B]}{(k_1 + k_2 + k_3'[B]) - \frac{k_3'[BH^+] k_3'[B]}{k_4 + k_3'[BH^+]}} \quad [9]$$

Substituting equations [8] and [9] in equation [5] gives equation [10].

$$\frac{d[P]}{dt} = \left\{ k_2 + \frac{k_4 k_3'[B]}{k_4 + k_3'[BH^+]} \right\} \left\{ \frac{k_1[S][B]}{k_1 + k_2 + k_3'[B] - \frac{k_3'k_3'[B][BH^+]}{k_4 + k_3'[BH^+]}} \right\} \quad [10]$$

If fluoride ion expulsion is the rate determining step, that is if $k_3'[BH^+] \gg k_4$ and $k_1 \gg k_2$, then equation [10] can be simplified to equation [11] and $k_{2,obs}$ would be given by equation [12].

$$\frac{d[P]}{dt} = \frac{k_1 k_2[S][B]}{k_1} + \frac{k_1 k_3' k_4[S][B]^2}{k_1 k_3' [BH^+]} \quad [11]$$

$$k_{2,obs} = \frac{k_{1,obs}}{[B]} = \frac{k_1 k_2}{k_1} + \frac{k_1 k_3' k_4[B]}{k_1 k_3'[BH^+]} \quad [12]$$

If $k_4 \gg k_3'[BH^+]$ and $k_1 \gg k_2 + k_3'[B]$, that is if fluoride ion

expulsion is not the rate determining step, then equation [10] can be simplified to equation [13] which gives equation [14] for $k_{2,obs}$.

$$\frac{d[P]}{dt} = \frac{k_1 k_2 [S][B]}{k_{-1}} + \frac{k_1 k_3 [S][B]^2}{k_{-1}} \quad [13]$$

$$k_{2,obs} = \frac{k_{1,obs}}{[B]} = \frac{k_1 k_2}{k_{-1}} + \frac{k_1 k_3 [B]}{k_{-1}} \quad [14]$$

If equation [14] is true then the amine catalysed and uncatalysed rate constants are given by equations [15] and [16] respectively.

$$k_3 = k_1 / k_{-1} k_3' = K_1 k_3' \quad [15]$$

$$k_2^{\circ} = k_1 / k_{-1} k_2 = K_1 k_2 \quad [16]$$

In this case, both catalysed and uncatalysed rate constants depend on the same equilibrium constant K_1 and hence they both should show similar temperature dependence, which is not observed from the kinetic results.

Alternatively, the observed temperature dependence of the catalysed and uncatalysed rate constants could be explained if equation [12] is valid. If equation [12] is true then the catalysed and uncatalysed rate constants are given by equations [17] and [18] respectively.

$$k_3 = (k_1 / k_{-1}) (k_3' / k_{-3}' [BH^+]) k_4 = K_1 K_3 k_4 / [BH^+] \quad [17]$$

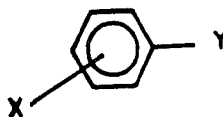
$$k_2^0 = k_1 / k_{-1} k_2 = K_1 k_2 \quad [18]$$

In this case, the catalysed and uncatalysed rate constants could have different temperature dependences if the equilibrium constants K_1 and K_3 have different temperature dependences. Unlike rate constants, it is possible for equilibrium constants to either increase or decrease with increasing temperature. Thus if K_3 decreases with increasing temperature, the catalysed reaction would show a much smaller ΔH^\ddagger than the uncatalysed reaction and it could even be negative.

Therefore, it is concluded that the mechanism of the reaction is that shown in Scheme 14 with fluoride ion expulsion as the rate-determining step.

2.4 The Hammett relationship.

The Hammett relationship is a linear free energy relationship which was introduced by Hammett (91) following the catalysis law proposed by Brønsted and Pederson (92). This relationship is applicable to equilibrium reactions of a series of substituted aromatic compounds. The substituents (X) in the benzene ring influence the reaction that occurs on the side chain (Y).



Hammett derived the relationship between the equilibrium constant (or rate constant) of the substituted compound and that of unsubstituted compound (X=H). The simplest form of the relationship is given by equation [19].

$$\log K = \log K_0 + \sigma\rho \quad [19].$$

where, K and K_0 are the equilibrium constants for a particular equilibrium for substituted and unsubstituted aromatic compounds respectively. σ is the substituent constant and ρ is the reaction constant.

A similar relationship can be applied to rate constants. This equation applies only for *para* and *meta* substituents. Since *ortho* substituents are closer to the reaction site, their influence on the reaction differs from *meta* and *para* substituents in that steric factors may be involved. Dissociation of *meta* and *para* substituted benzoic acids in water at 25°C was considered as the reference reaction for ρ so that it was unity for this series of equilibria.

Therefore, for benzoic acid, equation [19] can be rewritten as equation [20] and [21].

$$\log K = \log K_0 + \sigma \quad [20]$$

$$\log K - \log K_0 = pK_0 - pK = \sigma \quad [21]$$

Where K_0 and K are the dissociation constants of unsubstituted and substituted benzoic acids respectively.

The substituent constants, σ 's, were derived from equation [21]. In addition to these σ values, some other sets of sigma values such as σ^+ , σ^- , σ^0 , σ_1 and σ_R have also been proposed (93-97). These σ values correlate linearly with the logarithm of the equilibrium constants or rate constants of other series of reactions. The slope of the $\log K$ (or $\log k$) vs σ plot varies from one reaction to another. This slope is used as a measure of the sensitivity of the particular

reaction to the substituent effects.

A positive ρ value is found for reactions which are accelerated by electron withdrawing substituents such as $-\text{NO}_2$, $-\text{CHO}$ etc. The Hammett relationship has been applied to a large number of reactions (93-95) since it was introduced and is the most widely investigated linear free energy relationship. The sign and magnitude of ρ gives useful information about the transition state of the reaction considered. Therefore, it is worth while to study such a relationship for the results obtained in System 1.

The catalysed and uncatalysed rate constants for the five substrates at 25°C are collected in Table 11, from which it is clear that the reaction becomes slower when the aromatic ring is substituted with a less powerful electron-withdrawing substituent. Therefore, the reaction would be still slower with electron-donating substituents in the aromatic ring. Therefore, only substrates with electron-withdrawing substituents were chosen for our study. Substituents such as $-\text{COR}$, $-\text{CHO}$ and $-\text{COOR}$ are not suitable because, they could react directly with the nucleophile.

Table 11

The amine catalysed and uncatalysed rate constants (k_2° and k_3 respectively) at 25°C for the reaction of $(4\text{-XC}_6\text{H}_4)_2\text{C} = \text{CF}_2$ with piperidine in acetonitrile for various substituents.

Substituent	σ	σ^-	k_2° ($\text{l.mol}^{-1}.\text{s}^{-1}.$)	k_3 ($\text{l}^2.\text{mol}^{-2}.\text{s}^{-1}.$)	k_3 / k_2°
H	0.00	0.00	5.56×10^{-7}	9.93×10^{-5}	175
Br	0.23	0.26	2.07×10^{-5}	3.58×10^{-3}	173
CF_3	0.54	0.74	3.47×10^{-4}	1.42×10^{-1}	409
CN	0.66	0.90	4.34×10^{-3}	1.94	447
** NO_2	0.78	1.24	5.10×10^{-2}	82.4	1615

* extrapolated values from the activation parameters.

** obtained from ref (84).

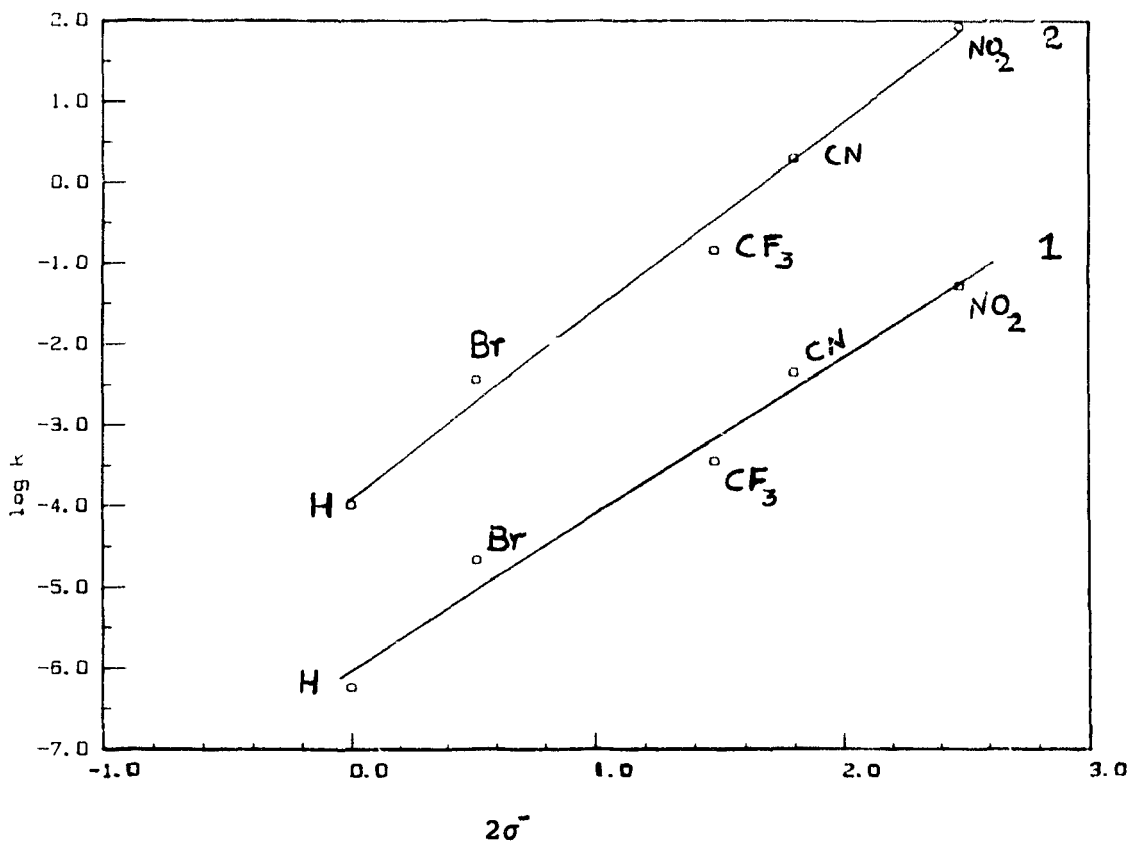


Figure 13: The Hammett plots for the amine catalysed and uncatalysed rate constants ($2\sigma^-$ vs k_2 and $2\sigma^-$ vs k_3) for the reaction of *para* substituted 1,1-difluoro-2,2-diphenylethylenes with piperidine in acetonitrile at 25°C. (1) uncatalysed reaction (2) catalysed reaction.

The substrates, 13 - 17, carry two identically substituted phenyl rings. Therefore, the substituent constants σ and σ' were multiplied by two, assuming that the substituent effects are additive, and the amine catalysed and uncatalysed rate constants were correlated with these values.

Correlation of the amine catalysed rate constants, k_3 , with σ gives a reaction constant $\rho = 3.54 \pm 0.36$ with a correlation coefficient 0.985 and correlation of the uncatalysed rate constants, k_2^0 , with σ gives a reaction constant $\rho = 2.99 \pm 0.25$ with a correlation coefficient 0.989.

Correlation of k_3 with σ' (Figure 13) gives a reaction constant $\rho = 2.31 \pm 0.14$ with a correlation coefficient 0.995 and in the case of k_2^0 the ρ value is 1.93 ± 0.16 with the correlation coefficient 0.990.

The positive values of ρ for both the amine catalysed and uncatalysed rate constants is evidence for the presence of increased negative charge in the transition state when compared to the reactant. The fact that the rate constants correlate better with the substituent constants σ' derived for substituted anilinium ions indicates that the negative charge is located on the carbon atom which is directly attached to the aromatic ring so that conjugation through the benzene ring can take place with the substituent group. This is in agreement with the proposed mechanism (Scheme 14).

Since the correlation of the rate constants with the

σ values is better and more appropriate than the correlation with the σ values, for the proposed mechanism, the reaction constants obtained from the correlation of rate constants with σ are used for further discussion.

The reaction constants obtained for both the amine catalysed and uncatalysed reactions are composite values. In the case of the uncatalysed reaction, the ρ value is obtained by addition of the ρ values for the zwitterion forming step and the expulsion of leaving group step (Scheme 14).

$$\text{That is, } \rho_{\text{uncat}} = \rho_{K_3} + \rho_{k_2}$$

$$\text{Similarly, } \rho_{\text{cat}} = \rho_{K_1} + \rho_{K_3} + \rho_{k_4}$$

If it is assumed that the reaction constants for leaving group expulsion in both the amine catalysed and the uncatalysed routes are approximately the same (ie, $\rho_{k_2} = \rho_{k_4}$), then the difference between ρ_{cat} and ρ_{uncat} would give the reaction constant for the proton transfer step.

$$\begin{aligned} \text{That is, } \rho_K &= \rho_{\text{cat}} - \rho_{\text{uncat}} \\ &= 2.31 - 1.93 \\ &= 0.38. \end{aligned}$$

Such a low reaction constant for the proton transfer step is reasonable because, as shown in Scheme 12, deprotonation takes place at the positive end of the zwitterion which would be influenced very little by the substituents on the phenyl ring. In addition, the reported values of 2.78

for the dissociation of anilinium ions where there is no carbon atom between the ammonium center and the phenyl ring and 0.72 for the dissociation of benzylammonium ions (98) where there is one carbon atom between the ammonium center and the phenyl ring also suggest that the value of 0.38 is reasonable for the proton transfer step, since there are two carbons between the ammonium center and the phenyl ring.

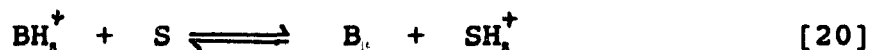
As mentioned above, the reaction constant for the uncatalysed reaction is the addition of the reaction constants for the zwitterion forming step and the leaving group expulsion step. Each of these steps would be influenced by the substituents in the opposite direction. The leaving group expulsion step would show a negative value because electron withdrawing substituents on the benzene ring slow down this step by stabilizing the negative charge. But formation of zwitterion would be facilitated by the electron withdrawing substituents and hence this step would show a positive value.

The observed reaction constant for the uncatalysed reaction (+ 1.93) indicates that the zwitterion forming step is more sensitive to the substituent effects than the expulsion of leaving group step. In the proposed mechanism, a late (product-like) transition state in the nucleophilic attack step and an early (reactant-like) transition state in the leaving group expulsion step would explain the observed reactant constants. This supports the assumption that the leaving group expulsion is the rate-determining step.

3. pK_a Measurements of Conjugate Acids of Amines in Acetonitrile.

3.1 General.

Dissociation of a conjugate acid of a base can be represented by equation [20].



where, B is the base, BH^+ is the conjugate acid of the base and S is the solvent.

Therefore, the dissociation constant (K_a) for the conjugate acid is given by equation [21], and the $\text{p}K_a$ of the conjugate acid is given by equation [22].

$$K_a = [\text{B}][\text{SH}^+]/ [\text{BH}^+] \quad [21]$$

$$\begin{aligned} \text{p}K_a &= - \log[\text{B}]/[\text{BH}^+] - \log[\text{SH}^+] \\ &= - \log[\text{B}]/[\text{BH}^+] - \log a_{\text{H}^+} \end{aligned} \quad [22]$$

It is clear that the dissociation constant depends on the nature of the solvent. Acetonitrile is a weaker base and much weaker acid than water, and its dielectric constant is lower than that of water. The autoprotolysis constant of acetonitrile is much lower than that of water. Therefore, acetonitrile acts as an excellent differentiating solvent for acids and bases. The behaviour of Brønsted acids and bases in acetonitrile has been studied using conductometric, polaro-

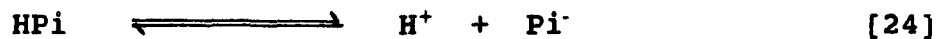
graphic, spectrophotometric, potentiometric measurements and various titrimetric methods.

Coetzee and co-workers have reported the pK_a values of the conjugate acids in acetonitrile for 35 bases of different structures (100). These values were obtained using a potentiometric method. Comparison of these values with those in water indicates that all protonated amines are much weaker acids in acetonitrile than in water. Although this statement is true for all the amines reported, and an average ΔpK_a value of 7.6 was found, no simple correlation was found between the pK_a values of the ammonium ions in acetonitrile and water.

Therefore, it is not possible to predict the pK_a value of an ammonium ion in acetonitrile from the corresponding pK_a value in water. It is also quite clear that interpretation of kinetic parameters obtained in acetonitrile using the pK_a values of ammonium ions in water would be inappropriate. Since the pK_a values of the conjugate acids for the amines used in our kinetic studies were not available in acetonitrile solvent in the literature, it was necessary to measure these values in our laboratory. In order to be consistent with the literature data, these measurements were carried out by exactly the same method described by Coetzee and Padmanabhan (101).

3.2 Results and Discussion.

An electrode of Ag/ 0.01M AgNO₃ in acetonitrile was used as the reference electrode and a general purpose glass electrode was used as the indicator electrode. The glass electrode was calibrated in picric acid - tetraethylammonium picrate buffers against the Ag/ 0.01M AgNO₃ in acetonitrile as the reference electrode. Tetraethylammonium picrate dissociates completely according to equation [23], up to 0.01M, and picric acid undergoes simple dissociation (equation [24]), up to 0.1M concentrations.



The hydrogen ion activity in a picric acid - tetraethylammonium picrate buffer in acetonitrile is given by equation [25].

$$a_{\text{H}^+} = K_{\text{HPi}} \frac{[\text{HPi}]}{[\text{Pi}^-]} \times \frac{f_0}{f_1} \quad [25]$$

According to the Nernst equation, the glass electrode potential is represented by equation [26].

$$E = E^{\circ} - \frac{RT}{F} \ln a_{H^+} = E^{\circ} - 2.303 \frac{RT}{F} \log a_{H^+} \quad [26]$$

where, E is the potential of the glass electrode, and

E° is the standard electrode potential (with reference to Ag/0.01M AgNO₃ electrode).

F is the Faraday number.

At 25° C, 2.303RT/F would be equal to 59 mV.

At constant ionic strength, f_0/f_1 in equation [25] would be constant and K_{HPi} is constant for a given solvent at a given temperature. Therefore, equation [26], together with equation [25] shows that the electrode potential, E, is proportional to $\log\{ [HPi]/ [Pi^-] \}$. Therefore, the calibration curve of the glass electrode, that is the plot of E against $\log\{ [HPi]/ [Pi^-] \}$, would be linear with a slope m, which is approximately equal to 59 mV at 25° c. Therefore, equation [27] represents the relationship between the electrode potential and the buffer ratio, where C is the intercept of the calibration curve.

$$E = m \log\{ [HPi]/[Pi^-] \} + C \quad [27]$$

Now, a relationship can be established from equations [25] and [27], between the electrode potential and the hydrogen ion activity in acetonitrile.

According to the reduced Debye - Hückel equation,

$$\log f_i = - 355 z_i^2 D^{-3/2} S^{1/2}$$

where, D is the dielectric constant of the solvent and S is the ionic strength.

Substituting D = 36.0 for acetonitrile, at S = 1 x 10⁻³,

$$f_i = 0.89 \text{ and } f_o = 1$$

Substituting these values in equation [25] gives equation [28]

$$\log [\text{HPi}] / [\text{Pi}] = \log a_{\text{H}} - \log K_{\text{HPi}} + \log 0.89 \quad [28]$$

Substituting equation [28] in equation [27] gives equation [29].

$$E_{\text{glass}} = m (\log a_{\text{H}^+} - \log K_{\text{HPi}} + \log 0.89) + C \quad [29]$$

Equation [29] relates the electrode potential with the hydrogen ion activity in acetonitrile. From equation [22], $\text{pK}_a = -\log a_{\text{H}^+}$ when $[\text{B}] / [\text{BH}^+] = 1$. If the electrode potential at this buffer ratio is E', then from equation [29],

$$-\log a_{\text{H}^+} = (C - E') / m - \log K_{\text{HPi}} + \log 0.89$$

$$\begin{aligned} \text{Therefore, } \text{pK}_a &= (C - E') / m - \log K_{\text{HPi}} + \log 0.89 \\ &= (C - E') / m + \text{pK}_a + \log 0.89 \quad [30] \end{aligned}$$

pK_a of picric acid has been reported as 11.0 in acetonitrile (102) and this has been adopted as a standard value.. Therefore, equation [30] can be rewritten as follows.

$$\text{pK}_a = (C - E') / m + 11.0 + \log 0.89$$

$$= (C - E') / m + 10.95 \quad [31]$$

The pK_a of the ammonium ion can be calculated from equation [31] by substituting the values for C, E' and m. C and m are obtained from the calibration curve for the picric acid - tetraethylammonium picrate buffer as intercept and slope respectively.

In order to obtain the value of E', the electrode potential of the glass electrode was obtained in five buffer solutions which contain constant concentration of amine picrate, constant concentration of tetraethylammonium perchlorate (inert electrolyte) and different concentrations of amine in acetonitrile. Then these electrode potentials were plotted against $\log([B]/ [BH^+])$. The value of E' is obtained as the intercept of this plot.

Table 12 shows the EMF values obtained for different ratios of picric acid and tetraethylammonium picrate, and Figure 14 shows the corresponding calibration curve. The slope of the plot, $m = 61.8 \pm 0.7$ and the intercept, $C = 76.2 \pm 0.4$.

The observed electrode potentials for different buffer ratios of amines are given in Table 13. These values are plotted against $\log ([B]/ [BH^+])$ in Figure 15.

Table 14 shows the calculated pK_a values for the amines studied.

Table 12

The observed EMF values of glass electrode for picric acid - tetraethylammonium picrate buffer solutions in acetonitrile.

$[\text{HPi}] \times 10^3$ (mol.l ⁻¹)	$[\text{TEAPi}] \times 10^3$ (mol.l ⁻¹)	EMF (mV)	$\log[\text{HPi}]/[\text{TEAPi}]$
0.502	1.029	57	-0.3115
1.005	1.029	76	-0.0105
2.511	1.029	101	0.3876
5.023	1.029	119	0.6885
10.050	1.029	138	0.9895

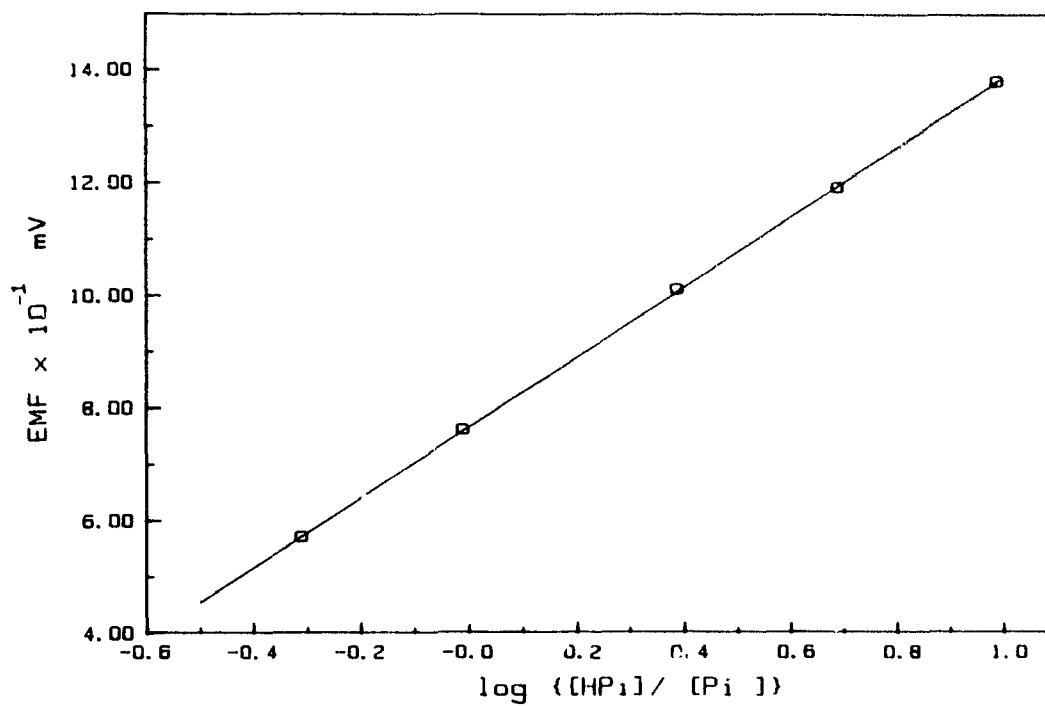


Figure 14: The calibration curve for glass electrode in acetonitrile.

Table 13

The electrode potentials of glass electrode in amine - amine picrate buffers for different buffer ratio in acetonitrile.

$[B] \times 10^4$ mol.l ⁻¹	$[BPi] \times 10^4$ mol.l ⁻¹	$[TEAClO_4] \times 10^4$ mol.l ⁻¹	$\log([B]/[BPi])$	EMF mV
<u>Piperidine</u>				
1.28	5.00	5.00	-0.5918	-389
2.55	5.00	5.00	-0.2924	-408
5.10	5.00	5.00	0.0086	-426
12.80	5.00	5.00	0.4082	-449
25.50	5.00	5.00	0.7076	-468
38.30	5.00	5.00	0.8842	-479
<u>1,2,3,4- tetrahydroisoquinoline</u>				
1.25	5.03	5.00	-0.6053	-278
2.50	5.03	5.00	-0.3043	-294
5.00	5.03	5.00	-0.0033	-312
12.49	5.03	5.00	0.3947	-337
24.99	5.03	5.00	0.6957	-355
37.48	5.03	5.00	0.8718	-366

continued

Table 13 (continued).

$[B] \times 10^4$ mol.l ⁻¹	$[BPi] \times 10^4$ mol.l ⁻¹	$[TEAClO_4] \times 10^4$ mol.l ⁻¹	$\log([B]/[BPi])$	EMF mV
<u>Thiomorpholine</u>				
1.25	5.03	5.00	-0.6050	-238
2.50	5.03	5.00	-0.3041	-255
5.00	5.03	5.00	-0.0031	-273
12.49	5.03	5.00	0.3950	-296
24.98	5.03	5.00	0.6959	-314
37.47	5.03	5.00	0.8721	-325
<u>N-methylpyrrolidine</u>				
1.24	5.00	5.00	-0.6049	-350
2.49	5.00	5.00	-0.3031	-367
4.98	5.00	5.00	-0.0021	-385
12.44	5.00	5.00	0.3951	-408
24.88	5.00	5.00	0.6969	-427
37.32	5.00	5.00	0.8729	-437

continued

Table 13 (continued).

[B] × 10 ⁴ mol.l ⁻¹	[BPi] × 10 ⁴ mol.l ⁻¹	[TEAClO ₄] × 10 ⁴ mol.l ⁻¹	log([B]/[BPi])	EMF mV
<u>N-methylpiperidine</u>				
1.33	4.97	5.00	-0.5716	-328
2.67	4.97	5.00	-0.2705	-344
5.33	4.97	5.00	0.0306	-362
13.33	4.97	5.00	0.4284	-385
26.66	4.97	5.00	0.7295	-402
40.00	4.97	5.00	0.9056	-414
<u>N-methylmorpholine</u>				
1.27	5.00	5.00	-0.5935	-181
2.55	5.00	5.00	-0.2924	-199
5.10	5.00	5.00	0.0086	-217
12.75	5.00	5.00	0.4065	-240
25.49	5.00	5.00	0.7076	-258
38.24	5.00	5.00	0.8837	-268

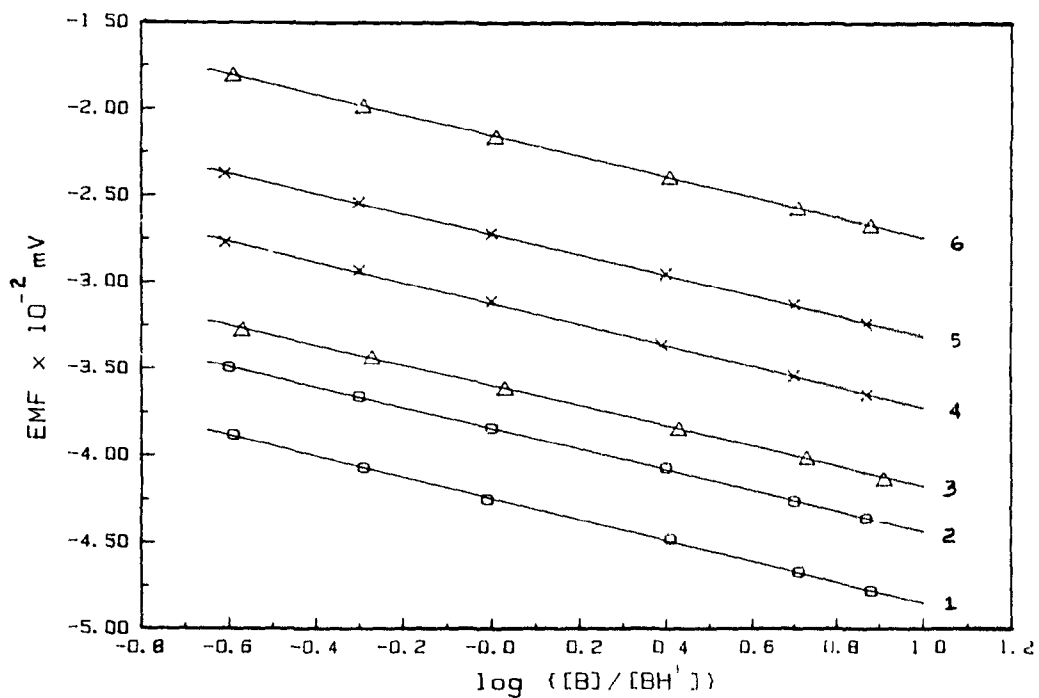


Figure 15: EMF vs $\log \{ [B]/ [BH^+] \}$ plots for different amines in acetonitrile at constant salt concentration. (1) piperidine, (2) N-methylpyrrolidine, (3) N-methylpiperidine, (4) 1,2,3,4-tetrahydroisoquinoline (5) Thiomorpholine and (6) N-methylmorpholine.

Table 14

The pK_a values of conjugate acids of amines in acetonitrile and water at 25°C.

Amine	pK_a in MeCN	pK_a in water	ΔpK_a
<u>Secondary amines</u>			
piperidine	19.06 \pm .09	11.22	7.84
1,2,3,4-tetra- hydroisoquinoline	17.25 \pm .07		
Thiomorpholine	16.60 \pm .06	9.00	7.60
<u>Tertiary amines</u>			
N-methylpyrrolidine	18.42 \pm .08	10.46	7.96
N-methylpiperidine	18.01 \pm .08	10.08	7.93
N-methylmorpholine	15.68 \pm .05	7.38	8.30
1,8-diazabicyclo[5.4.0]- undec-7-ene (DBU)	23.91 \pm .10		

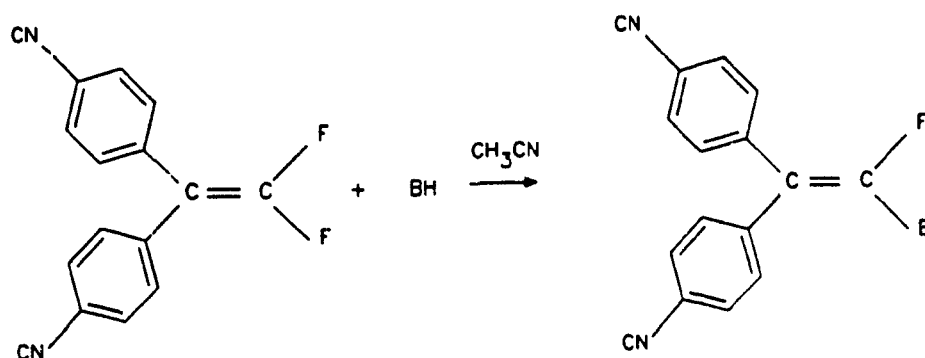
Although, the pK_a value for the conjugate acid of piperidine has been reported by Coetzee and his coworkers, it was measured in our laboratory in order to verify our results. The measured value 19.06 ± 0.09 is in good agreement with the reported value of 18.92 (100). An average value of 7.9 is obtained for ΔpK_a . This average value is comparable to 7.6 which was reported as the average value for ΔpK_a by Coetzee (100). The pK_a values listed in Table 14 will be used in the following chapters to analyse the kinetic results.

4. Kinetics of the reaction of 1,1-difluoro-2,2-di(4-cyano-phenyl)ethylene with amines.

4.1 General.

This chapter describes the study of the reaction of various amines with 1,1-difluoro-2,2-di(4-cyanophenyl)ethylene in acetonitrile (System 2).

System 2.



For BH = pyrrolidine, piperidine, morpholine, thiomorpholine, 1,2,3,4-tetrahydroisoquinoline, 1,1,3,3-tetramethylguanidine (TMG), and n-propylamine.

4.2 Results and discussion.

A preliminary, qualitative study of 1,1-difluoro-2,2-di(4-cyanophenyl)ethylene with different amines showed that the substrate is totally unreactive towards tertiary amines. Among the secondary amines, all the cyclic secondary amines studied were reactive while acyclic secondary amines react very slowly. This made acyclic secondary amines unsuitable for our kinetic studies. Although primary amines

were reactive towards the substrate, the enamines formed in the reactions were unstable. In most cases, the rate of disappearance of enamine was quite fast. Therefore, cyclic secondary amines were preferred for our kinetic studies. The absorption maxima (λ_{max}) of 1-fluoro-1-amino-2,2-di(4-cyanophenyl)ethylene for different amines are tabulated in Table 15, and the UV-Visible spectra for reactions with TMG and 1,2,3,4-tetrahydroisoquinoline are presented in Figures 16 and 17 respectively. The reactions were monitored at the wavelength where the corresponding product shows maximum absorption, and the pseudo first-order rate constants were calculated by the Guggenheim method (90) and are tabulated in Tables 16 to 21, together with their standard deviations. These rate constants are plotted against base concentrations in Figures 18 - 23.

Table 15

The absorption maxima of the monoamino product of the reaction of 1,1-difluoro-2,2-di(4-cyanophenyl)ethylene in acetonitrile with secondary and primary amines.

amine	λ_{\max} (nm)
pyrrolidine	349
piperidine	336
morpholine	329
thiomorpholine	327
1,2,3,4-tetrahydro- isoquinoline	332-336
1,1,3,3-tetramethyl- guanidine	355
n-propylamine	326

Figure 16: (1) The UV-Vis. spectra of 1,1-difluoro-2,2-di(4-cyanophenyl)ethylene [$6.2 \times 10^{-5} \text{M}$] and the reaction mixture of 1,1-difluoro-2,2-di(4-cyanophenyl)ethylene and 1,1,3,3-tetramethylguanidine [$1 \times 10^{-2} \text{M}$] in acetonitrile at different time after mixing. (2) immediately after mixing, (3) 1 min, (4) 2 min, (5) 5 min, (6) 15 min, (7) 30 min and (8) 18 hrs.

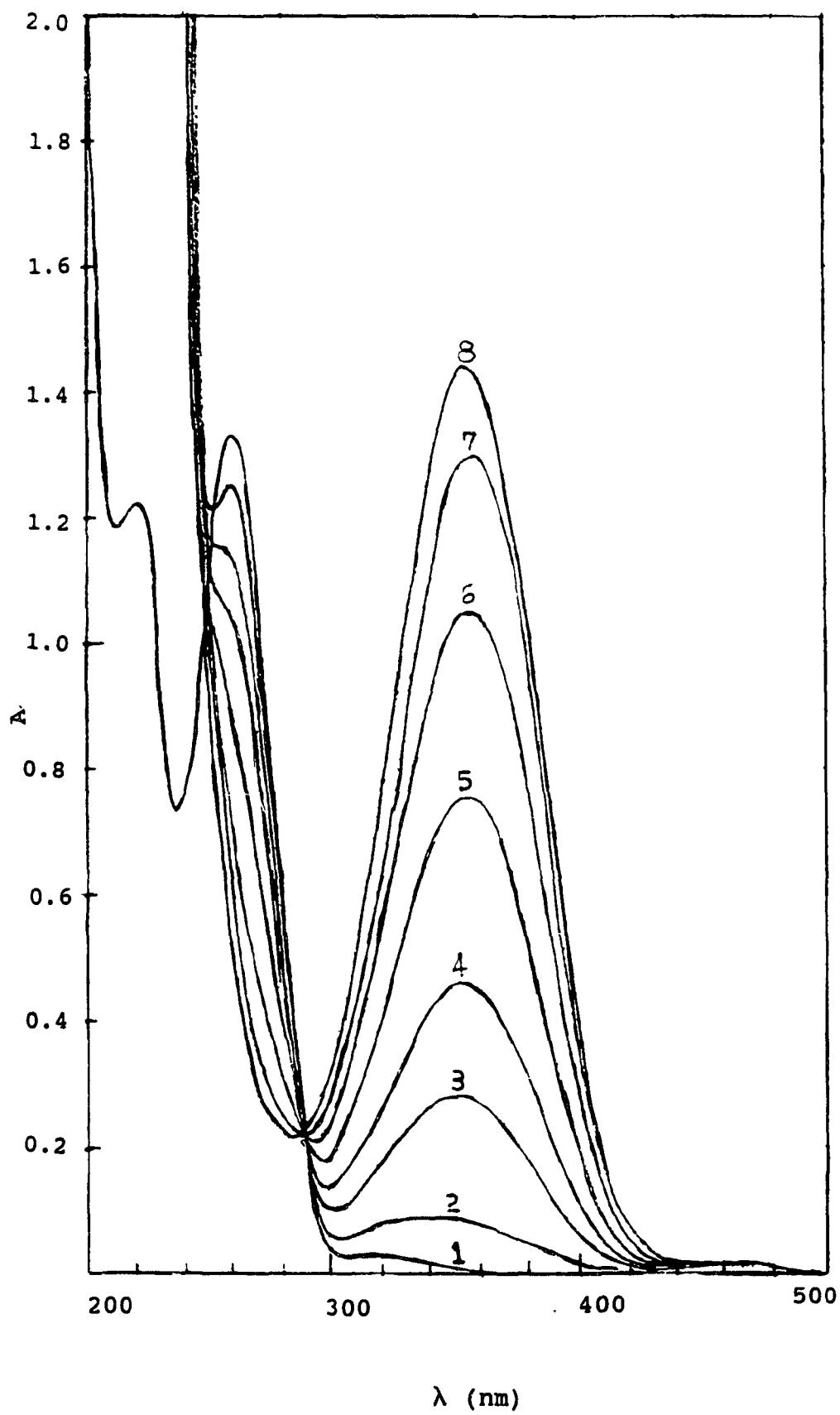


Figure 16

Figure 17: (1) The UV-Vis. spectra of 1,1-difluoro-2,2-di(4-cyanophenyl)ethylene [$5.4 \times 10^{-5} \text{M}$] and the reaction mixture of 1,1-difluoro-2,2-di(4-cyanophenyl)ethylene and 1,2,3,4-tetrahydroisoquinoline [$1 \times 10^{-2} \text{M}$] in acetonitrile at different time after mixing. (2) 1 min, (3) 2 min, (4) 4 min, (5) 10 min and (6) 1 hr.

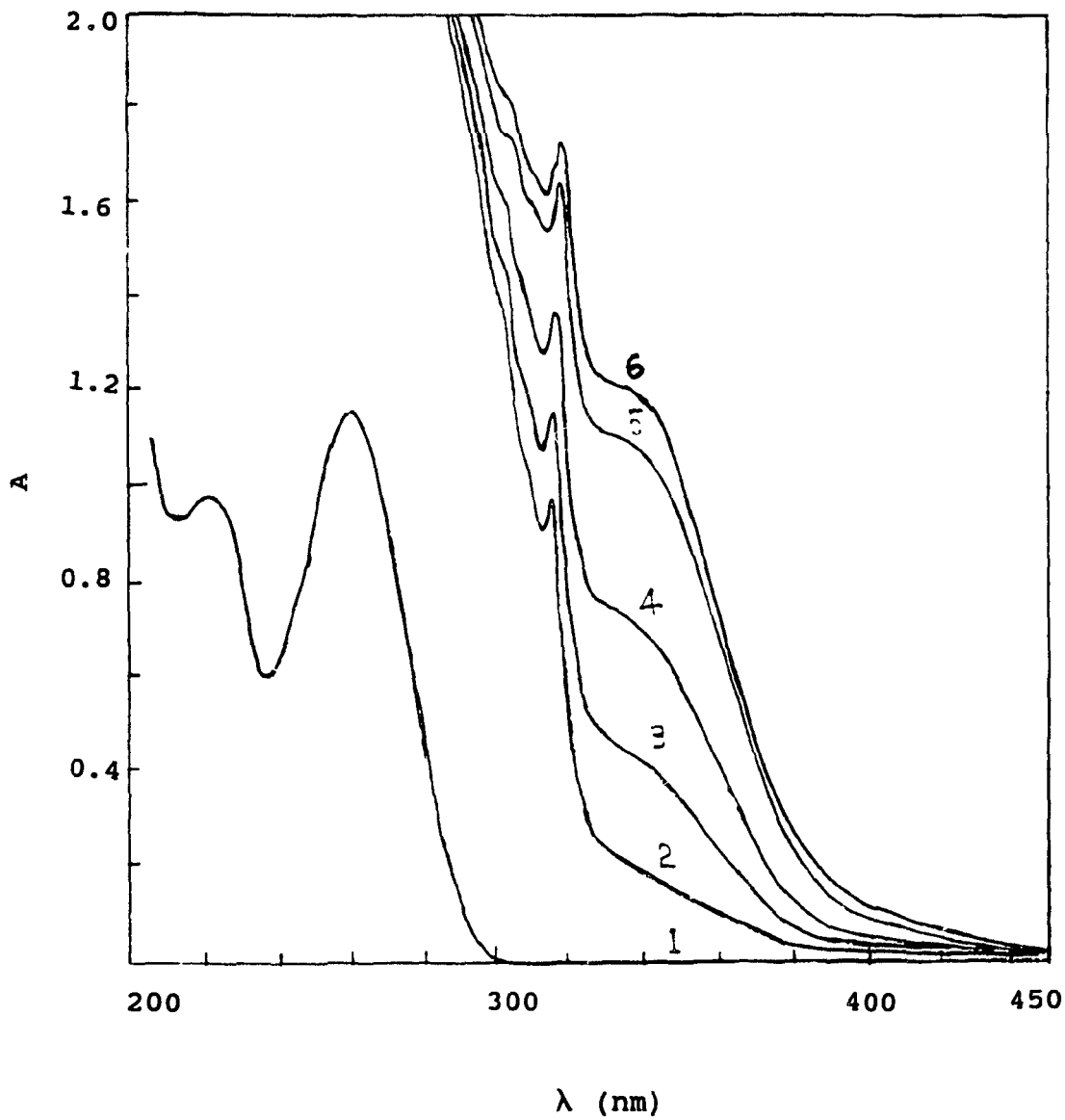


Figure 17

Table 16

The pseudo first-order rate constants and calculated second-order and third-order rate constants for the formation of 1-fluoro-1-pyrrolidino-2,2-di(4-cyanophenyl)ethylene from the reaction of 1,1-difluoro-2,2-di(4-cyanophenyl)ethylene with pyrrolidine in acetonitrile.

Temp. (°C)	[pyrr] x 10 ³ mol.l ⁻¹	k ₁ x 10 ⁴ (s ⁻¹)	k ₂ ^o x 10 ³ l.mol ⁻¹ .s ⁻¹	k ₃ l ² .mol ⁻² .s ⁻¹
15	1.05	1.90 ± .01		
	2.10	4.13 ± .02		
	3.15	6.96 ± .03	1.60 ± .02	19.0 ± .7
	3.98	9.44 ± .07		
	5.25	13.55 ± .09		
20	1.05	2.06 ± .01		
	2.09	4.61 ± .02		
	3.14	7.65 ± .03	1.78 ± .03	20.1 ± .9
	4.19	11.05 ± .05		
	5.24	14.63 ± .05		

continued

table 16 (continued).

Temp. (°C)	[pyrr] x 10 ³ mol.l ⁻¹	k ₁ x 10 ⁴ (s ⁻¹)	k ₂ ^o x 10 l.mol ⁻¹ .s ⁻¹	k ₃ l ² .mol ⁻² .s ⁻¹
25	1.05	2.33 ± .02		
	1.99	4.78 ± .03		
	2.99	7.86 ± .03	1.99 ± .01	20.9 ± .3
	3.98	11.28 ± .06		
	5.26	16.21 ± .07		
30	0.99	2.43 ± .02		
	1.99	5.27 ± .02		
	2.99	8.66 ± .04	2.21 ± .03	22.5 ± .8
	3.98	12.50 ± .06		
	4.98	16.48 ± .11		
35	0.99	2.71 ± .02		
	1.99	5.79 ± .03		
	2.99	9.49 ± .06	2.46 ± .04	23.3 ± 1.2
	3.98	13.33 ± .08		
	5.24	19.47 ± .12		

Table 17

The pseudo first-order rate constants and calculated second-order and third-order rate constants for the formation of 1-fluoro-1-morpholino-2,2-di(4-cyanophenyl)ethylene from the reaction of 1,1-difluoro-2,2-di(4-cyanophenyl)ethylene with morpholine in acetonitrile.

Temp. (°C)	[morph] x 10 ² mol.l ⁻¹	k ₁ x 10 ⁵ (s ⁻¹)	k ₂ ^o x 10 ⁴ l.mol ⁻¹ .s ⁻¹	k ₃ x 10 ² l ² .mol ⁻² .s ⁻¹
25	1.987	2.27 ± .01		
	2.981	5.33 ± .04		
	3.974	9.25 ± .06	1.33 ± .81	5.38 ± .19
	4.968	13.77 ± .04		
	5.961	19.80 ± .07		
30	2.016	2.71 ± .05		
	3.024	5.96 ± .05		
	4.032	10.16 ± .12	2.08 ± .44	5.72 ± .10
	5.040	15.39 ± .14		
	6.048	22.30 ± .07		

continued

table 17 (continued).

Temp. (°C)	[morph] x 10 ² mol.l ⁻¹	k ₁ x 10 ⁵ (s ⁻¹)	k ₂ ^o x 10 ⁴ l.mol ⁻¹ .s ⁻¹	k ₃ x 10 ² l ² .mol ⁻² .s ⁻¹
35	2.007	3.16 ± .03		
	3.004	6.80 ± .07		
	4.006	11.96 ± .08	2.80 ± .60	6.59 ± .14
	5.007	17.78 ± .09		
	6.009	25.41 ± .13		
40	2.007	3.33 ± .04		
	3.010	7.49 ± .06		
	4.013	12.79 ± .09	3.83 ± 1.13	6.77 ± .27
	5.017	18.76 ± .13		
	6.020	26.68 ± .33		
45	2.005	3.74 ± .03		
	3.008	8.14 ± .05		
	4.010	14.07 ± .09	4.25 ± .93	7.50 ± .22
	5.013	21.06 ± .22		
	6.015	29.33 ± .15		

Table 18

The pseudo first-order rate constants and calculated second-order and third-order rate constants for the formation of 1-fluoro-1-(1,2,3,4-tetrahydroisoquinolino)-2,2-di(4-cyanophenyl)ethylene from the reaction of 1,1-difluoro-2,2-di(4-cyanophenyl)ethylene with 1,2,3,4-tetrahydroisoquinoline (THIQ) in acetonitrile.

Temp. (°C)	[THIQ] x 10 ² mol.l ⁻¹	k ₁ x 10 ⁴ (s ⁻¹)	k ₂ ^o x 10 ³ l.mol ⁻¹ .s ⁻¹	k ₃ x 10 l ² .mol ⁻² .s ⁻¹
20	1.579	0.81 ± .007		
	2.368	1.65 ± .01		
	3.157	2.86 ± .02	1.04 ± .14	2.53 ± .04
	3.947	4.31 ± .02		
	4.736	6.22 ± .04		
25	1.914	1.35 ± .02		
	2.871	2.82 ± .01		
	3.828	5.14 ± .04	1.58 ± .64	2.95 ± .15
	4.785	7.66 ± .06		
	5.741	10.38 ± .08		

continued

table 18 (continued).

Temp. (°C)	[THIQ] x 10 ² mol.l ⁻¹	k ₁ x 10 ⁴ (s ⁻¹)	k ₂ ^o x 10 ³ l.mol ⁻¹ .s ⁻¹	k ₃ x 10 l ² .mol ⁻² .s ⁻¹
30	1.865	1.51 ± .03		
	2.797	3.07 ± .04		
	3.729	5.35 ± .04	2.15 ± .25	3.20 ± .06
	4.662	7.91 ± .08		
	5.594	11.21 ± .14		
35	1.579	1.39 ± .01		
	2.369	2.70 ± .01		
	3.159	4.81 ± .04	2.66 ± .50	3.86 ± .15
	3.948	7.15 ± .07		
	4.738	9.80 ± .11		
40	1.579	1.54 ± .01		
	2.369	3.24 ± .02		
	3.159	5.38 ± .04	3.48 ± .50	4.20 ± .15
	3.948	8.01 ± .06		
	4.738	10.92 ± .11		

Table 19

The pseudo first-order rate constants and calculated second-order and third-order rate constants for the formation of 1-fluoro-1-(thiomorpholino)-2,2-di(4-cyanophenyl)ethylene from the reaction of 1,1-difluoro-2,2-di(4-cyanophenyl)ethylene with thiomorpholine in acetonitrile at 25°C.

[thiomorph] x 10 ² mol.l ⁻¹	k ₁ x 10 ⁵ (s ⁻¹)	k ₂ ^o x 10 ⁴ l.mol ⁻¹ .s ⁻¹	k ₃ x 10 ² l ² .mol ⁻² .s ⁻¹
4.946	3.89 ± .06		
5.047	4.23 ± .04		
7.419	8.28 ± .04		
7.570	9.57 ± .09		
9.892	14.80 ± .10	1.00 ± .47	1.44 ± .05
10.090	16.36 ± .11		
12.366	22.97 ± .07		
12.620	24.39 ± .08		
15.140	34.51 ± .23		

Table 20

The pseudo first-order rate constants and calculated second-order and third-order rate constants for the formation of 1-fluoro-1-(n-propylamino)-2,2-di(4-cyanophenyl)ethylene from the reaction of 1,1-difluoro-2,2-di(4-cyanophenyl)ethylene with n-propylamine in acetonitrile.

Temp. (°C)	[prop] x 10 ³ mol.l ⁻¹	k ₁ x 10 ⁴ (s ⁻¹)	k ₂ ^o x 10 ² l.mol ⁻¹ .s ⁻¹	k ₃ x 10 l ² .mol ⁻² .s ⁻¹
15	4.805	1.14 ± .01		
	7.207	1.79 ± .01		
	9.609	2.44 ± .03	2.18 ± .05	3.99 ± .46
	12.012	3.15 ± .03		
	14.414	4.02 ± .02		
20	4.996	1.28 ± .02		
	7.494	2.16 ± .01		
	9.992	2.97 ± .02	2.52 ± .17	3.32 ± 1.62
	12.489	3.66 ± .03		
	14.987	4.41 ± .04		

continued.

table 20 (continued).

Temp. (°C)	[prop] x 10 ³ mol.l ⁻¹	k ₁ x 10 ⁴ (s ⁻¹)	k ₂ ^o x 10 ² l.mol ⁻¹ .s ⁻¹	k ₃ x 10 l ² .mol ⁻² .s ⁻¹
25	4.996	1.53 ± .03		
	7.494	2.51 ± .04		
	9.992	3.36 ± .05	2.93 ± .10	4.21 ± .94
	12.489	4.26 ± .08		
	14.987	5.34 ± .10		
30	4.979	1.89 ± .02		
	7.468	2.81 ± .03		
	9.958	4.15 ± .03	3.43 ± .16	6.32 ± 1.54
	12.447	5.13 ± .07		
	14.937	6.60 ± .09		
35	4.805	1.88 ± .02		
	7.207	2.99 ± .06		
	9.609	4.04 ± .06	3.67 ± .13	5.61 ± 1.25
	12.012	5.08 ± .09		
	14.414	6.57 ± .16		

Table 21

The pseudo first-order rate constants and calculated second-order rate constants for the formation of 1-fluoro-1-(1,1,3,3-tetramethylguanidino)-2,2-di(4-cyanophenyl)ethylene from the reaction of 1,1-difluoro-2,2-di(4-cyanophenyl)ethylene with 1,1,3,3-tetramethylguanidine (TMG) in acetonitrile.

Temp. (°C)	[TMG] x 10 ³ mol.l ⁻¹	k ₁ x 10 ⁴ (s ⁻¹)	k ₂ x 10 l.mol ⁻¹ .s ⁻¹
20	0.804	1.58 ± .01	
	1.608	2.96 ± .03	
	2.412	4.32 ± .03	1.74 ± .01
	3.216	5.77 ± .03	
	4.021	7.17 ± .04	
25	0.805	2.08 ± .02	
	1.610	3.96 ± .02	
	2.415	5.79 ± .07	2.38 ± .03
	3.220	7.73 ± .10	
	4.025	9.76 ± .09	

table 21 (continued).

Temp. (°C)	[TMG] x 10 ³ mol.l ⁻¹	k ₁ x 10 ⁴ (s ⁻¹)	k ₂ x 10 l.mol ⁻¹ .s ⁻¹
30	0.805	2.58 ± .01	
	1.610	5.01 ± .03	
	2.415	7.68 ± .15	2.95 ± .07
	3.220	9.70 ± .04	
	4.025	12.09 ± .02	
35	0.804	3.30 ± .02	
	1.608	6.32 ± .04	
	2.412	9.25 ± .09	3.73 ± .03
	3.216	12.50 ± .06	
	4.021	15.20 ± .05	
40	0.804	4.27 ± .02	
	1.609	8.15 ± .05	
	2.413	12.31 ± .06	4.52 ± .14
	3.218	15.33 ± .12	
	4.022	18.84 ± .08	

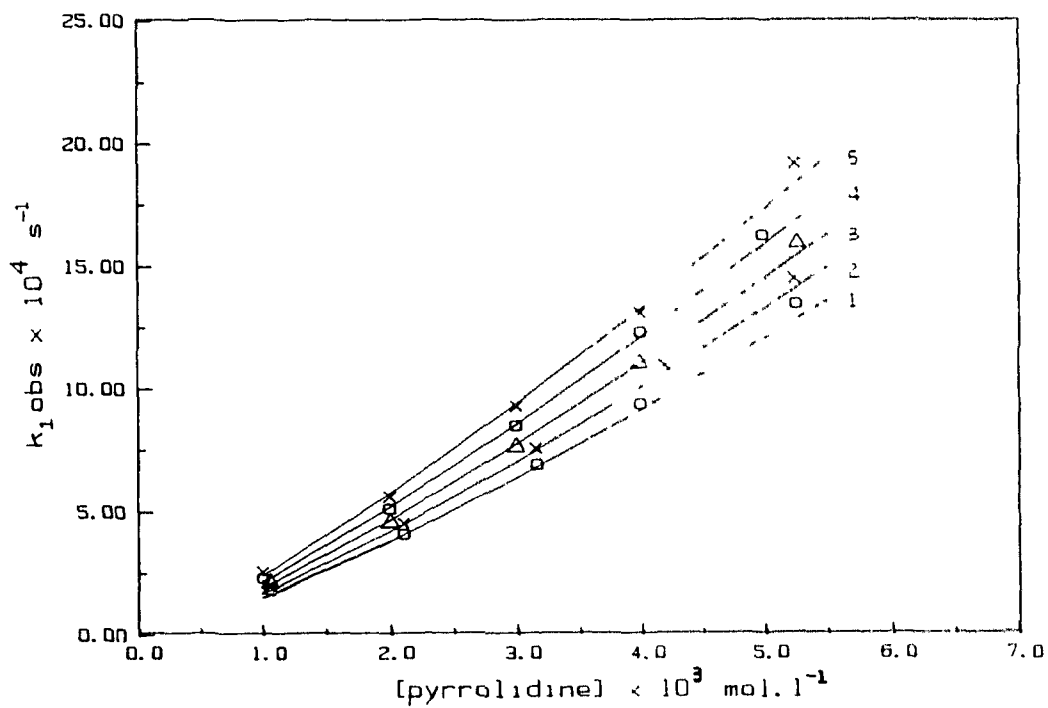


Figure 18: k_1 obs vs [pyrrolidine] plot for the reaction of 1,1-difluoro-2,2-di(4-cyanophenyl)ethylene with pyrrolidine in acetonitrile at different temperatures. (1) 15, (2) 20, (3) 25, (4) 30 and (5) 35°C.

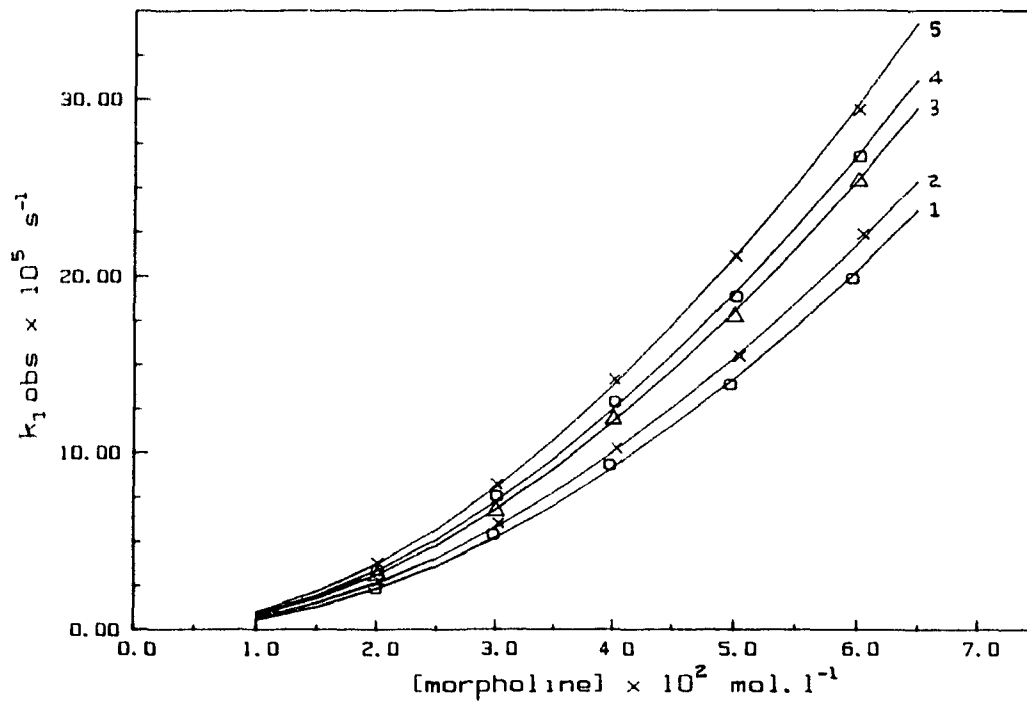


Figure 19: $k_1 \text{ obs}$ vs $[\text{morpholine}]$ plot for the reaction of 1,1-difluoro-2,2-di(4-cyanophenyl)ethylene with morpholine in acetonitrile at different temperatures. (1) 25, (2) 30, (3) 35, (4) 40 and (5) 45°C.

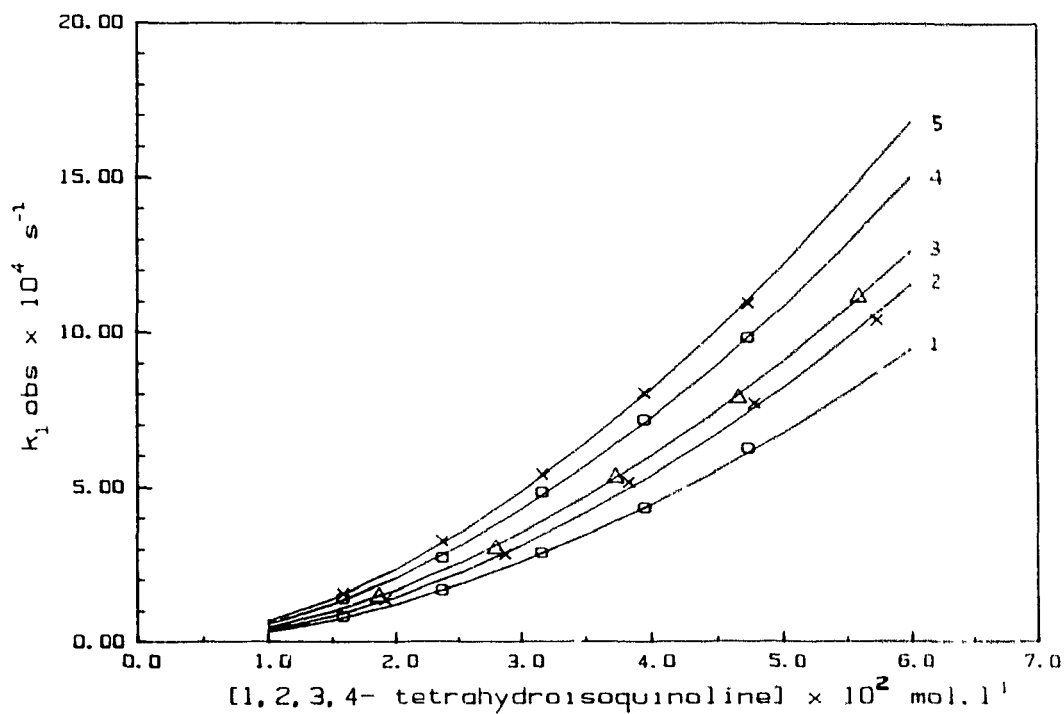


Figure 20: k_1, obs vs $[1,2,3,4\text{-tetrahydroisoquinoline}]$ plot for the reaction of 1,1-difluoro-2,2-di(4-cyanophenyl)- ethylene with 1,2,3,4-tetrahydroisoquinoline in acetonitrile at different temperatures. (1) 20, (2) 25, (3) 30, (4) 35 and (5) 40°C.

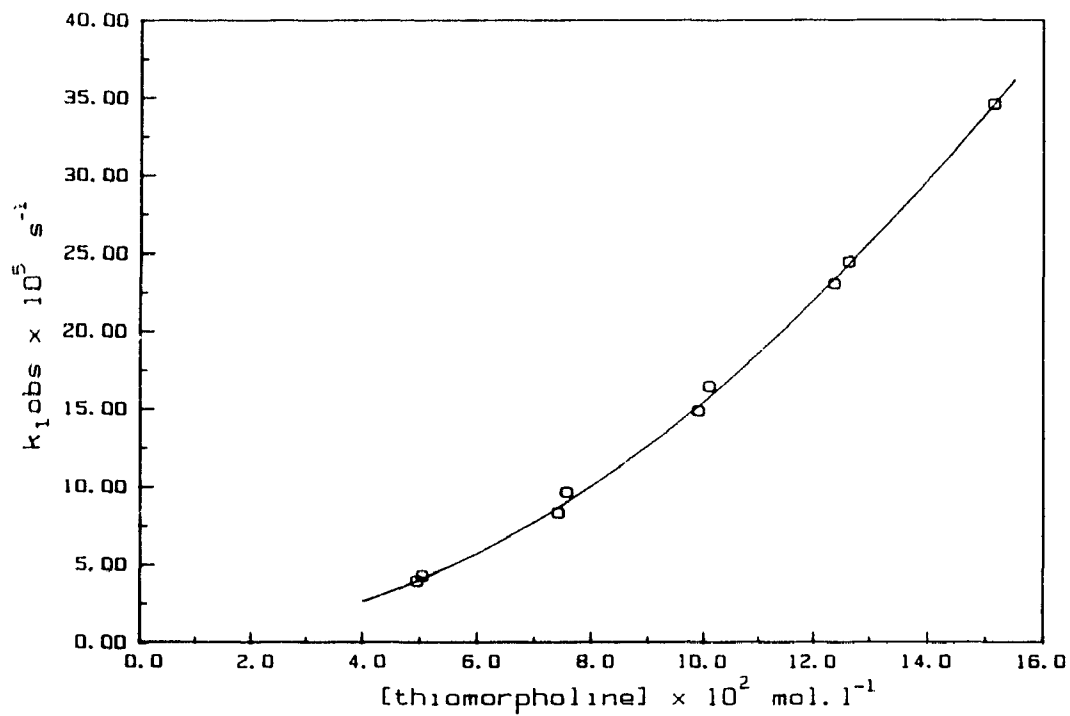


Figure 21: k_1 , obs vs [thiomorpholine] plot for the reaction of 1,1-difluoro-2,2-di(4-cyanophenyl)ethylene with thiomorpholine in acetonitrile at 25°C.

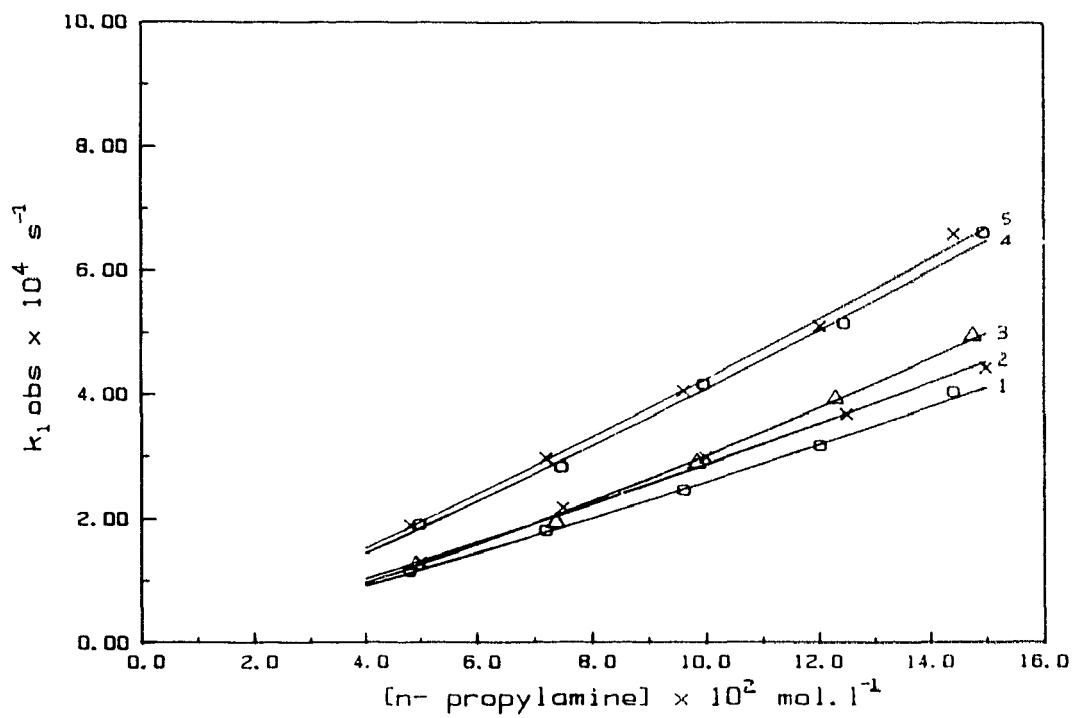


Figure 22: k_1 obs vs [n-propylamine] plot for the reaction of 1,1-difluoro-2,2-di(4-cyanophenyl)ethylene with n-propylamine in acetonitrile at different temperatures.

(1) 15, (2) 20, (3) 25, (4) 30 and (5) 35°C.

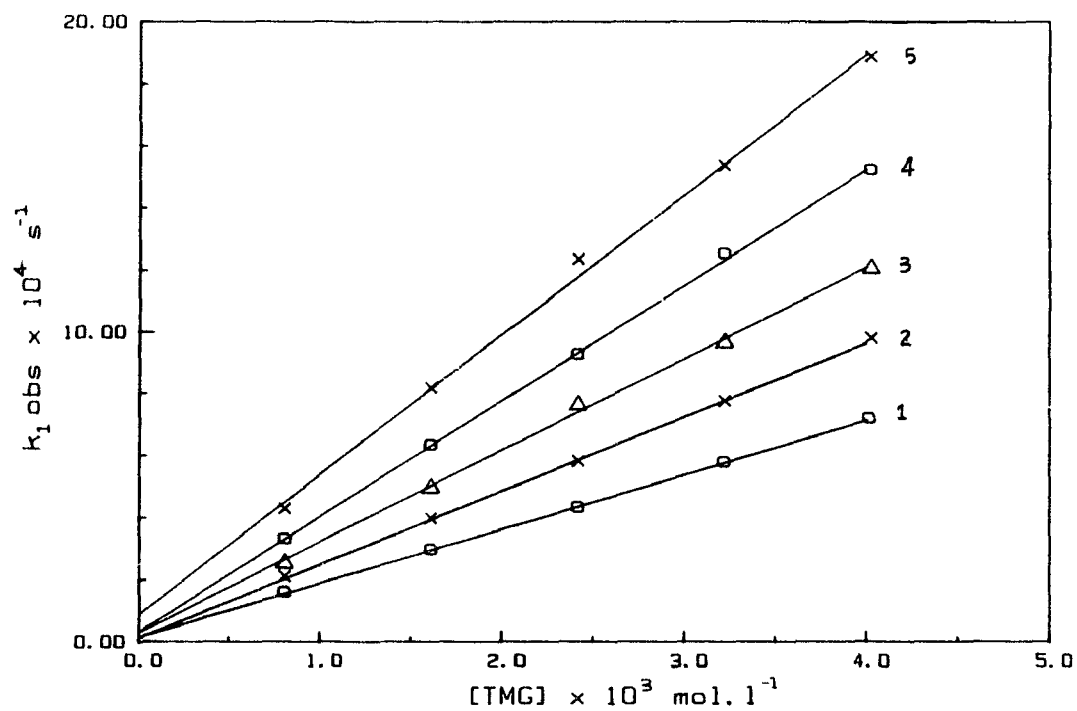


Figure 23: k_1, obs vs $[\text{TMG}]$ plot for the reaction of 1,1-difluoro-2,2-di(4-cyanophenyl)ethylene with 1,1,3,3-tetramethylguanidine in acetonitrile at different temperatures. (1) 20, (2) 25, (3) 30, (4) 35 and (5) 40°C.

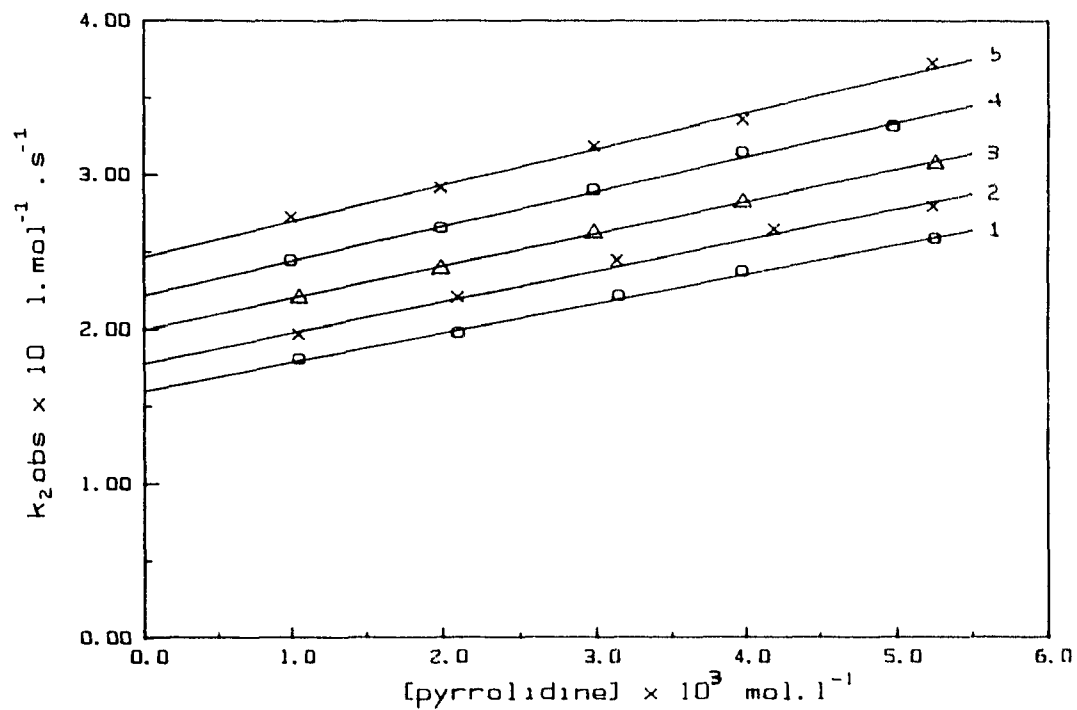


Figure 24: k_2 obs vs [pyrrolidine] plot for the reaction of 1,1-difluoro-2,2-di(4-cyanophenyl)ethylene with pyrrolidine in acetonitrile at different temperatures. (1) 15, (2) 20, (3) 25, (4) 30 and (5) 35°C.

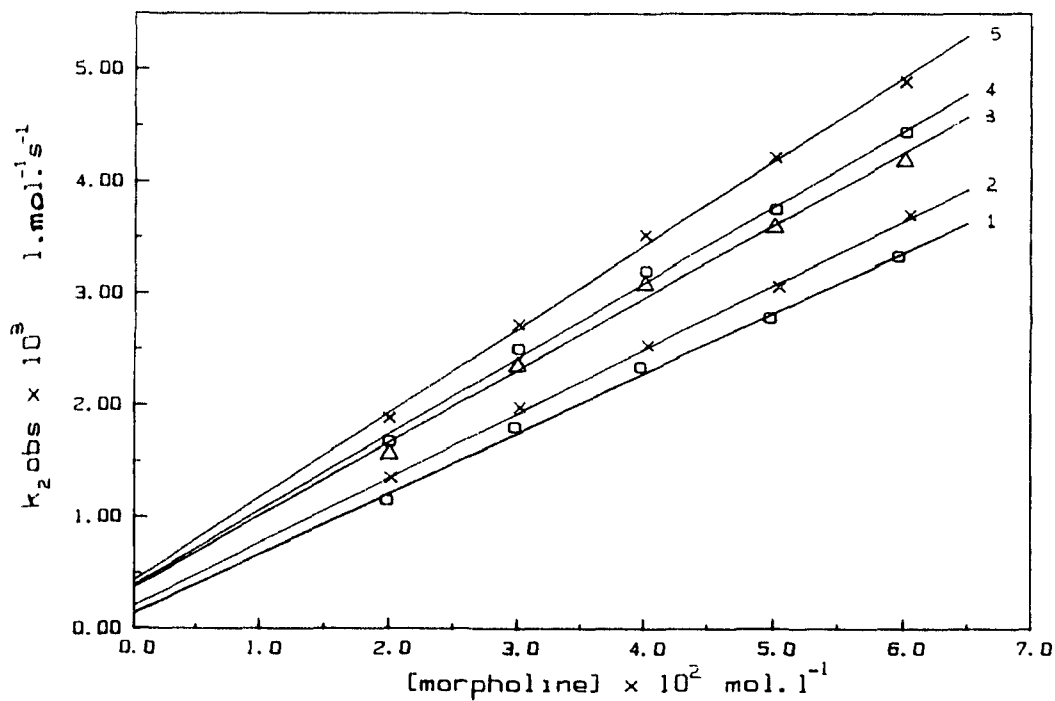


Figure 25: $k_2 \text{ obs}$ vs $[\text{morpholine}]$ plot for the reaction of 1,1-difluoro-2,2-di(4-cyanophenyl)ethylene with morpholine in acetonitrile at different temperatures. (1) 25, (2) 30, (3) 35, (4) 40 and (5) 45°C.

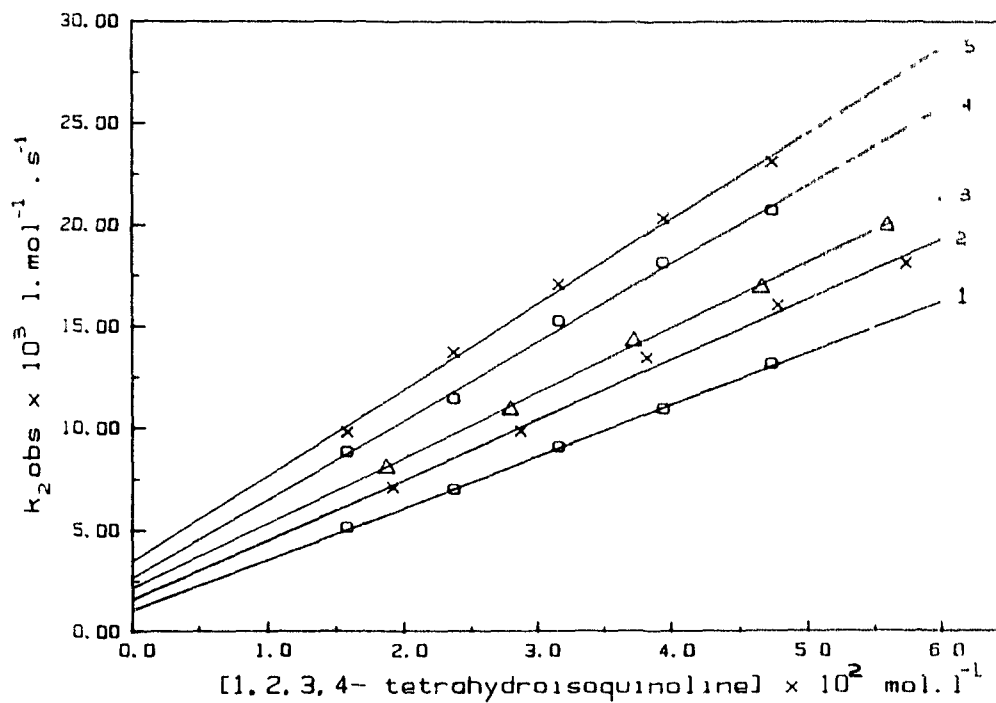


Figure 26: k_2 obs vs [1,2,3,4-tetrahydroisoquinoline] plot for the reaction of 1,1-difluoro-2,2-di(4-cyanophenyl)ethylene with 1,2,3,4-tetrahydroisoquinoline in acetonitrile at different temperatures. (1) 20, (2) 25, (3) 30, (4) 35 and (5) 40°C.

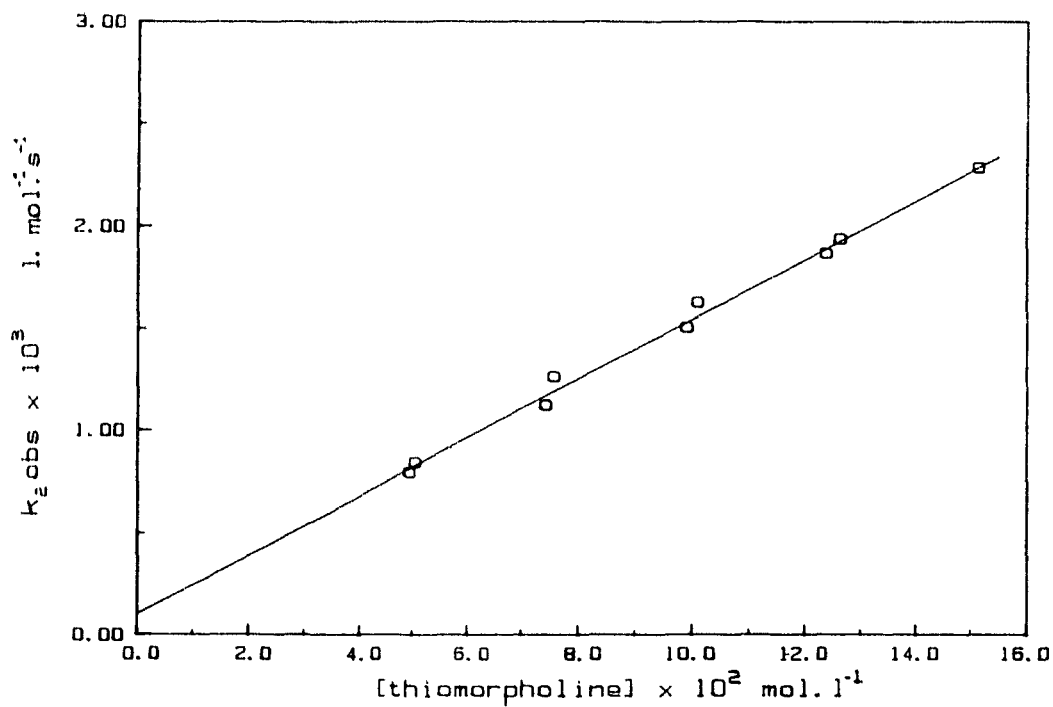


Figure 27: k_2 obs vs [thiomorpholine] plot for the reaction of 1,1-difluoro-2,2-di(4-cyanophenyl)ethylene with thiomorpholine in acetonitrile at 25°C.

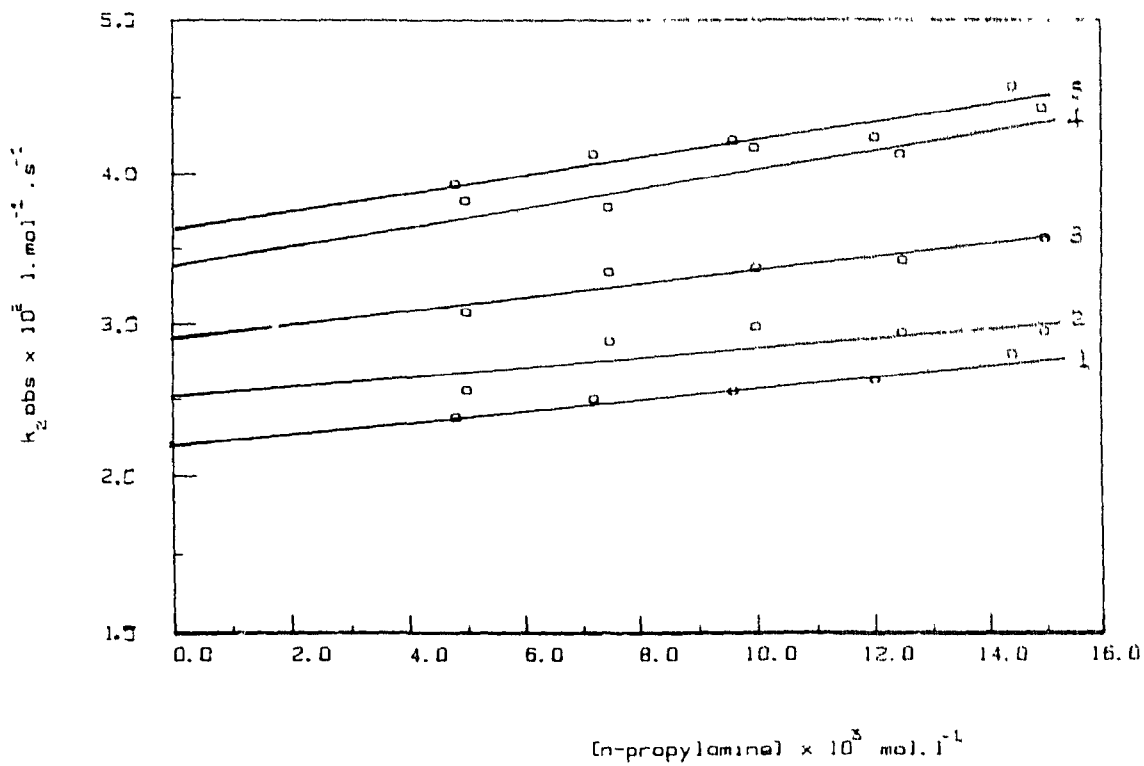


Figure 28: k_2 , obs vs [n-propylamine] plot for the reaction of 1,1-difluoro-2,2-di(4-cyanophenyl)ethylene with n-propylamine in acetonitrile at different temperatures. (1) 15, (2) 20, (3) 25, (4) 30 and (5) 35°C.

From Figures 18 to 23, it can be seen that the kinetic behaviour of pyrrolidine, morpholine, thiomorpholine and 1,2,3,4,-tetrahydroisoquinoline is similar to that of piperidine. The first order rate constants for these amines were fitted to equation (4) (Figures 24 to 27), and the calculated amine catalysed and uncatalysed rate constants and their standard deviations are tabulated in Tables 15 to 18 with the first- order rate constants.

Although n-propylamine behaves in the same way as other amines, the contribution of the catalytic route is negligible as can be seen from the k_3 / k_2° ratios from Table 20. For example, the ratio is 14 at 25°C. In order to verify the results, each set of measurements was repeated and in most cases the first order rate constants were reproduced within the experimental error. The contribution of the catalytic route under the experimental conditions ($k_3[B] / k_2^\circ$) was less than 20 percent. This causes the high standard error in the rate constants k_3 and in the activation parameters derived from them.

In contrast to the other amines, the observed pseudo first-order rate constants for 1,1,3,3-tetramethylguanidine (TMG) were linearly related to the amine concentrations (Figure 23), indicating the absence of a catalytic route. The reaction is only first-order with respect to amine. The calculated second-order rate constants are given in Table 21.

The activation parameters for amine catalysed and

uncatalysed reactions are tabulated in Table 22. For all the amines which react via both amine catalysed and uncatalysed routes, the enthalpy of activation for catalytic route is smaller than that for uncatalysed route. This is in agreement to the results obtained in the first system. In general, the enthalpy of activation for the amine catalysed and uncatalysed reaction decreases with the basicity of the amine.

Although TMG is the strongest base among the amines used, no catalysis was observed. This could be used as further evidence for the absence of route (c) in Scheme 12. Since TMG is the strongest base, it should show strong catalysis if route (c) were involved.

The second order rate constant for TMG is approximately 3 orders of magnitude less than one would predict from its pK_b value (Figure 29) assuming the same mechanism for TMG as for the other amines studied. In addition, 1,3 -diphenylguanidine which is a stronger base than morpholine does not react with this substrate. This shows that the guanidine bases react via a different mechanism.

Table 22

The activation parameters for the amine catalysed and uncatalysed reactions of 1,1-difluoro-2,2-di-(4-cyanophenyl)ethylene with amines in acetonitrile.

Amine	pK _a in CH ₃ CN	Act.parameters for uncatalysed reaction		Act.parameters for catalysed reaction	
		ΔH^\ddagger (kJ.mol ⁻¹)	ΔS^\ddagger (J.mol ⁻¹ .K ⁻¹)	ΔH^\ddagger (kJ.mol ⁻¹)	ΔS^\ddagger (J.mol ⁻¹ .K ⁻¹)
Pyrrolidine	19.58	14 ± .1	-213 ± 2	5 ± 0.5	-202 ± 2
Piperidine	18.92	26 ± 1	-202 ± 2	8 ± 1	-211 ± 4
1,2,3,4-tetra-					
hydroisoquinoline	17.25	42 ± 3	-157 ± 10	17 ± 1	-198 ± 4
Morpholine	16.61	44 ± 5	-171 ± 16	11 ± 1	-234 ± 4
n-Propylamine	18.22	17 ± 1	-216 ± 4	17 ± 8	-195 ± 29
TMG	23.30	34 ± 2	-145 ± 5		

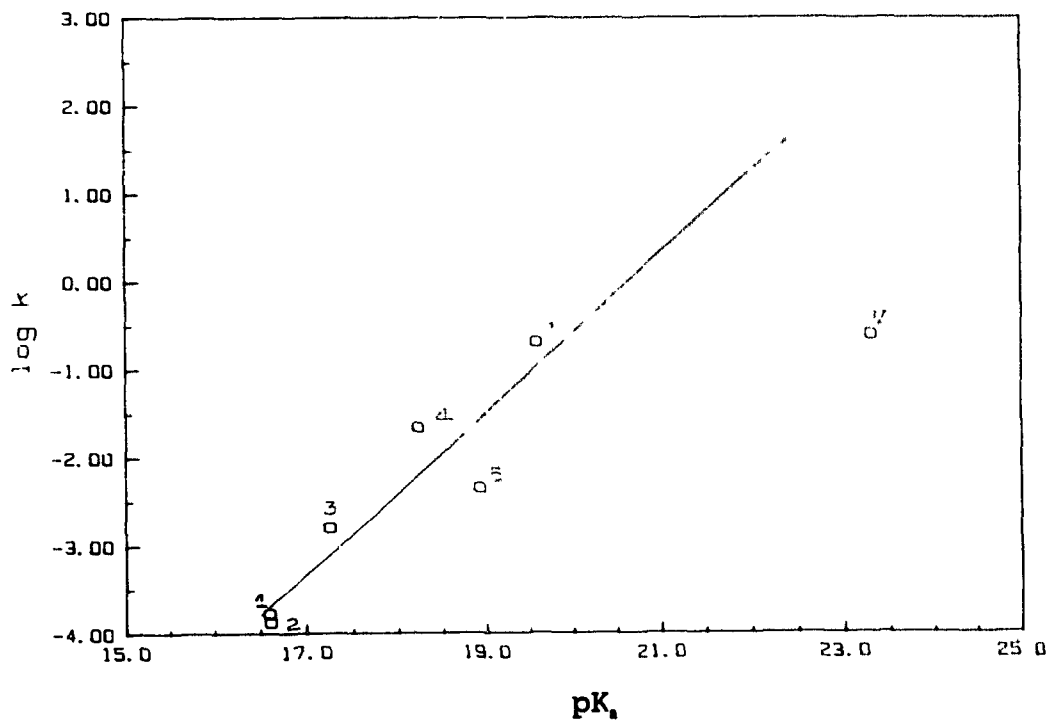
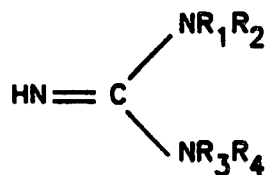


Figure 29: $\log k_2$ vs pK_a plot for the reaction of 1,1-difluoro-2,2-di(4-cyanophenyl)ethylene with various amines.

(1) thiomorpholine, (2) morpholine, (3) 1,2,3,4-tetrahydroisoquinoline, (4) n-propylamine (5) piperidine (6) pyrrolidine and (7) TMG.

The reaction of 1,1-difluoro-2,2-di(4-cyanophenyl)ethylene with TMG was studied in the presence of different concentrations of N-methylpyrrolidine and it was found that the N-methylpyrrolidine does not catalyse the reaction, even though N-methylpyrrolidine does catalyse the reaction of this substrate with piperidine. It was also found that 1,3-diphenylguanidine catalyses the reaction of 1,1-difluoro-2,2-di(4-cyanophenyl)ethylene with piperidine, and the catalytic rate constants for N-methylpyrrolidine (pK_a 18.42) and 1,3-diphenylguanidine (pK_a 17.90) are 1.46 and 0.46 $l^2 \cdot mol^{-2} \cdot s^{-1}$, respectively (Table 29, Chapter 5). These observations show that the absence of catalysis in the reaction of 1,1-difluoro-2,2-di(4-cyanophenyl)ethylene with TMG (pK_a 23.3) must be due to some special feature of the intermediate zwitterion and not due to the lack of power of TMG as a base catalyst.

Guanidine bases, 20, differ from other bases in two aspects. One of them is the presence of two other basic nitrogens and the other one is the presence of a double bond which causes extra stabilization of the positive charge in the zwitterion formed in the first step of the reaction.



20

R_1, R_2, R_3 and $R_4 = \text{H, alkyl or aryl}$.

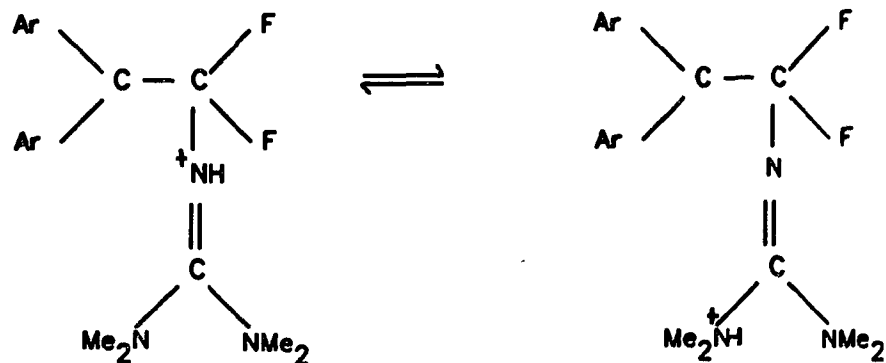
Absence of amine catalysis could be observed under the following conditions.

(1) The nucleophilic attack is the rate determining step.

In this case both amine catalysed and uncatalysed routes would be first order with respect to amine. If the presence of four bulky methyl groups in the TMG molecule could make the attack by TMG the slowest among the amines studied, and if the attack is slower than the fluoride ion expulsion, then the reaction would be first order with respect to amine even for amine catalysed route. But Figure 29 shows that the second order rate constant for TMG is the largest when compared with the other amines. Therefore, nucleophilic attack is not the rate determining step.

(2) Intramolecular catalysis.

Since there are two other basic centers (N_1 and N_2) in the TMG molecule, one of these basic centers might participate instead of an external amine molecule in the proton transfer step. That is,

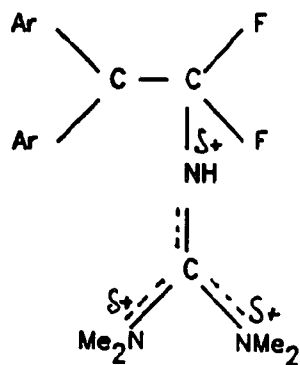


In this case again the amine catalysed route will be first order with respect to amine, because there is no additional amine molecule involved in the proton transfer step. In fact base catalysis was not observed in the reaction of 1,1-dicyano-2-p-dimethylaminophenyl-2-trifluoroethoxyethylene with 1,2- and 1,3-diaminopropane and their mono N,N-dimethyl derivatives in acetonitrile (103). A mechanism which involves intramolecular proton transfer to the second basic center has been proposed for this reaction. In this case, the second order rate constant was higher than the corresponding uncatalysed counterpart of the monoamines which is opposite to what was observed in the reaction of TMG with 1,1-difluoro-2,2-di-(4-cyanophenyl)ethylene. Moreover, the pK_a difference between the two basic centers in the 1,2- and 1,3-diaminopropane is much less than that in TMG. The pK_a difference in 1,2- and 1,3- diaminopropane ranges between 2-3 in water while in TMG the difference is more than 10 pK_a units. Therefore, the occurrence of intramolecular catalysis in the proton transfer step is very unlikely in the case of TMG.

- (3) The uncatalysed route is faster than the amine catalysed route.

In the zwitterion formed between 1,1-difluoro-2,2-di(4-cyanophenyl)ethylene and TMG, 21, the positive charge is delocalized in the amino part of the molecule. Due to the

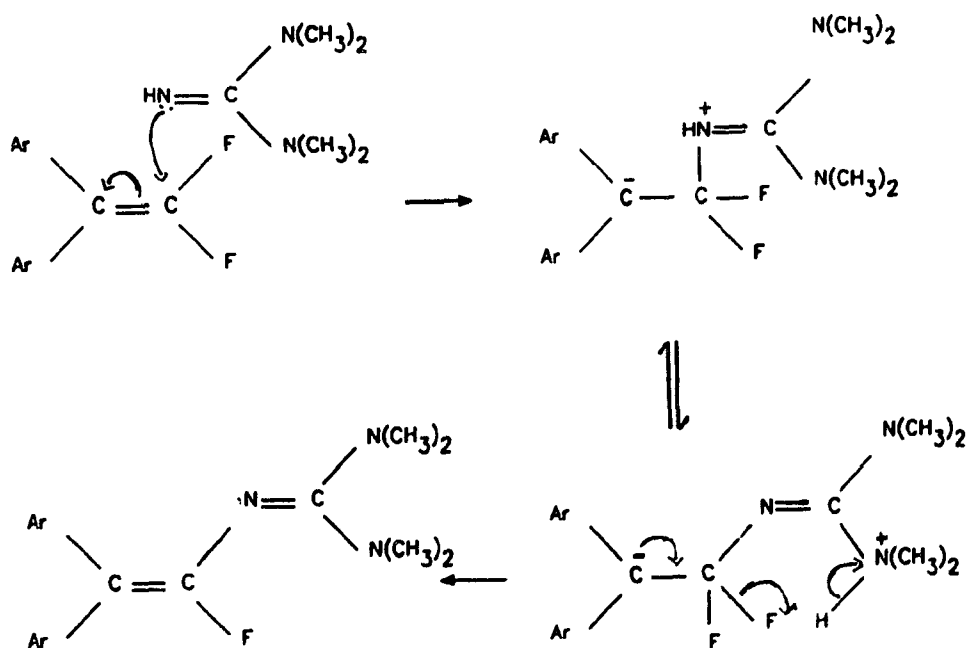
removed from the zwitterion. Therefore, the catalysed route is not observed.



21

In addition, the uncatalysed reaction could be the preferred path because it is assisted by a hydrogen bond as shown in Scheme 15.

Scheme 15



That is the reaction is not catalysed in the proton transfer step but is internally catalysed in the F expulsion step.

4.3 The Brønsted relationship.

Brønsted relationship is again a linear free energy relationship presented in two forms in equations [34] and [35].

$$k_A = G_A (K_A)^\alpha \quad [34]$$

$$k_B = G_B (K_B)^\beta \quad [35]$$

where, k_A and k_B are the catalytic constants for acid and base catalysis and K_A and K_B are the equilibrium constants for dissociation of acid and protonation of base respectively. G_A , G_B , α and β are constants for a reaction which involves a series of catalysts with different acidic or basic strengths. α and β are known as Brønsted coefficients.

This relationship was derived by Brønsted and Pedersen (92), in order to correlate the rates of general-acid base catalysed decomposition of nitramide. In fact, this was the first example of a linear free energy relationship

between rate and equilibrium constants. This is also known as the Brønsted catalysis law. In most cases the exponents α and β are positive and less than unity (92). The magnitude of these exponents may give information about the extent of proton transfer in the transition state.

According to the Brønsted catalysis law, the logarithm of the rate constant for a general-acid-catalysed reaction is a linear function of the pK_a value of the acid. A similar relationship applies for general-base-catalysed reactions. This law is restricted to series of acids and bases which are similar in structure.

The catalysed and uncatalysed rate constants for the reaction of 1,1-difluoro-2,2-di(4-cyanophenyl)ethylene with various amines at 25°C are tabulated in Table 23 together with the pK_a values of the conjugate acids of the amines in acetonitrile. The catalysed rate constants show a linear correlation with the pK_a values (in acetonitrile) of the amines (Figure 30). The Brønsted plot for the catalysed rate constants gives a slope 0.85 ± 0.14 with the correlation coefficient 0.95.

This value is very similar to the one reported for the reaction of 2,2-di(4-nitrophenyl)-1,1-difluoroethylene with amines in acetonitrile (84). The Brønsted coefficients in both cases are considerably higher than for reaction which involve proton transfer from a saturated carbon atom to amines. For example, the Brønsted coefficients of 0.55 ± 0.06

have been reported for the reaction of substituted and unsubstituted 1-aryl-1-nitroethane with piperidine, piperazine and morpholine in water (105). Similarly, the reaction of 4-nitrophenylcyanomethane and its deuterated analog with 2,2,6,6-tetramethylpiperidine, 1,2,2,6,6-pentamethylpiperidine and 3,3,6,9,9-pentamethyl-2,10-diazabicyclo[4.4.0]dec-1-ene in acetonitrile gives a Brønsted coefficient closer to 0.5 (106).

Therefore, the high Brønsted coefficient observed for the reaction of 1,1-di(4-cyanophenyl)-2,2-difluoroethylene and 2,2-di(4-nitrophenyl)-1,1-difluoroethylene with various amines again suggests that the proton is extensively transferred in the transition state of the proton transfer step of catalysed reaction. Thus route (c) in Scheme 12 is less likely than route (b).

The uncatalysed rate constants for the amines other than TMG also show a linear correlation with pK_a . Since the amines act as nucleophile in the uncatalysed reaction, the linear correlation shows that the nucleophilicity of these amines is parallel to their basicity. The negative deviation of TMG suggests that TMG is a much weaker nucleophile than it is a base.

Table 23

The amine catalysed and uncatalysed rate constants (k_2 and k_3 , respectively) at 25°C for the reaction of 1,1-difluoro-2,2-di(4-cyanophenyl)ethylene with various amines.

Amine	pK_a in CH_3CN	k_3 ($l^2 \cdot mol^{-2} \cdot s^{-1}$)	k_2 ($l \cdot mol^{-1} \cdot s^{-1}$)
Pyrrolidine	19.58	20.9	1.99×10^{-1}
Piperidine	19.06	1.94	4.34×10^{-3}
n-Propylamine	18.22	8.22×10^{-1}	2.16×10^{-2}
1,2,3,4-tetra- hydroiso- quinoline	17.25	2.95×10^{-1}	1.58×10^{-3}
Morpholine	16.61	5.38×10^{-2}	1.33×10^{-4}
Thiomorpholine	16.60	1.41×10^{-2}	1.67×10^{-4}
TMG	23.30		2.38×10^{-1}

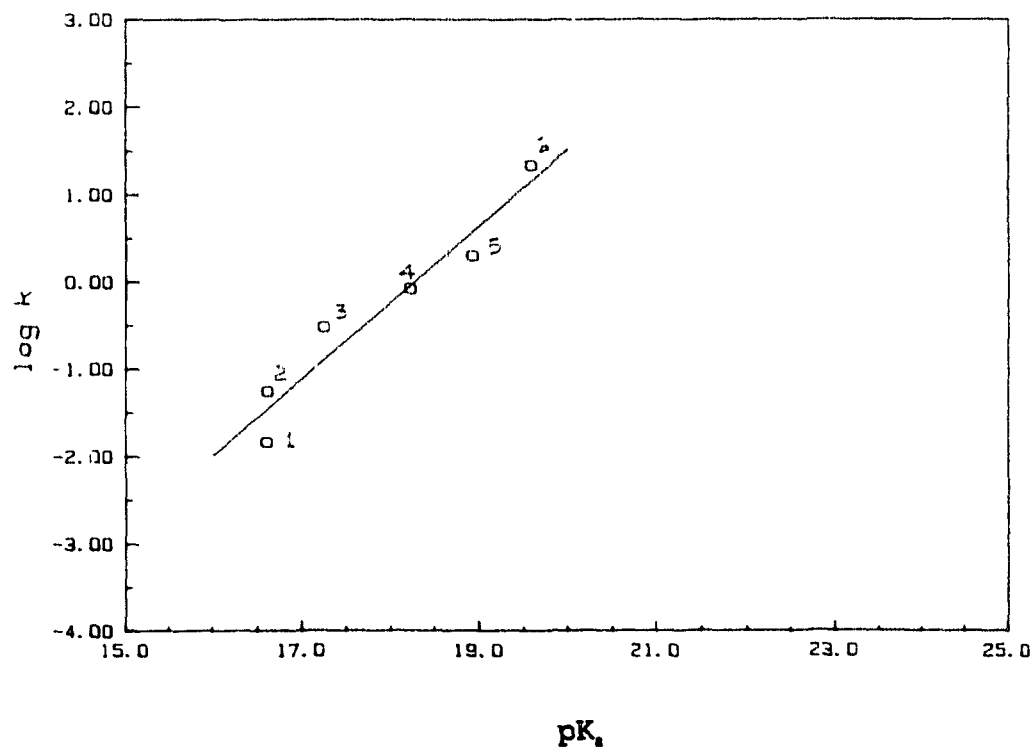


Figure 30: $\log k$, vs pK_b plot for the reaction of 1,1-difluoro-2,2-di(4-cyanophenyl)ethylene with various amines.

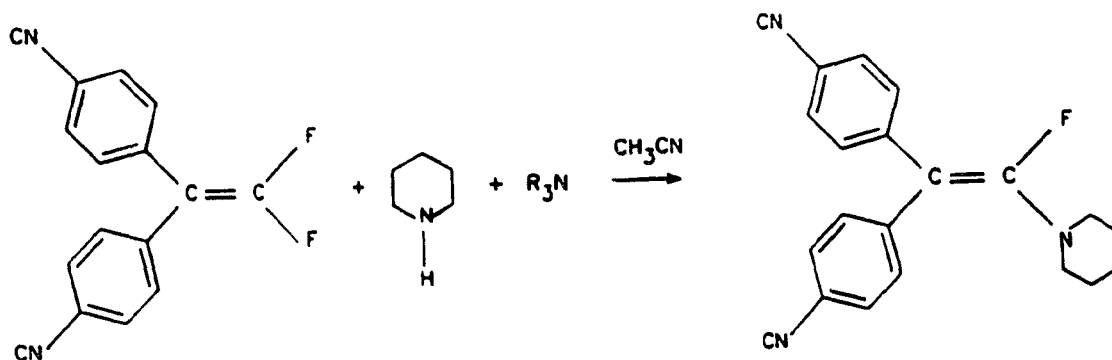
(1) thiomorpholine, (2) morpholine, (3) 1,2,3,4-tetrahydroisoquinoline, (4) n-propylamine (5) piperidine and (6) pyrrolidine.

5. Kinetics of the reaction of 1,1-difluoro-2,2-di-(4-cyanophenyl)ethylene with piperidine in the presence of added tertiary amines.

5.1 General.

In the study of the reaction of 1,1-difluoro-2,2-diphenylethylene and its *para* substituted analogs with various amines (Chapters 2 & 4), it was found that except in the case of TMG, the reaction is catalysed by amines. It was also suggested that the amine catalysis takes place in the proton transfer step. If this is true, then tertiary amines, which do not react with the substrate themselves, should also catalyse the reaction. In fact, in a preliminary study, it was found that the reaction of 1,1-difluoro-2,2-di(4-cyanophenyl)ethylene with piperidine is catalysed by added tertiary amines. Therefore, in this chapter, the reaction of 1,1-difluoro-2,2-di(4-cyanophenyl)ethylene with piperidine has been studied in presence of added tertiary amines (System 3).

System 3



For R_3N = N-methylpyrrolidine, N-methylpiperidine, N-methylmorpholine, 1,3-diphenylguanidine and DBU.

Although, 1,3-diphenylguanidine is not a tertiary amine, it was found that it does not react with the substrate. Therefore, this amine was used as a catalyst and its catalytic rate constant was calculated.

5.2 Results and Discussion.

The reaction is catalysed by added tertiary amines. In presence of added amine, equation [4] is extended to equation [36].

$$k_{2,obs} = k_2^{\circ} + k_3 [\text{piperidine}] + k_{cat} [\text{amine}] \quad [36]$$

$$\text{where } k_{2,obs} = k_{1,obs} / [\text{piperidine}]$$

At constant concentrations of the substrate and piperidine, $k_{2,obs}$ would be linearly related to the concentration of tertiary amine and the slope of this plot would be the catalytic rate constant.

Therefore, the concentration of piperidine was kept constant and the concentration of tertiary amine was varied. The observed pseudo first-order rate constants at various concentration of tertiary amines are tabulated in Tables 24 - 28. The observed second-order rate constants correlate linearly with the concentration of the tertiary amines (Figures 31 to 35). The slope of the plot gives the catalytic

rate constant of added tertiary amine. The calculated catalytic rate constants of amines and their standard deviations are tabulated in Table 29 together with the pK_a values of the conjugate acids of the tertiary amines.

Table 24

The pseudo first-order rate constants for the formation of 1-fluoro-1-piperidino-2,2-di(4-cyanophenyl)ethylene from the reaction of 1,1-difluoro-2,2-di(4-cyanophenyl)ethylene* with piperidine** in presence of N-methylpyrrolidine in acetonitrile.

[N-methylpyrrolidine] x 10 ³ mol.l ⁻¹	k _i x 10 ⁴ s ⁻¹
4.02	1.31 ± .01
8.04	1.59 ± .01
12.06	2.10 ± .03
16.08	2.40 ± .03
20.10	2.90 ± .04

* initial concentration 2.5 x 10⁻⁵ mol.l⁻¹.

** initial concentration 6.79 x 10⁻³ mol.l⁻¹

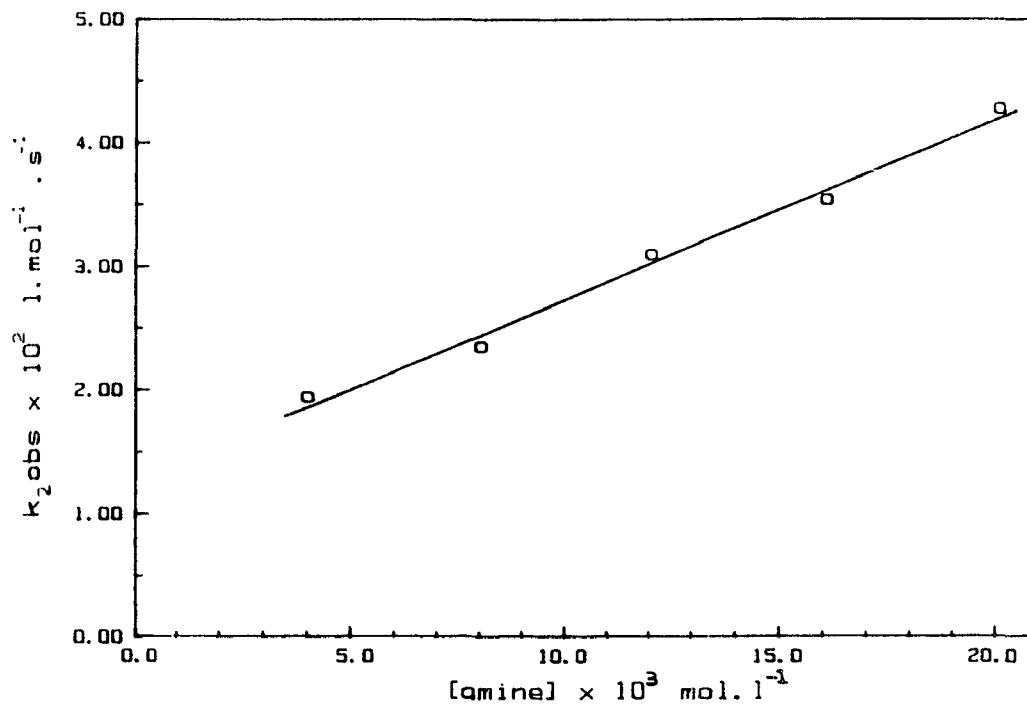


Figure 31: $k_{2,obs}$. vs [amine] plot for the reaction of 1,1-difluoro-2,2-di(4-cyanophenyl)ethylene with piperidine in presence of different concentration of N-methylpyrrolidine.

Table 25

The pseudo first-order rate constants for the formation of 1-fluoro-1-piperidino-2,2-di(4-cyanophenyl)ethylene from the reaction of 1,1-difluoro-2,2-di(4-cyanophenyl)ethylene* with piperidine** in presence of N-methylpiperidine in acetonitrile.

[N-methylpiperidine] x 10 ² mol.l ⁻¹	k ₁ x 10 ⁴ s ⁻¹
1.46	1.44 ± .01
2.92	1.68 ± .01
4.38	1.89 ± .01
5.84	2.04 ± .01
7.30	2.29 ± .01

* initial concentration 2.5 x 10⁻⁵ mol.l⁻¹.

** initial concentration 7.25 x 10⁻³ mol.l⁻¹

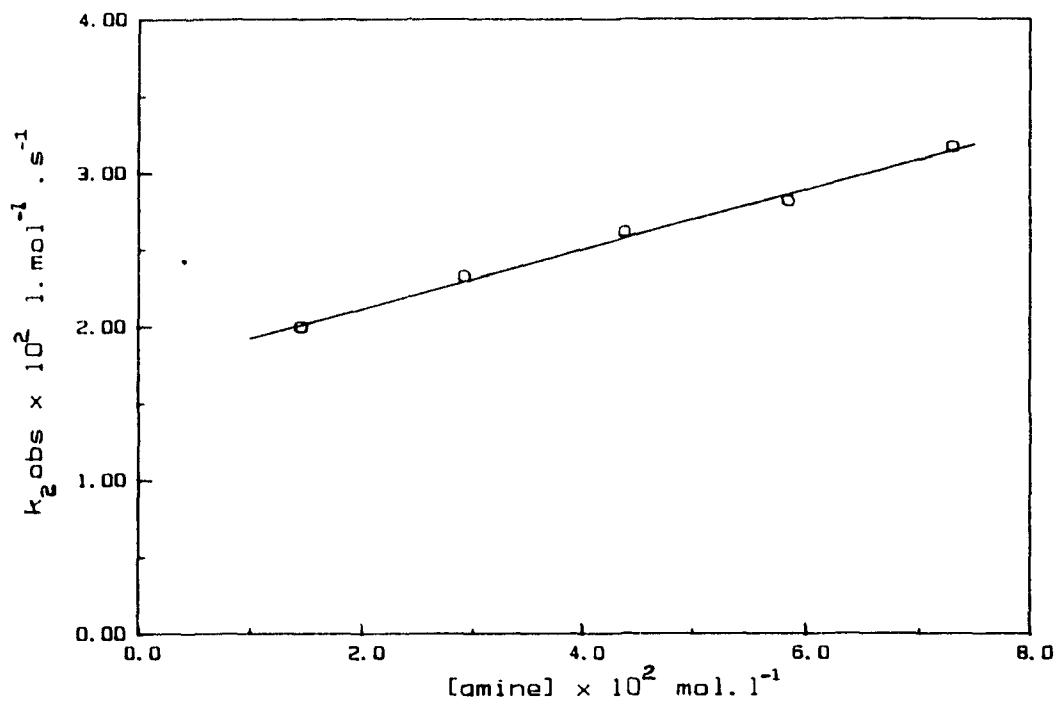


Figure 32: $k_{2,obs}$. vs $[\text{amine}]$ plot for the reaction of 1,1-difluoro-2,2-di(4-cyanophenyl)ethylene with piperidine in the presence of different concentration of N-methylpiperidine.

Table 26

The pseudo first-order rate constants for the formation of 1-fluoro-1-piperidino-2,2-di(4-cyanophenyl)ethylene from the reaction of 1,1-difluoro-2,2-di(4-cyanophenyl)ethylene* with piperidine** in presence of N-methylmorpholine in acetonitrile.

[N-methylmorpholine] x 10 mol.l ⁻¹	k ₁ x 10 ⁴ s ⁻¹
0.549	1.43 ± .01
1.099	1.74 ± .01
1.648	2.01 ± .01
2.197	2.28 ± .01
2.747	2.60 ± .01

* initial concentration 2.5×10^{-5} mol.l⁻¹.

** initial concentration 6.96×10^{-3} mol.l⁻¹

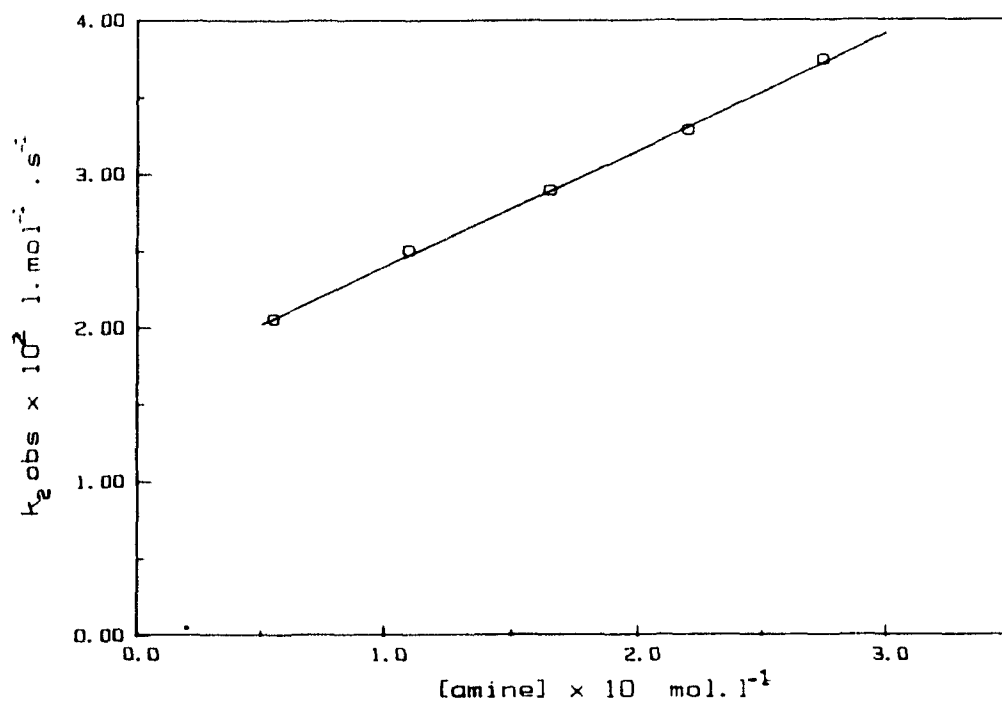


Figure 33: k_{obs} . vs [amine] plot for the reaction of 1,1-difluoro-2,2-di(4-cyanophenyl)ethylene with piperidine in the presence of different concentration of N-methylmorpholine.

Table 27

The pseudo first-order rate constants for the formation of 1-fluoro-1-piperidino-2,2-di(4-cyanophenyl)ethylene from the reaction of 1,1-difluoro-2,2-di(4-cyanophenyl)ethylene* with piperidine** in presence of 1,8-diazabicyclo[5.4.0]-undec-7-ene (DBU) in acetonitrile.

[DBU] $\times 10^5$ mol.l ⁻¹	$k_1 \times 10^4$ s ⁻¹
2.22	2.40 \pm .01
4.43	3.17 \pm .02
6.65	3.80 \pm .04
8.87	4.52 \pm .07
11.09	5.19 \pm .05

* initial concentration 2.5×10^{-5} mol.l⁻¹.

** initial concentration 7.05×10^{-3} mol.l⁻¹

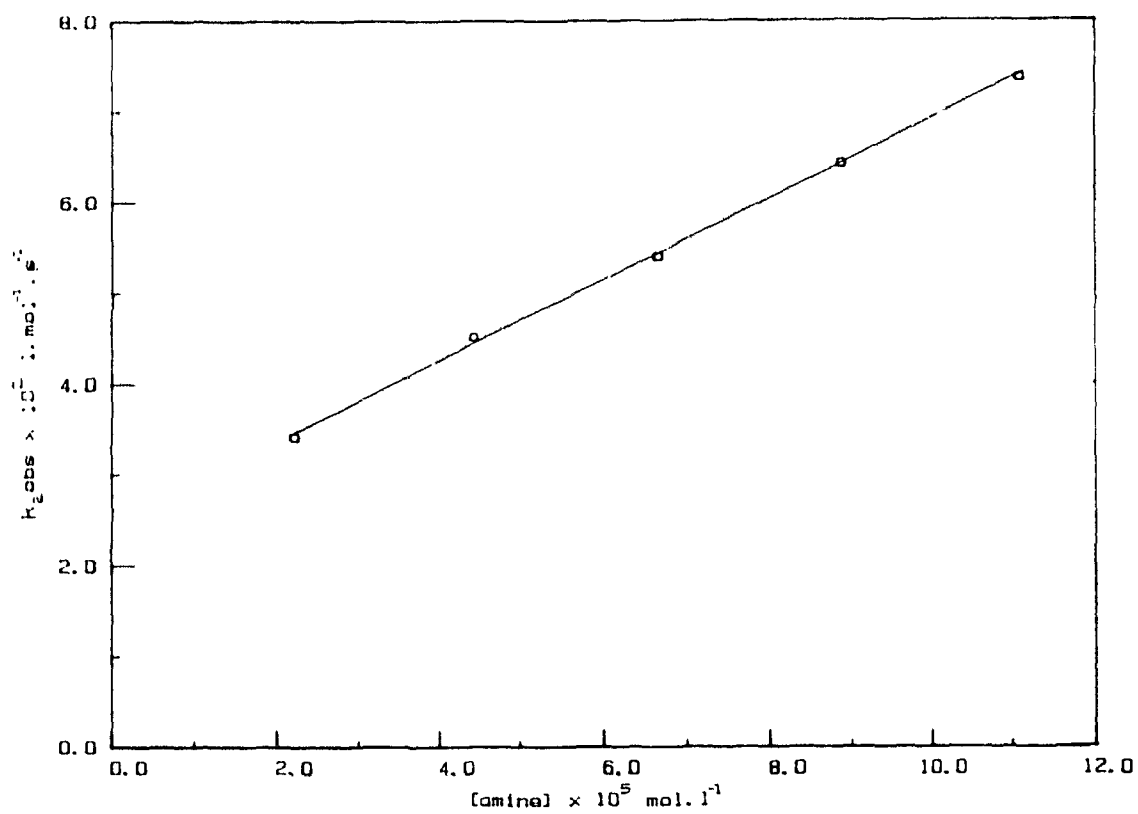


Figure 34: k_{obs} . vs [amine] plot for the reaction of 1,1-difluoro-2,2-di(4-cyanophenyl)ethylene with piperidine in the presence of different concentration of DBU.

Table 28

The pseudo first-order rate constants for the formation of 1-fluoro-1-piperidino-2,2-di(4-cyanophenyl)ethylene from the reaction of 1,1-difluoro-2,2-di(4-cyanophenyl)ethylene* with piperidine** in presence of 1,3-diphenylguanidine in acetonitrile.

[1,3-diphenylguanidine] x 10 ² mol.l ⁻¹	k ₁ x 10 ⁴ s ⁻¹
1.19	1.55 ± .01
2.38	1.97 ± .01
3.57	2.34 ± .01
4.76	2.68 ± .02
5.95	3.06 ± .04

* initial concentration 2.5 x 10⁻⁵ mol.l⁻¹.

** initial concentration 6.85 x 10⁻³ mol.l⁻¹

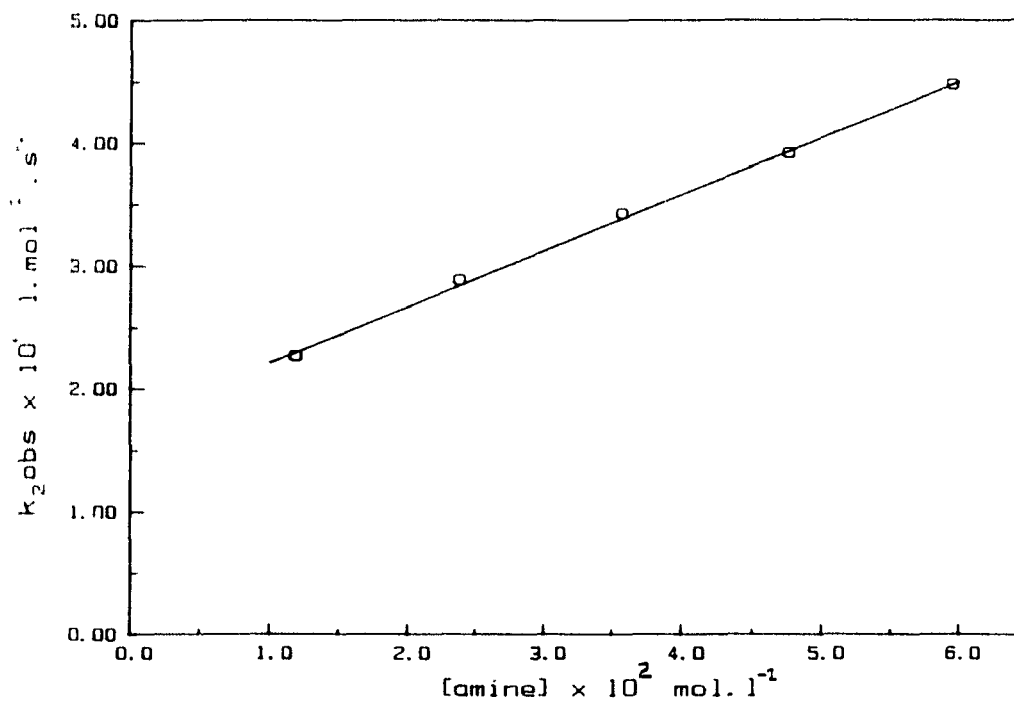


Figure 35: $k_{2,obs}$. vs [amine] plot for the reaction of 1,1-difluoro-2,2-di(4-cyanophenyl)ethylene with piperidine in the presence of different concentration of 1,3-diphenylguanidine.

Table 29.

The catalytic rate constants of tertiary amines at 25°C

Amine	pK_a in CH_3CN	rate constant $l^2 \cdot mol^{-2} \cdot s^{-1}$.
N-methylpyrrolidine	18.42	$1.46 \pm .10$
N-methylpiperidine	17.99	$1.90 \pm .08 \times 10^{-1}$
N-methylmorpholine	15.68	$7.50 \pm .10 \times 10^{-2}$
1,3-diphenyl- guanidine	17.90	$4.58 \pm .09 \times 10^{-1}$
DBU	23.91	$4.42 \pm .07 \times 10^{-2}$

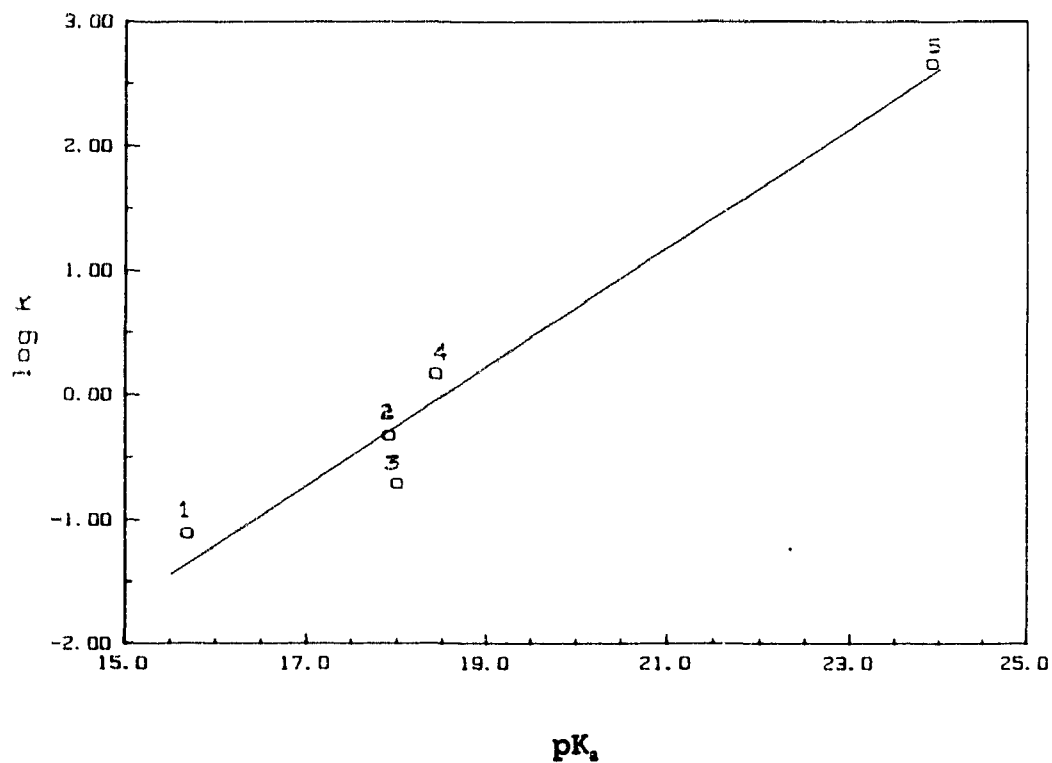
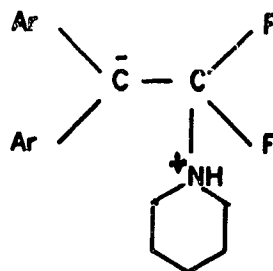


Figure 36: $\log k_{cat}$ vs pK_a plot for the reaction of 1,1-difluoro-2,2-di(4-cyanophenyl)ethylene with piperidine in the presence of different tertiary amines. (1) N-methylmorpholine, (2) 1,3-diphenylguanidine, (3) N-methylpiperidine, (4) N-methyl-

The catalytic rate constants for N-methyl amines are lower than the corresponding secondary amines. This can be attributed to the lower pK_a values of these amines when compared to the secondary amines. The catalytic rate constants of tertiary amines also show linear correlation with the pK_a values of the amines in acetonitrile (Figure 36). The slope of the plot in this case is 0.48 ± 0.08 and the correlation coefficient is 0.96. This slope is rather small when compared to that of secondary and primary amines. This can be explained by considering the proton transfer steps in System 2 and System 3. In System 2, when different amines are used, these amines take part in both formation of zwitterion and proton transfer. Also, in the proton transfer step the structure of both zwitterion and the amine changes when different amines are used. But in System 3, the proton transfer takes place from the same zwitterion 22 to different tertiary amine. That is, in proton transfer step in System 3, only the amine is changed not the zwitterion.



The higher Brønsted coefficient obtained in System 2 is due to the participation of the amines in both steps. That is, the slope obtained in System 2, refers to the formation of carbanion from the olefin while in System 3, the slope refers to the formation of carbanion from the zwitterion,²². In addition, due to the steric hindrance, the extent of proton transfer in the transition state would be less for tertiary amines when compared to the secondary amines and hence the tertiary amines give smaller Brønsted coefficient than the secondary amines.

5.3 Summary.

The reaction of 1,1-difluoro-2,2-diphenylethylene and its *para* substituted analogs with different amines leads to monosubstituted and disubstituted products. Formation of disubstituted product is much slower than the formation of monosubstituted product. In most cases, the disubstituted product was not observed under the experimental conditions. Since the carbon-carbon double bond in the substrate is activated by fluorine towards nucleophilic attack, substitution of one fluorine atom by an amine molecule makes the double bond less reactive towards the nucleophile. Therefore, formation of disubstituted product becomes slower than the formation of monosubstituted product.

The kinetics for the formation of monosubstituted product have been studied. The kinetics of the reaction of 1,1-difluoro-2,2-diphenylethylene and its parasubstituted analogs with piperidine (System 1) and the reaction of 1,1-difluoro-2,2-di(4-cyanophenyl)ethylene with different amines (System 2) and the reaction of 1,1-difluoro-2,2-di(4-cyanophenyl)ethylene with piperidine in presence of tertiary amines (System 3) have been studied.

In the study of the reaction of 1,1-difluoro-2,2-diphenylethylene and its *para* substituted analogs with piperidine, it was found that the reaction proceeds by an amine catalysed and uncatalysed routes. The rate constants and the activation parameters for the amine catalysed and the uncatalysed reactions have been obtained. Although no intermediate was observed directly under the experimental conditions, the negative enthalpy of activation for the amine catalysed reaction (Table 10, X = H and NO₂) and the large entropy of activation for both the amine catalysed and the uncatalysed reaction suggest that the reaction is not a single step reaction. The large negative entropy of activation is attributed to the formation of zwitterion. Three alternate routes (Scheme 12) were proposed for the formation of mono substituted product. Among these three routes, (b) and (c) are amine catalysed reactions and route (a) is uncatalysed reaction.

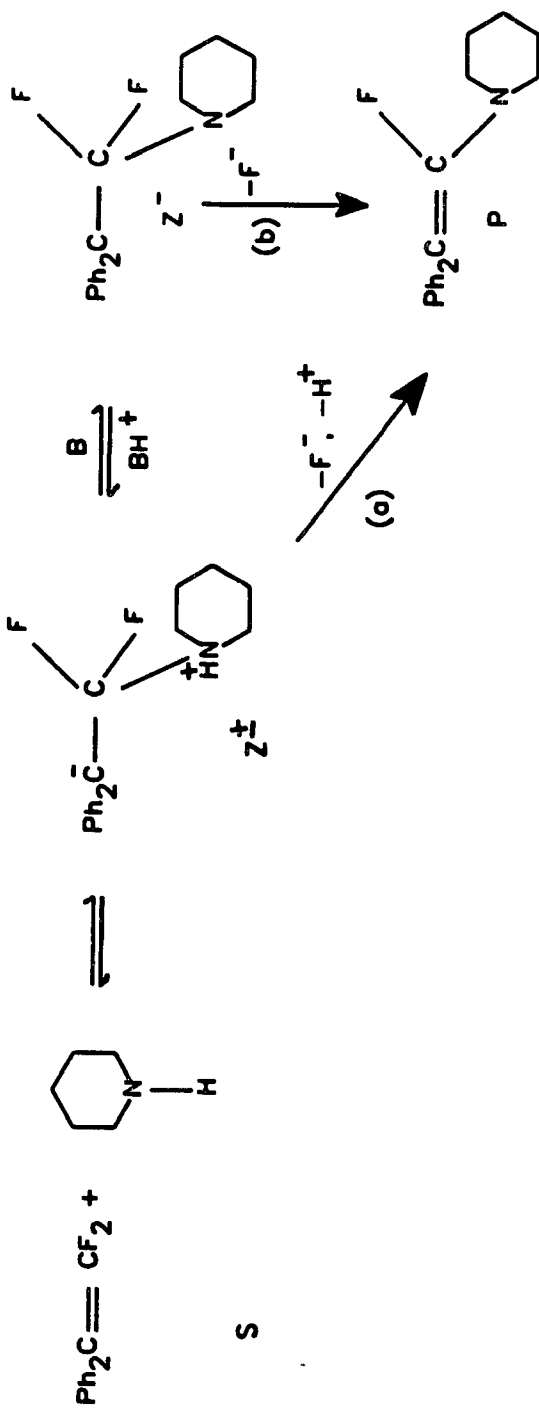
Among the two amine catalysed reactions, route (c) proceeds via the α,β -adduct which is usually a stable intermediate. Therefore, if the reaction proceeds via this route, then it would be possible to observe this intermediate. But no such intermediate was observed under the experimental conditions. Furthermore, in the reaction of 1,1-difluoro-2,2-di(4-nitrophenyl)ethylene with amines, it was found that the adduct is formed only after the formation of enamine (84).

In the study of the reaction of 1,1-difluoro-2,2-di(4-cyanophenyl)ethylene with different amines, the reaction with 1,1,3,3-tetramethylguanidine (TMG), the strongest base studied, did not show amine catalysis. If the amine catalysis observed in the case of other amines was due to route (c), then, being a strong base, TMG would show strong amine catalysis. This is contrary to the experimental observation.

These facts suggest that the reaction does not proceed via route (c). Therefore, route (c) was rejected and the experimental results are discussed with reference to Scheme 16.

The mechanism proposed in Scheme 16 is similar to the one proposed by Rappoport (7,56) and Bernasconi (41). In view of the low nucleofugality of fluoride ion, the leaving group expulsion is considered to be the rate determining step. This consideration accounts for the observed behaviour of the activation parameters as explained in terms of rate equations (Chapter 1).

Scheme 16



Most of the examples of nucleophilic vinylic substitution reactions reported in the literature, follow the addition-elimination mechanism in which nucleophilic attack is the rate determining step (26). This includes the reaction of activated vinylic carbons with thiolates and phenolates (37). Substitution reactions by amines on vinylic carbon activated by cyano groups have been reported in several solvents and these reactions proceed via the addition elimination mechanism. In most cases, the nucleophilic attack is rate determining but in some the proton transfer is rate determining (103). Thus the results reported in this thesis provide some uncommon examples of nucleophilic vinylic substitution reactions which proceed via the addition-elimination mechanism in which the leaving group expulsion is rate determining.

The Hammett correlation has been found for the amine catalysed and uncatalysed rate constants of the reaction of 1,1-difluoro-2,2-diphenylethylene and its para substituted analogs with piperidine. A reaction constant $\rho_{\text{uncat}} = 1.93 \pm 0.16$ for the uncatalysed reaction and a reaction constant $\rho_{\text{cat}} = 2.31 \pm 0.14$ for the amine catalysed reaction was obtained. These reaction constants seem reasonable for the proposed mechanism. These reaction constants yield 0.38 as the reaction constant for the proton transfer step. This value also fits well if the zwitterion (Z^+) is placed as the next member in the anilinium ion ($\rho = 2.78$) and benzylammonium ion ($\rho = 0.72$) series.

In the study of the reaction of 1,1-difluoro-2,2-di(4-cyanophenyl)ethylene with different amines, it was found that except TMG, the amines react via an amine catalysed and uncatalysed routes. TMG reacts only via uncatalysed route. The rate constants for amine catalysed and uncatalysed reactions show Brønsted relationship. The uncatalysed rate constant for TMG shows a negative deviation from the Brønsted plot. The Brønsted plot for the amine catalysed reaction gives a slope $\beta = 0.85 \pm 0.14$. A similar value has been reported for the reaction of 1,1-difluoro-2,2-di(4-nitrophenyl)ethylene with amines (84). The absence of amine catalysis in the case of TMG has been explained considering the structure of the zwitterion in which the positive charge is stabilized by delocalization. The absence of amine catalysis in the case of TMG also shows how the reaction mechanism is influenced by the structure of the nucleophile.

The reaction of 1,1-difluoro-2,2-di(4-cyanophenyl)ethylene with piperidine in the presence of added tertiary amines shows that the reaction is catalysed by tertiary amines and other amines such as 1,3-diphenylguanidine that are not reactive with the substrate themselves. The catalytic rate constants for different tertiary amines again showed a Brønsted relationship but with a slope of 0.48 ± 0.08 . This Brønsted coefficient is low when compared to the Brønsted coefficient for the amine catalysed reaction of secondary amines.

6. EXPERIMENTAL

6.1 General

Infrared spectra were obtained on a Perkin-Elmer 283B spectrophotometer. The NMR spectra were recorded on Varian EM-360L and Nicolet 360NB spectrophotometer. The mass spectra were obtained on a CEC-21-104 mass spectrometer. The uncorrected melting points were obtained on a Fisher-Johns melting point apparatus. Kinetic measurements were carried out on a Varian-Cary 219 spectrophotometer.

6.2 Solvents

Methanol was refluxed with freshly prepared magnesium methoxide and then distilled.

Dimethyl formamide was purified by azeotropic distillation with benzene and then dried over barium oxide and then distilled fractionally under vacuum. The middle fraction was used.

n-Pentane was dried over sodium and then distilled over fresh sodium.

HPLC grade acetonitrile was dried by distillation over P_2O_5 and then distilled fractionally over calcium hydride. The middle fraction corresponding to the literature boiling point was used.

6.3 Reagents

Amines were dried over potassium hydroxide pellets and then distilled fractionally over fresh potassium hydroxide. The middle fractions corresponding to the literature boiling points were used.

Synthesis of 1,1-difluoro-2,2-diphenylethylene and its *para* substituted analogs:

1,1-difluoro-2,2-diphenylethylene was synthesised according to the method described by Fuqua and co-workers (107), using the following reaction.



The sodium chlorodifluoroacetate required for this synthesis was also synthesised according to the method described by Fuqua and co-workers (108).

4,4'-Dibromobenzophenone, 4,4'-dicyanobenzophenone and 4,4'-di(trifluoromethyl)benzophenone were synthesised in order to synthesise *para* substituted analogs of 1,1-difluoro-2,2-diphenylethylene using the same method. An attempt to synthesise 1,1-di(4-cyanophenyl)-2,2-difluoroethylene using the same procedure was not successful. Therefore, the method

described by Naae and Burton (109) was used for the synthesis via the following reaction.



Hexamethylphosphorotriamide (HMPT) required for this synthesis was prepared from phosphorous trichloride using the method described by Mark (110).

Synthesis of Sodium Chlorodifluoroacetate (108):

A solution of chlorodifluoroacetic acid (0.758 moles, 99.0g) in methanol(150ml.) was added slowly to a cooled, stirred solution of sodium hydroxide(0.758 moles, 30.35g) in methanol(350ml) while maintaining the temperature below 40°C. The methanol was removed under vacuum and the salt was pulverized and dried overnight at room temperature under vacuum. The salt was again dried in the same way immediately before use.

Synthesis of 1,1-difluoro-2,2-diphenylethylene (107):

A solution of benzophenone(0.1 mole, 18.22 g) and tributylphosphine(0.11 mole, 22.26 g) in DMF(20ml.) was stirred at 160°C. A solution of sodium chlorodifluoro acetate

(0.2 mole, 30.7 g) in DMF (100 ml.) was slowly added to the above solution over a period of one hour. The flask contents were flash distilled under vacuum to remove DMF and the inorganic substance was removed by treating the residue with benzene and then by filtration. Then the benzene was evaporated and the olefin was separated by column chromatography using n-pentane as the eluent, (yield 9 %). IR(neat, μ): 5.85, 6.68, 6.90, 8.00, 8.22, 10.10, 13.10 and 14.35; $^1\text{H-NMR}$ (δ ppm, CDCl_3): 7.0-7.5 (m); $^{19}\text{F-NMR}$ (ppm, CDCl_3): -38 (s) (std. $\text{F}_2\text{CBr}\cdot\text{CH}_2\text{Br}$); M. S. (m/z): 216 (100 %), 217 (15.4 %).

Synthesis of 4,4'-dibromobenzophenone (111):

Anhydrous aluminum chloride (68.25g, 0.51mol) and dry carbon tetrachloride (150 ml) were placed in a one litre three-necked round-bottom flask fitted with a mechanical stirrer, dropping funnel and a reflux condenser connected with a trap for absorbing the hydrogen chloride evolved. The mixture was cooled to 10-15°C and bromobenzene (7.5 ml) was added at once. Once the reaction had started, the reaction mixture was cooled again and a mixture of bromobenzene (97 ml, total of 1.005mol) and carbon-tetrachloride (82.5 ml, total of 2.205mol) was added slowly so that the temperature remained between 5-10°C. The stirring was continued for about three hours and the temperature was maintained below 10°C

during this period.

The reaction mixture was allowed to stand for about twelve hours at room temperature and then water (75 ml) was added slowly with stirring. The resulting mixture was then steam distilled and the distillate was extracted with benzene. The benzene layer was dried and evaporated to obtain the crude product. Crystallisation of the crude product in benzene gave 60g 4,4'-dibromobenzophenone (yield 69%). m.p. 174.5 - 175°C. $^1\text{H-NMR}$ (δ ppm, CDCl_3): 7.6 (s); M. S. (m/z) : 342 (25.97%), 341 (8.27%), 340 (52.54%), 339 (5.25%), 338 (26.78%), 261 (6.05), 259 (6.15%), 185 (98.46%), 184 (7.83%), 183 (100%), 157 (31.92%), 156 (10.58%), 155 (32.93%), 79 (31.14).

Synthesis of 4,4'-dicyanobenzophenone (112):

Dry N,N-dimethylformamide (40 ml), p,p'-dibromobenzophenone (40 g, 0.118 moles) and cuprous cyanide (25.4 g, 0.284 moles) were placed in a round bottom flask, equipped with the reflux condenser, stirring bar and drying tube. The mixture was heated to reflux using an oil bath and was allowed to reflux for 9 hours. Then, the mixture was poured into a litre of hot 10% aqueous sodium cyanide solution. The resulting mixture was heated on a steam bath. While heating, an orange solid appeared on the top. The mixture was extracted with benzene. The benzene layer was washed with water, dried with anhydrous magnesium sulfate and then the benzene was

evaporated. The resulting solid was purified by column chromatography using 9:1 petroleum ether-diethyl ether as eluent. Evaporation of solvent afforded 14g p,p'-dicyanobenzophenone (yield 51%). m.pt. 159 - 160°C; ¹H-NMR (δppm, CDCl₃): 7.9 (s); M. S. (m/z) : 233 (5.38), 232 (29.59), 131 (9.65), 130 (100), 103 (3.37), 102 (39.24).

Synthesis of 4,4'-di(trifluoromethyl)benzophenone (113):

A solution of 4-trifluoromethylbenzotrile (4.05 g, 0.0235 moles) in ether (10 ml) was added slowly with stirring, to a solution of 4-(trifluoromethyl)phenylmagnesium bromide prepared from 4-(trifluoromethyl)bromobenzene (11.25 g, 0.05 moles) and magnesium (1.215 g, 0.05 moles) in ether (25 ml). The reaction mixture was kept at room temperature for 12 hours. The resulting solid product was treated with a mixture of ice and dilute hydrochloric acid and then the mixture was heated for 10 - 15 minutes. The resulting mixture was extracted with ether and the ether layer was washed with water and dried with anhydrous magnesium sulfate. The ether was evaporated and the remaining solid was crystallised from hot ethanol after being treated with charcoal. m.pt. 108 - 108.5°C; ¹H-NMR (δppm, CDCl₃): 7.9 (s); M. S. (m/z) : 319 (5.07), 318 (28.53), 300 (1.39), 299 (7.57), 174 (9.09), 173 (100), 146 (3.17), 145 (38.58).

Synthesis of Hexamethylphosphoroustriamide (HMPT) (110):

A solution of anhydrous dimethylamine (100 g) in anhydrous ether (250 ml) was placed in a one litre three-necked round bottom flask equipped with a reflux condenser, drying tube and a dropping funnel. A solution of phosphorus trichloride (25 ml, 0.29 moles) in anhydrous ether (250 ml) was added slowly from the dropping funnel, to the round bottom flask. The temperature of the mixture was maintained below 15°C during this process. When the addition was over, the reaction mixture was allowed to warm up to room temperature, and kept at this temperature overnight. The resulting slurry was filtered and the residue was washed well with dry ether. The washing solution was combined with the filtrate and the ether was evaporated and then the remaining liquid was distilled under vacuum, to get hexamethylphosphoroustriamide (yield 30 g, 80%). The product was a colourless liquid.

Synthesis of 1,1-difluoro-2,2-di(4-bromophenyl)ethylene (109):

A solution of HMPT (8 ml, 0.044 mole) in DMF was added slowly from a dropping funnel to a round bottom flask which contained a cooled slurry of p,p'-dibromobenzophenone (5 g, 0.0147 mole), dibromodifluoromethane (2.02 ml, 0.022 mole) and DMF (30 ml). The reaction mixture was stirred and the

temperature was maintained at 0°C during the addition. After the addition was completed, the mixture was stirred overnight at room temperature. TLC analysis using pentane as the eluent showed the presence of two compounds in the mixture, one of which was the unreacted ketone, in addition to the other side products which do not move with the eluent. After evaporation of the DMF, the sticky residue was separated on a column using pentane as the eluent. Evaporation of the solvent yielded 4.15 g unreacted ketone and 0.156 g of 1,1-difluoro-2,2-di(4-bromophenyl)-ethylene (yield 17%). m.p. 83-84°C; ¹H-NMR (δppm, CDCl₃): 7.1 (d, J = 8 Hz), 7.6 (d, J=8 Hz); M. S. (m/z) : 376 (49.61), 375 (17.71), 374 (100), 373 (12.80), 372 (51.70), 322 (< 5), 215 (12.70), 214 (81.09).

Synthesis of 1,1-difluoro-2,2-di(4-cyanophenyl)ethylene:

A procedure similar to the one used for the synthesis of 1,1-difluoro-2,2-di(4-bromophenyl)ethylene was used. The product was isolated by column chromatography using pentane - ether (1 : 5) mixture as the eluent (yield 10%). m.pt. 138 - 139°C; ¹H-NMR (δppm, CDCl₃): 7.4 (d, J = 8 Hz), 7.7 (d, J=8 Hz); M. S. (m/z) : 267 (18.13), 266 (100), 217 (4.02), 216 (17.37), 215(46.38), 129 (36.49), 113(23.85).

Synthesis of 1,1-difluoro-2,2-di(4-trifluoromethyl-phenyl)ethylene:

A procedure similar to the one used for the synthesis of 1,1-difluoro-2,2-di-(4-bromophenyl)ethylene was used. The product was isolated by column chromatography using pentane as the eluent. (yield 10%), $^1\text{H-NMR}$ (δppm , CDCl_3): 7.4 (d, $J = 8$ Hz), 7.7 (d, $J=8$ Hz); M. S. (m/z) : 353 (18.48), 352 (100), 333 (18.06), 283 (17.58), 233 (19.22), 214 (21.01).

Synthesis of tetraethylammonium perchlorate ($\text{Et}_4\text{N}^+\text{ClO}_4^-$):

A hot 1M aqueous solution of tetraethylammonium-chloride (100 ml) was added slowly, with stirring to an equivalent amount of a hot 1 M aqueous solution of sodium perchlorate. After cooling in ice water, the precipitate was filtered on a buchner funnel and washed with cold distilled water, until the wash liquid was free from chloride. Then the salt was recrystallised from water and dried at 60°C in a vaccum oven.

Synthesis of Tetraethylammonium picrate :

A saturated aqueous solution of picric acid was

titrated with a 20% aqueous solution of tetraethylammonium hydroxide to the equivalence point detected by potentiometer. The solution was then evaporated until crystallisation occurred. The product was recrystallised twice, first from water and then from 95% ethanol and then dried over P_2O_5 at room temperature in a vacuum desiccater.

Synthesis of picrates of amines :

An ethanolic solution of amine (0.5-1.5 g) was titrated with a saturated ethanolic solution of picric acid to the equivalent point detected by a potentiometer. The salts were then recrystallised twice from ethanol and washed with ethanol and dried under vacuum.

6.4 Kinetic measurements

The acetonitrile and the amines used for the kinetics were distilled freshly for each set of measurements. The reaction was followed by monitoring the appearance of mono-substituted olefin, under pseudo first-order conditions. The solutions were prepared freshly in acetonitrile just before the kinetic measurements.

The reaction between 1,1-difluoro-2,2-diphenylethylene and piperidine was the slowest one among the

reactions studied. In this case, the concentration of the substrate was $4 \times 10^{-3} \text{M}$ and the concentration of the amine varied between 3.03×10^{-1} and $7.07 \times 10^{-1} \text{M}$. The reaction was carried out in small cells (Figure 37) which were designed with a side valve to pass nitrogen and with a silicon rubber septum at the mouth to withdraw a sample from time to time without opening the system. This allowed us to carry out the reaction under nitrogen, free from moisture, oxygen and carbon dioxide.

The solutions were mixed in the cell under nitrogen via the side arm of the cell, and the cell was closed immediately. Then the reaction mixtures were kept in an oil bath maintained at the required temperature. Samples (0.05 mL) were withdrawn by means of a syringe at half - hour intervals and diluted with acetonitrile (3 mL) directly in cuvettes; then the absorbances of the resulting solutions were measured.

All other reactions were carried out in tightly closed cuvettes in a thermostated compartment of the spectrophotometer and the reaction was followed by monitoring the absorbance of the reaction mixture at constant time intervals.

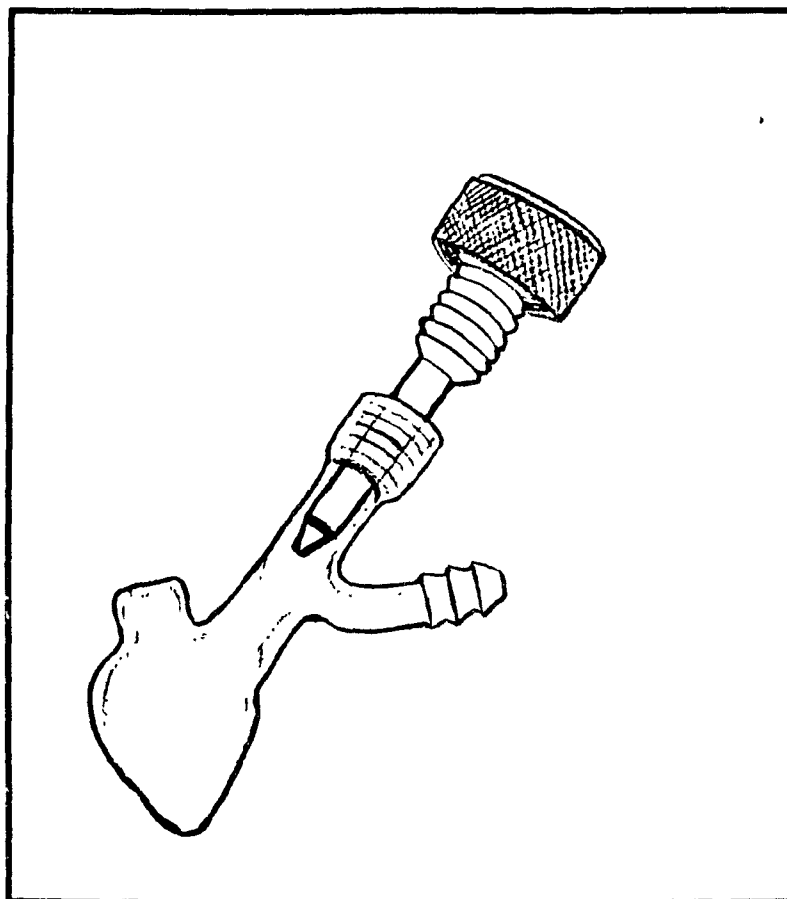


Figure 37: The cell used for the kinetic measurements of the reaction of 1,1-difluoro-2,2-diphenylethylene with piperidine in acetonitrile.

The reactions were carried out in presence of large excess of base so that pseudo first-order rate constants were obtained. The kinetics of the first step of the reaction were followed by monitoring the absorbance at the λ_{\max} of the corresponding product. Two sample sets of kinetic readings are given in Tables 30 and 32, and the absorbance of the reaction mixture is plotted as a function of time in Figures 38 and 40.

The observed pseudo first-order rate constants ($k_{1\text{obs}}$) were calculated by the Guggenheim method. The Guggenheim method is used widely for the calculation of first-order rate constants when the infinity reading for a reaction is not available. In this case, measurements A_1, A_2, A_3, \dots are made at times t_1, t_2, t_3, \dots and a second series of measurements A_1', A_2', A_3', \dots are made at times $t_1 + \Delta, t_2 + \Delta, t_3 + \Delta, \dots$. Where Δ is a constant time increment. If A_∞ is the infinity reading of A, then for a first order reaction,

$$A_\infty - A_1 = (A_\infty - A_0)e^{-kt_1} \quad [37]$$

$$\text{and} \quad A_\infty - A_1' = (A_\infty - A_0)e^{-k(t_1 + \Delta)} \quad [38]$$

subtracting [38] from [37] gives,

$$A_1' - A_1 = (A_\infty - A_0)e^{-kt_1}(1 - e^{-k\Delta}) \quad [39]$$

$$\begin{aligned} \text{Therefore, } \ln (A_1' - A_1) &= \ln (A_\infty - A_0) (1 - e^{-k\Delta}) - kt, \\ &= \text{constant} - kt, \end{aligned} \quad [40]$$

Equation [40] can be generalized for any A and A'. That is,

$$\ln (A' - A) = -kt + \text{constant} \quad [41]$$

A plot of $\ln(A' - A)$ versus t is linear and its slope would give the first-order rate constant.

For accurate results, Δ should be at least one and preferably two or three times the half-life of the reaction.

Two sets of corresponding points were chosen from the kinetic readings for this calculation, so that the second set begins no sooner than the third half life of the reaction. Table 31 shows the two sets of points chosen from the sample readings shown in Table 30. Resulting Guggenheim plot is shown in Figure 39. As shown in this Figure, the Guggenheim plots were linear for all the kinetic runs with correlation coefficient greater than 0.9998. The observed pseudo first-order rate constant and standard deviation calculated by a linear least squares fit from the sample Guggenheim plot was $1.149 \pm 0.003 \times 10^{-4} \text{ s}^{-1}$.

Table 30

The absorbance of the reaction mixture of 1,1-difluoro-2,2-di(4-trifluoromethylphenyl)ethylene* and piperidine** in acetonitrile at 20°C monitored at 310 nm at different time.

pt #	t (min) (t = 0 at time of mixing)	A
0	0	-
1	15	0.1693
2	45	0.3287
3	75	0.4562
4	105	0.5637
5	135	0.6494
6	165	0.7171
7	195	0.7729
8	225	0.8167
9	255	0.8546
10	285	0.8865
11	315	0.9104
12	345	0.9303

continued

table 30 (continued).

pt #	t (min) (t = 0 at time of mixing)	A
13	375	0.9462
14	405	0.9602
15	435	0.9701
16	465	0.9781
17	495	0.9860
18	525	0.9920
19	555	0.9972
20	585	1.0012
21	615	1.0040
22	645	1.0068
23	675	1.0092
24	705	1.0108

* initial concentration = 7.09×10^{-5} mol. l^{-1}

** initial concentration = 2.83×10^{-2} mol. l^{-1}

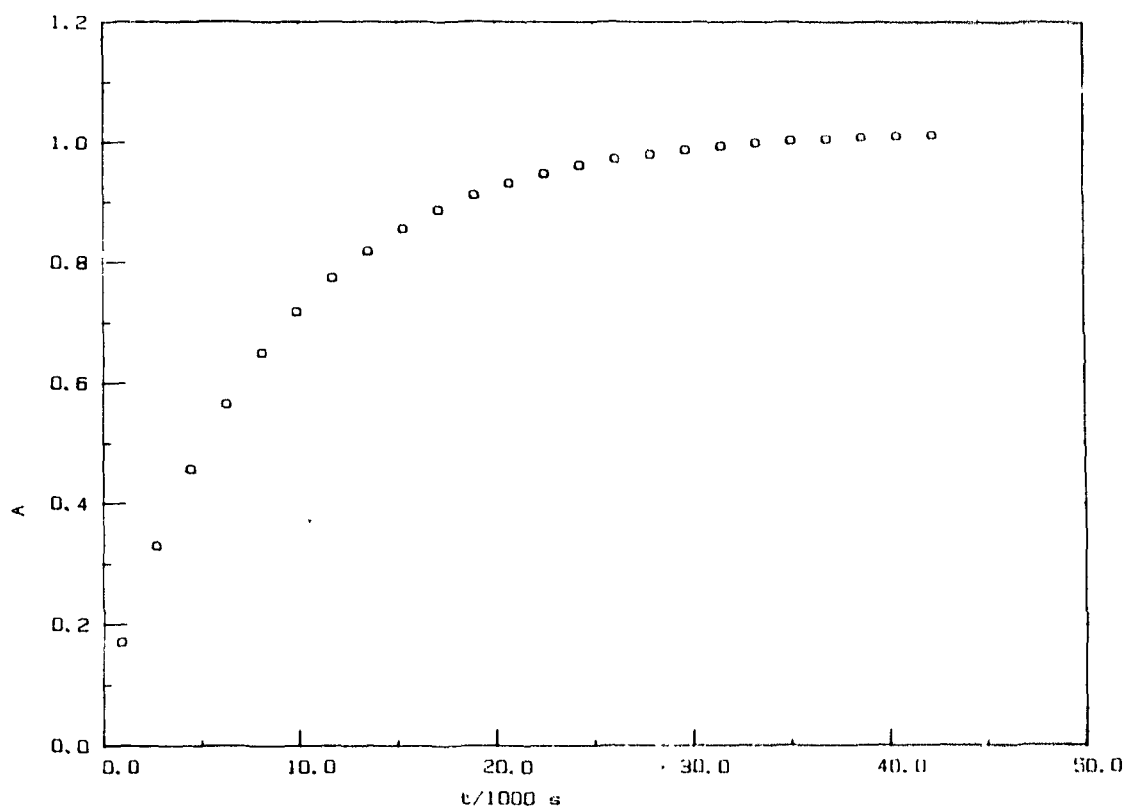


Figure 38: The kinetic curve for the reaction of 1,1-difluoro-2,2-di(4-trifluoromethylphenyl)ethylene ($7.09 \times 10^{-5} \text{ mol.l}^{-1}$) with piperidine ($2.83 \times 10^{-2} \text{ mol.l}^{-1}$) at 20°C in acetonitrile.

Table 31

The two sets of points chosen from Table (29), for the calculation of pseudo first-order rate constant by Guggenheim method.

pt #	A_1	A_2	$\ln(A_2 - A_1)$
1	0.1693	0.8546	-0.3779
2	0.3287	0.8865	-0.5836
3	0.4562	0.9104	-0.7892
4	0.5637	0.9303	-1.0034
5	0.6494	0.9462	-1.2147
6	0.7171	0.9602	-1.4143
7	0.7729	0.9701	-1.6235
8	0.8167	0.9781	-1.8239
9	0.8546	0.9860	-2.0295

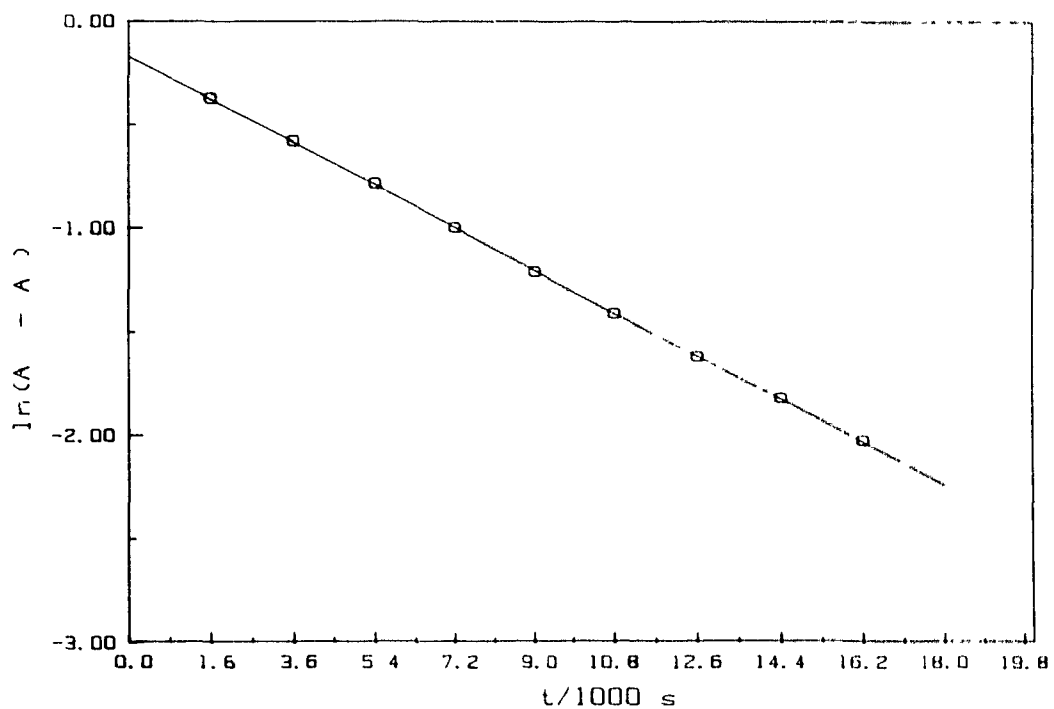


Figure 39: The Guggenheim plot for the reaction of 1,1-difluoro-2,2-di(4-trifluoromethylphenyl)ethylene ($7.09 \times 10^{-5} \text{ mol.l}^{-1}$) with piperidine ($2.83 \times 10^{-2} \text{ mol.l}^{-1}$) at 20°C in acetonitrile.

The interval (in half-lives) between the two sets of points in a Guggenheim plot Δ is given by the equation [42].

$$\Delta = \frac{[(n + \Delta n) \times \text{timebase}] \times k_1}{\ln 2}$$

where, n = number of points in each set.

Δn = number of points left between the two sets.

k_1 = first order rate constant.

and the time base is the time interval between two consecutive readings.

In the given example (table 30 & 31),

$n = 9$, $n = 0$, timebase = 1800 s.

and $k_1 = 1.15 \times 10^{-4} \text{ s}^{-1}$.

Therefore, $\Delta = \{[(9 + 0) \times 1800] \times 1.15 \times 10^{-4}\} / \ln 2$
 $= 2.7 \text{ half lives}$

Table 32

The absorbance of the reaction mixture of 1,1-difluoro-2,2-diphenylethylene* and piperidine** in acetonitrile at 50°C at 310 nm.

pt #	t (min) (t = 0 at time of mixing)	A
0	0	-
1	15	0.0175
2	45	0.0284
3	75	0.0375
4	105	0.0475
5	135	0.0568
6	165	0.0661
7	195	0.0750
8	225	0.0855
9	255	0.0945
10	285	0.1025
11	315	0.1110
12	345	0.1205

continued

table 32 (continued).

pt #	t (min) (t = 0 at time of mixing)	A
13	375	0.1290
14	405	0.1375
15	435	0.1462
16	1365	0.3409
17	1395	0.3455
18	1425	0.3515
19	1455	0.3575
20	1485	0.3625
21	1515	0.3675
22	1545	0.3715
23	1575	0.3755
24	1605	0.3800

* initial concentration = 4×10^{-3} mol. l^{-1}

** initial concentration = 3.03×10^{-1} mol. l^{-1}

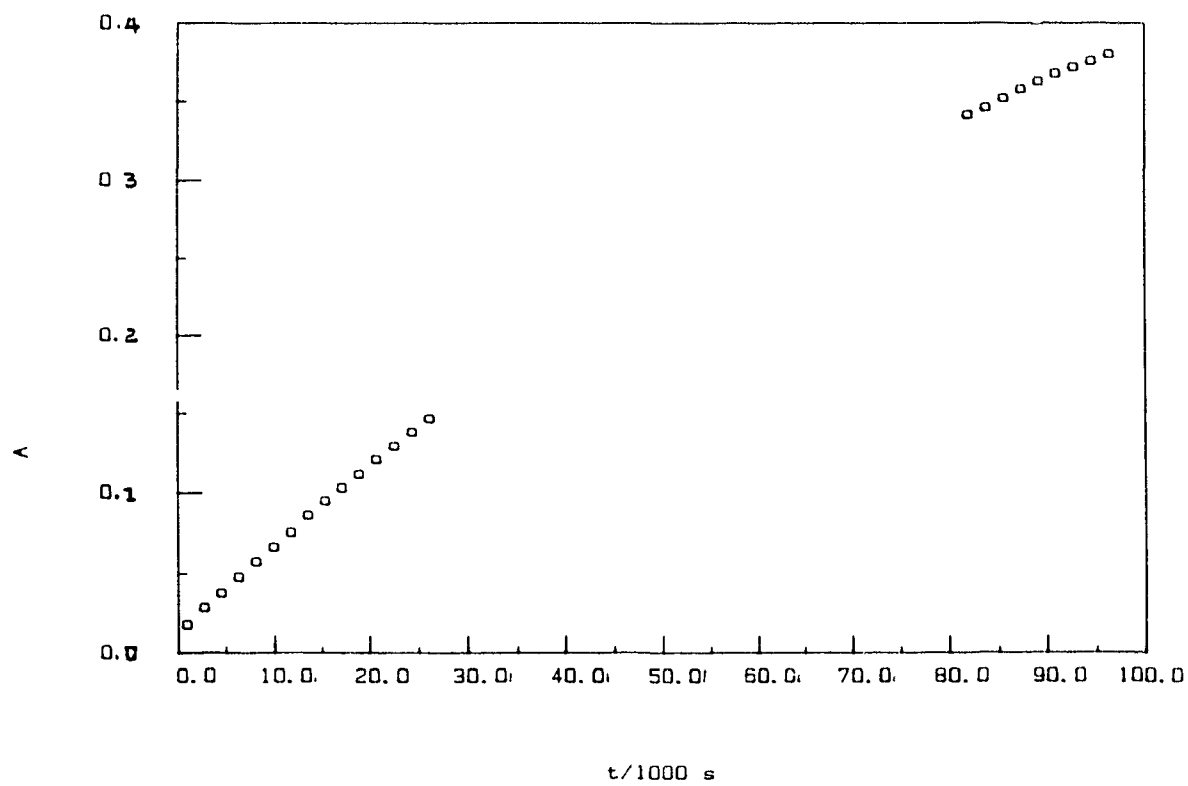


Figure 40: The kinetic curve for the reaction of 1,1-difluoro-2,2-diphenylethylene ($4 \times 10^{-3} \text{ mol.l}^{-1}$) with piperidine ($3.03 \times 10^{-1} \text{ mol.l}^{-1}$) at 50°C in acetonitrile.

The Table 33 shows the two sets of points chosen from the sample readings given in Table 32. The resulting Guggenheim plot is shown in Figure 41.

The calculated pseudo first order rate constant was $(8.4 \pm 0.3) \times 10^{-6} \text{ s}^{-1}$.

For this example, $n = 8$, $\Delta n = 36$ and the time base = 1800s.

Therefore, $\Delta = \{[(8 + 36) \times 1800] \times 8.4 \times 10^{-6}\} / \ln 2$
 $= 0.96 \text{ half lives.}$

Table 33

The two sets of points chosen from Table (31), for the calculation of pseudo first-order rate constant by Guggenheim method.

pt #	A_1	A_2	$\ln(A_2 - A_1)$
1	0.0475	0.3455	-1.2107
2	0.0568	0.3515	-1.2218
3	0.0660	0.3575	-1.2327
4	0.0750	0.3625	-1.2465
5	0.0855	0.3675	-1.2658
6	0.0945	0.3715	-1.2837
7	0.1025	0.3755	-1.2982
8	0.1110	0.3800	-1.3130

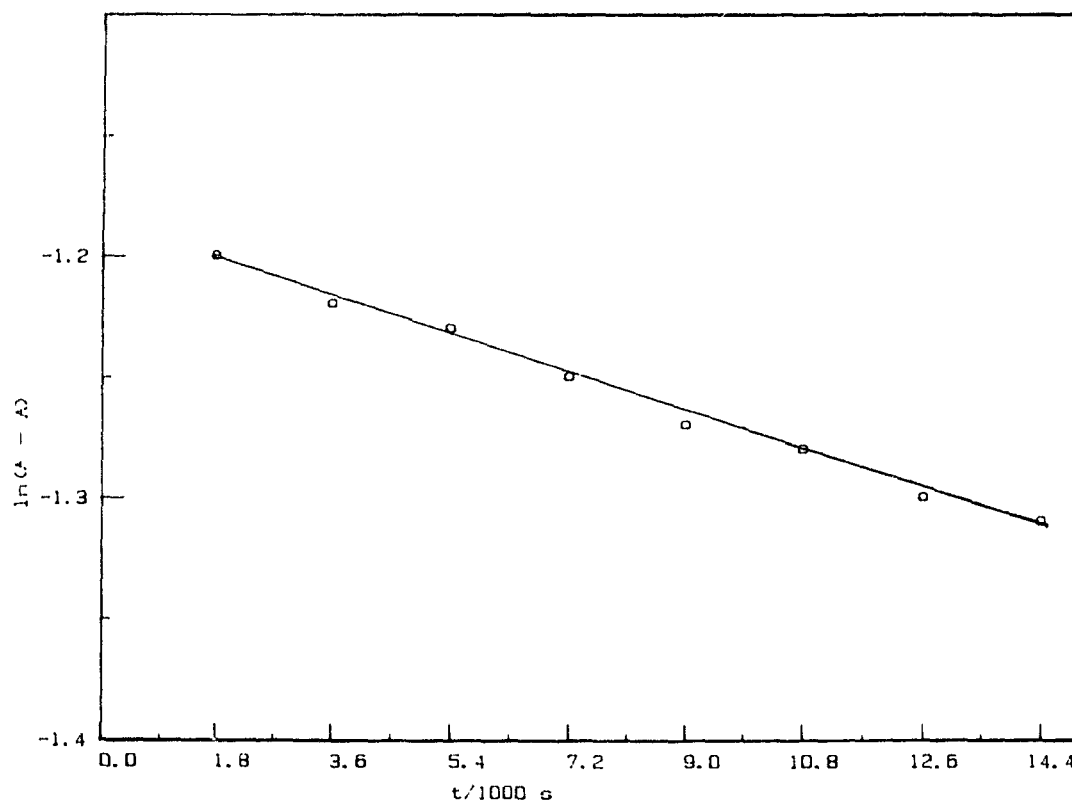


Figure 41: The Guggenheim plot for the reaction of 1,1-difluoro-2,2-diphenylethylene ($4 \times 10^{-3} \text{ mol.l}^{-1}$) with piperidine ($3.03 \times 10^{-1} \text{ mol.l}^{-1}$) at 50°C in acetonitrile.

6.5 EMF measurements of buffer solutions.

A general purpose glass electrode was used as the indicator electrode. When not in use, the glass electrode was kept in distilled water, and before each measurement, the electrode was washed with absolute ethanol, dried in a stream of dry nitrogen and immersed in distilled acetonitrile at least for two hours. The reference electrode was a flowing junction silver- 0.01M silver nitrate in acetonitrile halfcell. This cell was constructed as described by Kolthoff and Chantooni (102). An Orion Research model 601A pH- meter was used for the EMF measurement.

An H- shaped cell was constructed as described by Coetzee and Padmanabhan (101). The dimensions of the one vertical arm of this cell were chosen so that this arm could accommodate the glass electrode together with a minimum 5ml of buffer solution under study. This arm was also equipped with a stopcock at the bottom in order to drain the solution after each measurement.

The other vertical arm of the cell was considerably smaller. The horizontal section of the cell was about 10 - 12mm in diameter and about 5cm in length. This horizontal compartment, which is the salt bridge, was sealed on both side with two fine porosity sintered glass discs inserted on both ends. This compartment was also provided with vertical inlet and outlet tubes for the introduction and removal of salt

bridge solution. The reference electrode and the H- shaped cell were equipped with water jacket (Figure 42) in order to thermostat the system. During the measurement, the system was thermostated at 25°C.

All the solutions were prepared just before the measurement. The smaller vertical arm and the horizontal section of the H- shaped cell were filled with 0.1M solution of tetraethylammonium perchlorate in acetonitrile, and the side arm of the reference electrode was dipped into this vertical arm. The buffer solution under study was added to the other vertical arm of the cell and the glass electrode was placed in the buffer solution. All the compartments were tightly closed to avoid contamination with moisture and carbon dioxide.

The glass electrode was calibrated using picric acid - tetraethylammonium picrate buffers. The EMF values of five buffers which contain $1 \times 10^{-3}M$ tetraethylammonium picrate and different concentrations of picric acid were obtained.

The buffers of the bases were prepared so that the concentrations of tetraethylammonium perchlorate and picrate of base under study was constant and both equal to $5 \times 10^{-4}M$. The concentrations of base was changed between 3×10^{-4} and $4 \times 10^{-3}M$. Therefore, the total ionic strength in the base buffers is equal to that of the picric acid buffers.

In each case the equilibrium was reached in about 10 - 15 minutes, and the EMF values were very stable.

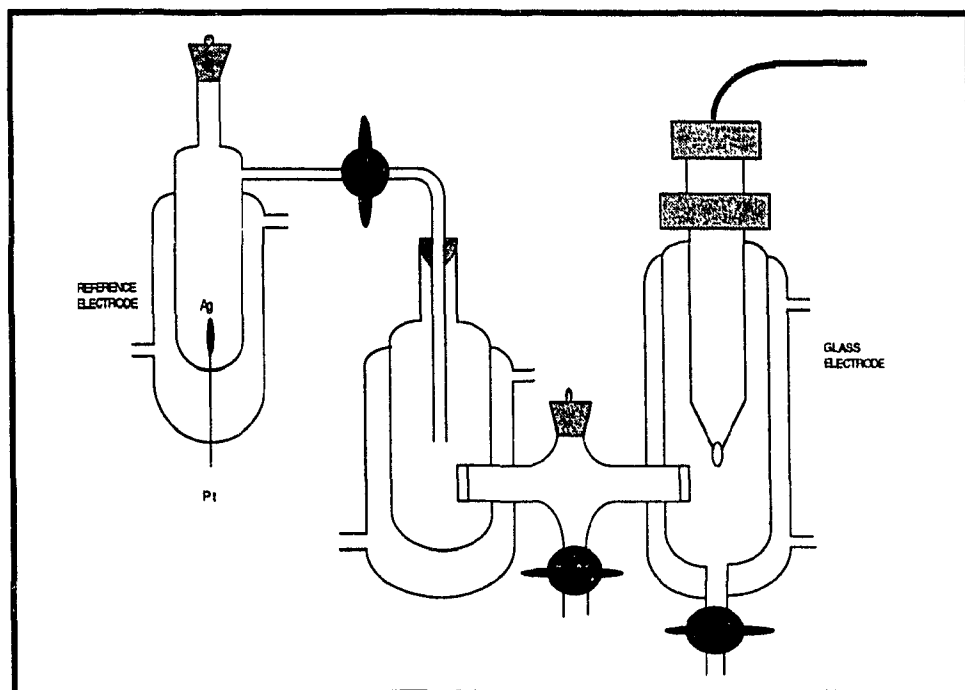


Figure 42: The H-shaped cell that was used for the pK_a measurements.

REFERENCES

- (1) A. Lapworth. *Nature* **115**, 625 (1925)
- (2) C. K. Ingold. *J. Chem. Soc.* 1120 (1933)
- (3) C. K. Ingold. "Structure and Mechanism in Organic Chemistry", Cornell Univ. Press, Ithaca, N.Y. 1953 p. 200.
- (4) J. F. Bunnett. *Annu. Rev. Phys. Chem.* **14**, 271 (1963)
- (5) C. F. Bernasconi and D. J. Carre. *J. Am. Chem. Soc.* **101**, 2698 (1979).
- (6) C. F. Bernasconi, R. A. Renfrow, and P. R. Tia. *J. Am. Chem. Soc.* **108**, 4541 (1986).
- (7) Z. Rappoport and R. Ta-Shma. *J. Chem. Soc. (B)*., 871 (1971).
- (8) C. F. Bernasconi, K. A. Howard and A. Kanavarioti. *J. Am. Chem. Soc.* **106**, 6827 (1984).
- (9) F. Freeman. *Chem. Rev.* **80**, 329 (1980).
- (10) C. F. Bernasconi and G. D. Leonardizzi. *J. Am. Chem. Soc.* **104**, 5133 (1982).
- (11) C. F. Bernasconi and S. Fornarrini. *J. Am. Chem. Soc.* **102**, 5329 (1980).
- (12) C. F. Bernasconi and G. D. Leonarduzzi. *J. Am. Chem. Soc.* **102**, 1361 (1980).
- (13) G. Modena. *Acc. Chem. Res.* **4**, 73 (1971).
- (14) E. F. Silversmith and D. Smith. *J. Org. Chem.* **23**, 427

- (1958).
- (15) A. J. Kirby and C. J. Logan. *J. Chem. Soc. Perkin Trans. II*, 642 (1978).
- (16) C. M. Evans and A. J. Kirby. *J. Am. Chem. Soc.* **104** 4705 (1982).
- (17) C. M. Evans and A. J. Kirby. *J. Chem. Soc. Perkin Trans. II*, 1259 (1984).
- (18) K. R. Hanson and E. A. Havir, "The Enzymes", P. D. Boyer, Academic Press, N.Y., 3rd edition, Vol.7, p.75 (1972).
- (19) M. Tieco, L. Testaferri, M. Tingoli, D. Chianelli, and M. Montanucci. *J. Org. Chem.* **48**, 4795 (1983).
- (20) M. Tieco, L. Testaferri, M. Tingoli, D. Chianelli, and M. Montanucci. *Tetrahedron Lett.* **25**, 4975 (1984).
- (21) R. G. Pearson, H. Sobel, and J. Songstad. *J. Am. Chem. Soc.* **90**, 319 (1968)
- (22) Z. Rappoport. *Adv. Chem. Ser.* **215**, 399 (1987).
- (23) E. D. Bergmann, D. Ginsburg, and R. Papo. "Organic Reactions" (John Wiley & Sons, Inc., N.Y.) Vol. 10, 1959, p. 179.
- (24) H. A. Bruson. "Organic Reactions" (John Wiley & Sons, Inc., N.Y.) Vol. 5, 1954, p. 79.
- (25) P. B. D. de la Mare, In "Progress in stereochemistry", W. Klyne and P. B. D. de la Mare eds. Butterworth, London. 1958. vol. 2, p. 90.
- (26) S. Patai and Z. Rappoport. In "The chemistry of

- alkenes", S. Patai eds. Interscience, London. 1964.
p. 469.
- (27) Z. Rappoport. *Adv. Phys. Org. Chem.* 7, 1 (1969).
- (28) C. F. Bernasconi. *Tetrahedron* 45, 4017 (1989).
- (29) C. F. Bernasconi and C. J. Murray. *J. Am. Chem. Soc.* 106, 3257 (1984).
- (30) C. F. Bernasconi and R. D. Bunnell. *J. Org. Chem.* 53, 2001 (1988).
- (31) C. F. Bernasconi, J. P. Fox, A. Kanavarioti, and M. Panda *J. Am. Chem. Soc.* 108, 2372 (1986).
- (32) S. Patai and Z. Rappoport. *J. Chem. Soc.* 383 (1962)
- (33) S. Patai and Z. Rappoport. *J. Chem. Soc.* 396 (1962)
- (34) H. von Pechmann. *Chem. Ber.* 33, 3323 (1900).
- (35) M. Takebayashi. *Chem. Abstr.* 46, 8608 (1952).
- (36) G. Modena, U. Tonellato, and F. Naso. *Chem. Comm.* 1363 (1968).
- (37) Z. Rappoport. *Recl. Trav. Chim. Pays- Bas.* 104, 309 (1985).
- (38) Z. Rappoport. *Acc. Chem. Res.* 14, 7 (1981).
- (39) C. F. Bernasconi, R. B. Killion. Jr., J. Fassberg, and Z. Rappoport. *J. Am. Chem. Soc.* 111, 6862 (1989).
- (40) C. F. Bernasconi, R. B. Killion. Jr., J. Fassberg, and Z. Rappoport. *J. Am. Chem. Soc.* 112, 3169 (1990).
- (41) C. F. Bernasconi, R. B. Killion. Jr., J. Fassberg, and Z. Rappoport. *J. Org. Chem.* 55, 4568 (1990).
- (42) C. F. Bernasconi, J. Fassberg, R. B. Killion. Jr.,

- D. F. Schuck, and Z. Rappoport. *J. Am. Chem. Soc.* **113**, 4937 (1991).
- (43) V. Gold. *J. Chem. Soc.* 1430 (1951).
- (44) D. R. Kelsey and R. G. Bergman. *J. Am. Chem. Soc.* **93**, 1953 (1971)
- (45) S. I. Miller. *Tetrahedron*, **33**, 1211 (1977).
- (46) P. J. Stang, M. G. Magnum, D. P. Fox, and P. Haak. *J. Am. Chem. Soc.* **96**, 4562 (1974).
- (47) P. J. Stang, Z. Rappoport, M. Hanack, and L. R. Subramanian. "Vinyl Cations", Academic Press, N. Y., 1979, chap.5 and 6.
- (48) A. Pross. *Acc. Chem. Res.* **18**, 212 (1985).
- (49) E. C. Ashby and A. B. Goel. *J. Am. Chem. Soc.* **103**, 4983 (1981).
- (50) S. K. Chung. *J. chem. Soc., Chem. Commun.* 480 (1982).
- (51) L. Ebersson. *Adv. Phys. Org. Chem.* **18**, 79 (1982).
- (52) B. Avramovitch and Z. Rappoport. *J. Am. Chem. Soc.* **110**, 911 (1988).
- (53) C. F. Bernasconi. *Adv. Phys. Org. Chem.* **27**, 205 (1992).
- (54) C. F. Bernasconi. *Acc. Chem. Res.* **25**, 9 (1992).
- (55) C. F. Bernasconi and D. F. Schuck. *J. Org. Chem.* **57**, 2365 (1992).
- (56) Z. Rappoport and R. Ta-Shma. *J. Chem. Soc.(B)*. 1461 (1971).
- (57) B. Avramovitch, P. Weyerstahl, and Z. Rappoport. *J. Am. Chem. Soc.* **109**, 6687 (1987).

- (58) W. Dmowski. *J. Fluorine Chem.* 21, 201 (1982).
- (59) Z. Rappoport and P. Peled. *J. Chem. Soc. Perkin Trans. II*, 616 (1973).
- (60) D. Cohen, R. Bar, and S. S. Shaik. *J. Am. Chem. Soc.* 108, 231 (1986).
- (61) R. D. Chambers and R. H. Mobbs. *Adv. Fluorine Chem.* 4, 50 (1965).
- (62) W. E. Hanford and G. W. Rigby. U. S. Pat. no. 2, 409, 274, Oct. 15. 1946. *Chem. Abs.* 41, 982b (1947).
- (63) W. T. Miller, Jr., E. W. Fager, and P. H. Griswold. *J. Am. Chem. Soc.* 70, 431 (1948).
- (64) K. N. Makarov, L. L. Gervits, A. Cheburkov, and I. L. Knunyants. *J. Fluorine Chem.* 10, 323 (1977).
- (65) W. Dmowski. *J. Fluorine Chem.* 15, 299 (1980).
- (66) J. D. Park, C. M. Snow, and J. R. Lacher. *J. Am. Chem. Soc.* 73, 2342 (1951).
- (67) W. T. Miller, Jr. and A. H. Fainberg. *J. Am. Chem. Soc.* 79, 4164 (1957).
- (68) A. H. Fainberg and W. T. Miller, Jr.. *J. Am. Chem. Soc.* 79, 4170 (1957).
- (69) J. H. Fried and W. T. Miller, Jr.. *J. Am. Chem. Soc.* 81, 2078 (1959).
- (70) W. T. Miller, Jr., J. H. Fried and H. Goldwhite. *J. Am. Chem. Soc.* 82, 3091 (1960).
- (71) J. D. Park, J. R. Lacher, and J. R. Dick. *J. Org. Chem.* 31, 1116 (1966).

- (72) H. F. Koch and A. J. Kielbania, Jr.. J. Am. Chem. Soc. 92, 729 (1970).
- (73) H. F. Koch, J. G. Koch, and D. B. Donovan. J. Am. Chem. Soc. 103, 5417 (1981).
- (74) Shaw Guan Su. Diss. Abs. Int B. 42(5), 1898 (1981).
- (75) C. V. Maffeo, G. Marchese, F. Naso, and L. Ronzini. J. Chem. Soc. Perkin Trans. I. 92 (1979).
- (76) Cart G. Krespan, Frederic A. Van Catledge, Bruce E. Smart. J. Am. Chem. Soc. 106, 5544 (1984).
- (77) K. T. Leffek, A. Jarczewski, G. Schroeder, W. Galezowski, and U. Maciejewska. Can. J. Chem. 63, 576 (1985).
- (78) A. Jarczewski, G. Schroeder, and M. Dworniczak. J. Chem. Soc. Perkin Trans. II. 55 (1986).
- (79) C. F. Bernasconi. MTP Int. Rev. Sci. Org. Chem., Ser. One. 3, 33 (1973).
- (80) J. Miller, " Aromatic Nucleophilic Substitution ", American Elsevier, New York (1968).
- (81) A. F. Popov, I. F. Perepichka, and L. I. Kostenko. J. Chem. Soc. Perk. Trans. II., 395 (1989).
- (82) I. F. Perepichka, A. F. Popov, L. I. Kostenko, T. V. Artyomova, and J. Kovac. Studies in organic Chemistry 35, 462 (1988).
- (83) I. F. Perepichka, L. I. Kostenko, A. F. Popov and A. Yu. Chervinskii. Zh. Org. Khim., 24, 822 (1988).
- (84) K. T. Leffek and U. Maciejewska. Can. J. Chem. 64, 2274

- (1986).
- (85) Z. Rappoport and D. Ladkani. *Chem. Scr.* **5**, 124 (1974).
- (86) Yu. V. Zeifman, E. G. Ter-Gabrielyan, N. P. Gambaryan, and I. L. Knunyants. *Usp. Khim.* **53**, 431 (1984).
- (87) Yu. V. Zeifman, E. G. Ter-Gabrielyan, N. P. Gambaryan, and I. L. Knunyants. *Russ. Chem. Rev.* **53**, 256 (1984).
- (88) B. A. Shainyan. *Usp. Khim.* **55**, 942 (1986).
- (89) B. A. Shainyan. *Russ. Chem. Rev.* **55**, 511 (1986).
- (90) E. A. Guggenheim. *Philos. Mag.* **2**, 538 (1926).
- (91) L. P. Hammett. *J. Am. Chem. Soc.* **59**, 96 (1937).
- (92) L. N. Bronsted and K. J. Pedersen. *Z. phys. Chem.* **108**, 185 (1924).
- (93) J. Shorter. *Q. Rev. Chem. Soc.* **24**, 433 (1970).
- (94) J. Shorter. "Advances in linear Free Energy Relationships". N. B. Chapman and J. Shorter, Eds., Plenum, London (1972).
- (95) J. E. Leffler and E. Grunwald. "Rates and Equilibria of Organic Reactions". Wiley, N.Y. (1963).
- (96) P. R. Wells. "Linear Free Energy Relationships". Academic Press, N. Y. (1968).
- (97) L. P. Hammett. "Physical Organic Chemistry", N.Y., McGraw - Hill.
- (98) H. H. Jaffe. *Chem. Rev.* **53**, 191 (1953).
- (99) A. I. Biggs and R. A. Robinson. *J. Chem. Soc.* 388 (1961).
- (100) J. F. Coetzee. *Prog. Phys. Org. Chem.* **4**, 45 (1967).

- (101) J. F. Coetzee and G. R. Padmanabhan. *J. Am. Chem. Soc.* **87**, 5005 (1965).
- (102) I. M. Kolthoff and M. K. Chantooni, Jr. *J. Am. Chem. Soc.* **87**, 4428 (1965).
- (103) Z. Rappoport and P. Peled. *J. Am. Chem. Soc.* **101**, 2682 (1979).
- (104) R. P. Bell. "The Proton In Chemistry", Cornell Univ. Press, Ithaca, N.Y. p194 (1973).
- (105) F. G. Bordwell and W. J. Boyle, Jr. *J. Am. Chem. Soc.* **94**, 3907 (1972).
- (106) M. Dworniczak and K. T. Leffek. *Can. J. Chem.* **68**, 1657 (1990).
- (107) S. A. Fuqua, W. G. Duncan and R. M. Silverstein. *J. Org. Chem.* **30**, 2543 (1965).
- (108) S. A. Fuqua, W. G. Duncan and R. M. Silverstein. *J. Org. Chem.* **30**, 1027 (1965).
- (109) D. G. Naeae and D. J. Burton. *Syn. Comm.* **3**, 197 (1973).
- (110) V. Mark. *Org. Syn.* **46**, 42 (1966).
- (111) C. S. Marvel and W. M. Sperry. *Org. Syn., Coll. Vol.* **1**, 95.
- (112) R. W. Humphreys and D. R. Arnold. *Can. J. Chem.* **55**, 2286 (1977).
- (113) J. Lichtenberger and F. Weiss. *Bull. Soc. Chim. France.* 587 (1962).